UNIVERSIDAD DE LA REPÚBLICA
FACULTAD DE AGRONOMÍA

IDENTIFICACIÓN Y ANÁLISIS DE COMPONENTES CLAVES EN LA EFICIENCIA DEL USO DE LA RADIACIÓN EN ARROZ

por

Gastón Eduardo Quero Corrallo

TESIS presentada como uno de los requisitos para obtener el título de Doctor en Ciencias Agrarias

Montevideo
URUGUAY
Abril 2020

Tesis aprobada por el tribunal integrado por Dr. Ariel Castor Tabó, Dra. María Fernanda Cerdá Bresciano, y Dr. Ing Juan Pablo Oliver Deferrari, el 3 de Junio de 2020 .

Autor: Biol. Prof. (Msc.) Gastón Eduardo Quero Corrallo. Director: Dr. Julio Omar Borsani Cambón.

Dedico este trabajo a mi madre

AGRADECIMIENTOS

A los miembros del tribunal por tomarse el tiempo de revisar y corregir mi trabajo.

A Omar Borsani director de esta tesis por darme un espacio en su laboratorio y creer en mi trabajo.

A Victoria Bonnecarrère por su permanente apoyo durante todo el proceso de mi doctorado, y ayudarme a escribir y corregir los artículos que componen esta tesis.

A Lucía Gutiérrez por las horas de docencia, correcciones y aportes, que hicieron posible la finalización de mi formación de Doctorado.

A Sebastián Fernández por construir las ideas que hicieron posible este trabajo.

Al todo el grupo de Bioquímica y Fisiología Vegetal del Dpto. de Biología Vegetal de Facultad de Agronomía, especialmente a Luis Viega por su compañerismo y apoyo en todas las actividades diarias.

A Sebastián Simondi por su amistad incondicional, sin la cual mi trabajo no hubiera sido posible. Además sabe matemáticas.

TABLA DE CONTENIDO

Página

RESUMEN

Una de las principales limitantes del rendimiento del arroz en regiones de alta productividad es la capacidad intrínseca de cada genotipo de convertir la energía de sol en biomasa. Esta capacidad puede entenderse como la eficiencia en el uso de la luz (LUE). La LUE se puede determinar a nivel de toda la planta o al nivel del aparato fotosintético (rendimiento cuántico). El objetivo de esta tesis fue analizar la dependencia del cultivar con respecto a LUE a nivel de planta y rendimiento cuántico utilizando cuatro cultivares de arroz y cuatro ambientes de luz. Para lograr esto, se desarrollaron dos sistemas de iluminación: Light System I que genera entornos de luz blanca (400 - 700 nm) y Light System II que genera un entorno de luz azul-roja (una banda entre 400 - 500 nm y otra banda entre 600 - 700 nm). La partición de energía en PSII se determinó por el rendimiento cuántico de tres procesos de desexcitación usando parámetros de fluorescencia de clorofila. El daño de PSII solo se incrementó por bajos niveles de energía en ambientes de luz blanca, lo que condujo a una disminución en los procesos fotoquímicos debido al cierre de los centros de reacción. Se puede concluir que todos los cultivares de arroz evaluados en este estudio fueron sensibles a los bajos niveles de radiación, pero la respuesta fue dependiente del cultivar. No hubo una relación genotípica clara entre LUE y rendimiento cuántico. Por otro lado, a través de una estrategia MA, se identificaron 32 genes en el genoma del arroz asociados con los principales parámetros que definen el rendimiento cuántico de PSII. Nuestro trabajo muestra la asociación entre los complejos de captación de luz y el rendimiento cuántico potencial de PSII, así como la relación entre las regiones que codifican proteínas unidas a PSI en la distribución de energía durante el proceso fotoquímico de la fotosíntesis. Esta tesis abre nuevas líneas de trabajo centradas en establecer los mecanismos de acción de la calidad espectral de la luz en PSI y cómo esto define la partición de energía de PSII.

Palabras clave: arroz, eur, led, fotoquímica, fotosistemas

IDENTIFICATION AND ANALYSIS OF KEY COMPONENTS IN THE EFFICIENCY OF THE USE OF RADIATION IN RICE

SUMMARY

One of the main limitations of rice yield in regions of high productive performance is the light-use efficiency (LUE). LUE can be determined at the whole-plant level or at the photosynthetic apparatus level (quantum yield). The aim of this thesis was to analyze the cultivar dependence regarding LUE at the plant level and quantum yield using four rice cultivars and four light environments. To achieve this, two in-house Light Systems were developed: Light System I which generates white light environments (spectral quality of 400–700 nm band) and Light System II which generates a blue-red light environment (spectral quality of 400–500 nm and 600–700 nm bands). Energy partition in PSII was determined by the quantum yield of three de-excitation processes using chlorophyll fluorescence parameters. The damage of PSII was only increased by low levels of energy in white environments, leading to a decrease in photochemical processes due to the closure of the reaction centers. In conclusion, all rice cultivars evaluated in this study were sensible to low levels of radiation, but the response was cultivar dependent. There was not a clear genotypic relation between LUE and quantum yield. Through a GWAS strategy, 32 genes of rice genome associated with the main parameters that define the quantum yield of PSII in rice were identified. Our work shows the association between light-harvesting complexes and the potential quantum yield of PSII, as well as the relationship between regions that code for PSI-linked proteins in energy distribution during the photochemical process of photosynthesis. This thesis opens new lines of work focused on establishing the mechanisms of action of the spectral quality of light in PSI and how this defines the energy partition of PSII.

Keywords: rice, rue, led, photochemistry, photosystems

1. CAPÍTULO I: INTRODUCCIÓN

El arroz (*Oryza sativa* L.) es uno de los principales cereales cultivados y representa la fuente primaria de alimento para un tercio de la población mundial (Khush, 2005). Las predicciones actuales indican que para el año 2025 la población mundial superará los 7 mil millones de personas. Por tanto, se estima que para mantener la seguridad alimentaria de la población mundial, sin afectar negativamente la base de los recursos, los países productores de arroz deberán aumentar sus rendimientos en casi 40% (Swaminathan, 2007, Khush, 2005). En este contexto Uruguay tiene un papel relevante ya que es el primer exportador de arroz de América Latina, participando con el 3 % del comercio de arroz a nivel internacional (Battello, 2008).

A nivel mundial los cultivares modernos de arroz tiene un rendimiento potencial teórico de 15 t ha^{-1} en las regiones templadas (Mitchell et al., 1998), mientras que a nivel local rendimiento potencial estimado es de 10 t ha^{-1} (Pérez de Vida, 2011). En tanto que, en los últimos 15 años el rendimiento alcanzable local (en condiciones experimentales) fue de 8 t ha^{-1}, mientras que para el mismo período el rendimiento comercial promedio logrado a nivel nacional fue de aprox. 7 ton ha^{-1} (Pérez de Vida y Macedo, 2013). En este sentido, el desafío que actualmente enfrenta el sector es tratar de disminuir la brecha existente entre el rendimiento potencial del arroz a nivel local y los rendimientos promedios logrados a nivel productivo nacional.

Entre los factores que afectan la producción, la captura y uso de la radiación solar son cruciales en la determinación del rendimiento potencial de los cultivos (van Ittersum y Rabbinge, 1997). En este sentido, las características funcionales y estructurales que definen los factores de intercepción y uso de la radiación de las variedades locales de arroz, podrían estar explicando las diferencias entre los rendimientos antes mencionados. Por tanto el desafío está, en tratar de establecer cuáles son las causas biológicas de los límites en rendimiento de las variedades que conforman el sistema arrocero uruguayo.

1.1 EFICIENCIA DEL USO DE LA RADIACIÓN: UN COMPONENTE CLAVE DE LA ECUACIÓN DE RENDIMIENTO

Basados en los modelos de crecimiento aceptados actualmente desarrollado por Monteith (1977) y revisado por Russell et al. (1989), el rendimiento de los cultivos puede ser descrito por las siguientes ecuaciones:

$$B = FCR * FI * S_t \quad [1]$$

$$Y = HI * FCR * FI * S_t \quad [2]$$

dónde B es la biomasa producida (g m^{-2}), FCR es el factor de conversión de la radiación el cual es un indicador de la eficiencia en el uso de la radiación (EUR) específica para un cultivo o genotipo (g MJ^{-1}), FI es la fracción de la radiación incidente interceptada por la canopia, S_t es la radiación total incidente (MJ m^{-2}) en un intervalo de tiempo dado, Y es el rendimiento en grano (g m^{-2}), HI es el índice de cosecha o fracción cosechable de la biomasa total del cultivo (en los cultivos como el arroz, es la fracción de grano/biomasa total de la parte aérea). La ecuación [1] provee un marco conceptual que permite la interpretación de la producción de biomasa en función de un factor de intercepción (FI) y un factor de conversión (FCR) (Long et al., 2006, Monteith, 1994).

Este marco conceptual ha sido ampliamente usado para el modelado de la producción de biomasa (Sadras et al., 2005, Jones et al., 1998, Williams et al., 1984). Como se muestra en la ecuación [2] la producción potencial está determinada por el producto combinado de la radiación incidente, las eficiencias de intercepción y conversión y el HI.

En este modelo FI está determinada por el tamaño y tipo de arquitectura de la canopia así como por la velocidad de desarrollo y cierre de la misma. En tanto que el FCR está determinado por la combinación de la tasa fotosintética de todas las hojas dentro de la canopia menos la pérdida por respiración (Stöckle y Kemanian, 2009).

Los niveles de rendimiento potencial se ven limitados debido a que los parámetros HI y FI están llegando a sus valores máximos, por lo que incrementos en el Y solo

pueden ser logrados a través de un incremento en el FCR, que a su vez está asociado a incrementos en la tasa de fotosíntesis, y/o disminución en la tasa de respiración (Long et al., 2006).

En tal sentido, la disección del FCR en una serie de rasgos fisiológicos tales como: estabilidad de la maquinaria fotosintética (fotosistemas), mecanismos de foto protección, tasa de fijación de CO_2, apertura estomática, etc., es una estrategia que permite estudiar mejor las relaciones funcionales que definen el rendimiento (Murchie et al., 2015, Monneveux y Ribaut, 2006, Blum, 1988).

Si bien la información disponible acerca de FCR es abundante, pocos artículos combinan la teoría, con la experimentación y la modelización para identificar que componentes están involucrados en las variaciones de FCR observados entre distintos genotipos (Stöckle y Kemanian 2009). Aquí la dificultad está en poder fenotipar correctamente materiales genéticamente relevantes (Berger et al., 2010) e identificar las regiones del genoma asociadas a tales rasgos de interés.

1.2 HIPÓTESIS DE TRABAJO

Se establecieron tres hipótesis de trabajo:

H1: La EUR varía entre los genotipos de arroz (Figura 1, H1).

H2: El FCR determina de las variaciones en la EUR en arroz (Figura 1, H2).

H3: La tasa de fotosíntesis es la responsable de las variaciones en el FCR en arroz (Figura 1, H3).

H4: Se pueden identificar genes involucrados en la respuesta diferencial del FCR en arroz (Figura 1, H4).

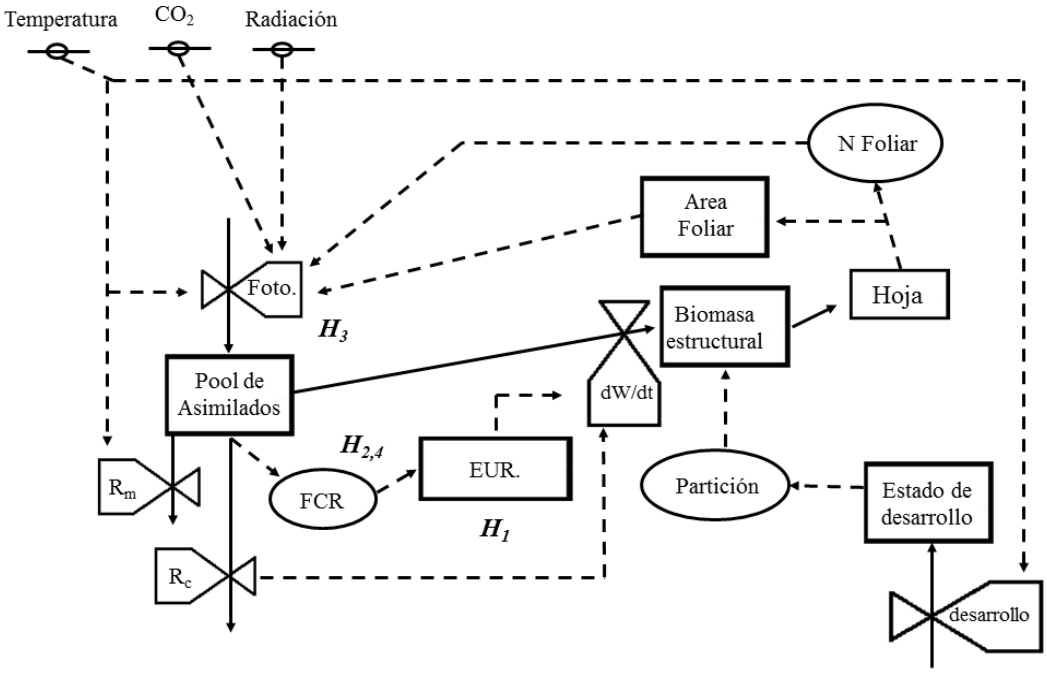

Figura 1. Esquema conceptual del modelo de conversión y balance de la energía propuesto. El esquema se realizó utilizando los símbolos de Forrester (1961), las cajas representan variables de estado, las válvulas representan tasas variables, las elipses representan variables intermedias, los círculos cruzados con líneas representan variables ambientales de entrada, las líneas sólidas representan flujo de materia, las líneas cortadas representan flujo de información. Los coeficientes genéticos son considerados como variables de entrada pero no están representados en el diagrama.

1.3 OBJETIVOS

1.3.1 Objetivo general

El objetivo general de este trabajo es identificar parámetros fisiológicos, bioquímicos y genéticos involucrados en la eficiencia del uso de la radiación con el fin de incluir nuevos marcadores de selección en los programas de mejoramiento de arroz.

1.3.2 Objetivos específicos

a. Identificar y caracterizar componentes que participen en la EUR en arroz.

b. Desarrollar una estrategia de selección a partir de marcadores fisiológicos para identificar genotipos con regiones genómicas asociadas a EUR diferencial.

c. Identificar genes claves en la EUR en arroz.

2. CAPÍTULO II:
HERRAMIENTAS GENÓMICAS PARA LA CARACTERIZACIÓN DE UNA POBLACIÓN DE MEJORAMIENTO E IDENTIFICACIÓN DE REGIONES DE GENOMA DE INTERÉS EN ARROZ.

El trabajo se concentró en el estudio de la estructura genética de la población utilizada para el análisis de mapeo asociativo de genoma completo (MA). Aquí se desarrollaron las herramientas informáticas para el análisis de MA y para identificación de haplotipos a partir de los loci identificados para los rasgos cuantitativos estudiados (QTL) que en este caso fueron rasgos de calidad.

Para poder analizar la estructura genética de la población de mapeo se desarrollaron algoritmos en el software libre R. Producto de ese desarrollo se obtuvieron como producto dos paquetes de R que se encuentran disponible en el *The Comprehensive R Archive Network* (CRAN). El primer paquete de R denominado *lmem.gwaser* (Gutiérrez et al., 2016) fue desarrollado para el control de la calidad de los marcadores genéticos y la implementación de diferentes modelos para el análisis de MA. El segundo paquete de R denominado *clustehap* (Quero et al., 2017) fue desarrollado para la identificación de haplotipos en la población de mapeo.

Este trabajo permitió obtener herramientas para el análisis de MA que luego fueron implementadas para la identificación de QTL asociados a rasgos de fotosíntesis. Los QTL identificados en este artículo serán utilizados como base para un futuro trabajo en el cual se estudiara la relación entre las regiones asociados la calidad del grano y aquellas identificadas para la eficiencia del uso de la radiación. Esto en arroz es particularmente importante ya que los incrementos de producción en arroz tienen sentido si se encuentran vinculados con niveles de alta calidad de grano.

2.1 GENOME-WIDE ASSOCIATION STUDY USING HISTORICAL BREEDING POPULATIONS DISCOVERS GENOMIC REGIONS INVOLVED IN HIGH-QUALITY RICE.

Published July 12, 2018

Genome-Wide Association Study Using Historical Breeding Populations Discovers Genomic Regions Involved in High-Quality Rice

Gastón Quero, Lucía Gutiérrez,* Eliana Monteverde, Pedro Blanco, Fernando Pérez de Vida, Juan Rosas, Schubert Fernández, Silvia Garaycochea, Susan McCouch, Natalia Berberian, Sebastián Simondi, and Victoria Bonnecarrère

G. Quero, Dep. of Plant Biology, College of Agriculture, Univ. de la República, Garzón 809, Montevideo, Uruguay; G. Quero, J. Rosas, S. Garaycochea, V. Bonnecarrère, Biotechnology Unit, Experimental Station Wilson Ferreira Aldunate, Instituto Nacional de Investigación Agropecuaria (INIA, National Institute of Agriculture Research), Ruta 48, Km 10, Rincón del Colorado, Canelones 90200, Uruguay; L. Gutiérrez, Dep. of Agronomy, Univ. of Wisconsin-Madison, 1575 Linden Dr., Madison, WI 53706; L. Gutiérrez, N. Berberian, Dep. of Statistics, College of Agriculture, Univ. de la República, Garzón 780, Montevideo, Uruguay; E. Monteverde, S. McCouch, Dep. of Plant Breeding and Genetics, Cornell Univ., Ithaca, NY 14850; P. Blanco, F. Pérez de Vida, J. Rosas, National Rice Research Program, Experimental Station INIA Treinta y Tres, INIA, Ruta 8, Km 281, Treinta y Tres 33000, Uruguay; S. Fernández, Information Technology Unit, INIA, Andes 1365 Piso 12, Montevideo, Uruguay; S. Simondi, Mathematics Area, College of Natural and Exact Sciences, Univ. Nacional de Cuyo, Padre Contreras 1300, Mendoza, Argentina.

ABSTRACT Rice (*Oryza sativa* L.) is one of the most important staple food crops in the world; however, there has recently been a shift in consumer demand for higher grain quality. Therefore, understanding the genetic architecture of grain quality has become a key objective of rice breeding programs. Genome-wide association studies (GWAS) using large diversity panels have successfully identified genomic regions associated with complex traits in diverse crop species. Our main objective was to identify genomic regions associated with grain quality and to identify and characterize favorable haplotypes for selection. We used two locally adapted rice breeding populations and historical phenotypic data for three rice quality traits: yield after milling, percentage of head rice recovery, and percentage of chalky grain. We detected 22 putative quantitative trait loci (QTL) in the same genomic regions as starch synthesis, starch metabolism, and cell wall synthesis-related genes are found. Additionally, we found a genomic region on chromosome 6 in the *tropical japonica* population that was associated with all quality traits and we identified favorable haplotypes. Furthermore, this region is linked to the *OsBEI* gene that codes for a starch branching enzyme I, which is implicated in starch granule formation. In *tropical japonica*, we also found two putative QTL linked to *OsBEII*, *OsDEP1*, and *OsDEP2*. Our study provides an insight into the genetic basis of rice grain chalkiness, yield after milling, and head rice, identifying favorable haplotypes and molecular markers for selection in breeding programs.

Abbreviations: GC, percentage of chalky grain; GWAS, genome-wide association study; INIA, Instituto Nacional de Investigación Agropecuaria (National Institute of Agriculture Research); LD, linkage disequilibrium; PCA, principal component analysis; PHR, percentage of head rice recovery; PVE, proportion of phenotypic value explained; QTL, quantitative trait loci; SNP, single nucleotide polymorphism; SSRG, starch synthesis-related genes; YAM, yield after milling.

CORE IDEAS

- Genome-wide association study (GWAS) for rice quality was performed in two breeding populations.
- Twenty-two putative quantitative trait loci (QTL) were associated to rice quality.
- A genomic region on chromosome 6 was associated with all quality traits in the *tropical japonica* population.
- Markers for favorable haplotypes are ready for immediate use for selection.

ONE OF THE MAIN CONCERNS of agricultural research today is intensifying agricultural production in a sustainable manner to feed the 9 billion people expected by 2050 (Godfray et al., 2010). Rice is a staple crop in Asia and Africa, where 3.5 billion people depend on rice for food energy (Food and Agriculture Organization of the United

Citation: Quero, R., L. Gutiérrez, E. Monteverde, P. Blanco, F. Pérez de Vida, J. Rosas, S. Fernández, S. Garaycochea, S. McCouch, N. Berberian, S. Simondi, and V. Bonnecarrère. 2018. Genome-wide association study using historical breeding populations discovers genomic regions involved in high-quality rice. Plant Genome 11:170076. doi: 10.3835/plantgenome2017.08.0076

Received 25 Aug. 2017. Accepted 9 Apr. 2018. *Corresponding author (gutierrezcha@wisc.edu).

Nations, 2009). The demand for rice continues to grow, especially in Asia and Africa, where people now require high-quality rice (Hsiaoping, 2005; Zader, 2011; Mohanty, 2013; Yu et al., 2013) regarding traits such as grain length, color, absence of broken grains, aroma, and flavor. The ability to meet this demand can be achieved by understanding the genetic basis of key production traits and accelerating the rate of genetic gain from cultivar development.

Grain quality is a complex quantitative trait (Fitzgerald et al., 2009). Quantitative trait loci mapping via GWAS (Jannink et al., 2001) has successfully identified genomic regions associated with complex traits in diverse crop species and provided targets for marker assisted selection (Begum et al., 2015). Early GWAS studies used large diversity panels to maximize the range of genetic variation and improve the power of detecting QTL (Kraakman et al., 2004; Gore et al., 2009; Huang et al., 2010, 2012; Famoso et al., 2011; Zhao et al., 2011; Chen et al., 2014; McCouch et al., 2016; Zhu et al., 2016). However, in the same way that traditional QTL studies were challenged by their lack of practical use because some of the favorable alleles of major-effect QTL were already fixed in elite germplasm (Langridge et al., 2001); the use of diverse and unadapted germplasm in GWAS studies may yield irrelevant genomic regions for breeding purposes (Kraakman et al., 2004). Furthermore, the genetic background interaction of QTL effects (Langridge et al., 2001) and QTL × environment interactions (Malosetti et al., 2004, 2016; Mathews et al., 2008; Gutiérrez et al., 2015) have been extensively reported, indicating that the choice of germplasm and environments used for mapping studies is relevant, especially regarding its future deployment. Therefore, studies looking for immediate applications in breeding use locally adapted germplasm to map QTL (Begum et al., 2015; Spindel et al., 2015) or nested association mapping with a locally adapted line serving as the common parent (Yu et al., 2008; Brachi et al., 2011; Kump et al., 2011; Tian et al., 2011; Mace et al., 2013; Maurer et al., 2015). The use of breeding populations has been successful in identifying QTL and favorable haplotypes in elite populations of tropical rice with phenotypic data specially generated for GWAS purposes (Begum et al., 2015). Besides the immediate advantage of using adapted germplasm, GWAS in local populations allows the discovery of adaptive alleles and allelic complexes, which may be locally common but globally rare (rare alleles) and therefore has the potential to unveil genetic variants that would otherwise be overlooked. Despite being potentially useful, rare alleles are often discarded by minor allele frequency filters when exploring natural variation (Jannink et al., 2001; Brachi et al., 2011; McCouch et al., 2016).

The main objective of this study was to identify genomic regions associated with rice grain quality in relevant adapted germplasm and to identify favorable haplotypes for selection. Specifically, we studied the genetic architecture of rice quality by conducting a GWAS analysis on a subtropical-adapted breeding population consisting of 637 elite rice lines representing two of the major subgroups of rice, *indica* and *tropical japonica*. Considering the extended linkage disequilibrium (LD) in this kind of population, we conducted a GWAS analysis that followed an appropriate analytical framework that involved a high-coverage genotyping strategy and a careful interpretation of population structure and phenotypic data. Candidate genes were predicted via an annotation approach. This strategy exploits existing breeding populations and historical phenotypic data, demonstrating that it is possible to use routine breeding data to perform haplotype selection.

MATERIALS AND METHODS

Plant Material

A total of 637 genotypes from the National Rice Breeding Program were used as the Uruguayan rice reeding GWAS population. The population included 324 *indica* lines, 310 *tropical japonica* lines, two *indica* cultivars [El Paso 144 (Yan et al., 2007) and INIA Olimar (Blanco et al., 2004)] and one *tropical japonica* cultivar [INIA Tacuarí (Blanco et al., 1993; Instituto Nacional de Semillas, 2017)]. Within the *indica* subpopulation, 228 genotypes originated from Instituto Nacional de Investigación Agropecuaria (INIA) breeding material and 98 from Fondo Latinoamericano de Arroz de Riego breeding material. All the individuals within a population, including the checks, share some level of common ancestry, and pedigree information was available from breeders.

Genotyping and Single Nucleotide Polymorphism Genotype Calling

Genotyping-by sequencing data were obtained for the 637 advanced inbred lines and cultivars. DNA was extracted from young leaf tissue from plants grown in the Biotechnology Unit in Las Brujas, Canelones, Uruguay. The extraction was conducted with the Qiagen DNeasy kit (www.qiagen.com/uy/, accessed 5 June 2018). Samples were submitted in 96-well plates and libraries were prepared using the protocol described by Elshire et al. (2011). Genotyping-by-sequencing library construction and sequencing were done at the Biotechnology Resource Center at Cornell University. Single nucleotide polymorphisms (SNPs) were called from fastq files via the TASSEL version 3.0 genotyping-by-sequencing pipeline (Glaubitz et al., 2014). Alignment to the Michigan State University Nipponbare reference genome version 7.0 (http://rice.plantbiology.msu.edu/pub/data/Eukaryotic_Projects/o_sativa/annotation_dbs/pseudomolecules/version_7.0/, accessed 14 June 2018) was performed with Bowtie version 2 (Langmead and Salzberg, 2012). Imputation of missing data was performed with the FILLIN algorithm implemented in TASSEL version 5.0 (Bradbury et al., 2007; Swarts et al., 2014) for the *indica* and *tropical japonica* genotypes separately. The average imputation accuracy was approximately 94% for both *indica* and *tropical japonica* datasets. Single nucleotide polymorphism markers that had more than 50% missing data after imputation, along with monomorphic SNPs and SNPs with a minor allele frequency smaller than 1% were removed from the analysis.

Grain Quality Phenotyping

Rice lines were evaluated in the field located in Paso de la Laguna, Treinta y Tres, Uruguay (33°15′S, 54°25′W) during the growing seasons (October–March) in 2010–2011, 2011–2012, and 2012–2013 in replicated experiments. Adjusted means for each line were obtained with mixed models to include experimental design components and spatial corrections (Supplemental File S1) using the model in Eq. [1]:

$$Y_{ijk} = \mu + \lambda_i + \beta_{j(i)} + \gamma_k + \varepsilon_{ijk} \quad [1]$$

where Y_{ijk} is the response variable, μ is the overall mean or intercept, λ_i is a random variable associated with the *i*th trial with $\lambda_i \sim N(0, \sigma^2_\lambda)$, $\beta_{j(i)}$ is a random variable associated with the *j*th block nested within the *i*th trial with $\beta_{j(i)} \sim N(0, \sigma^2_\beta)$, γ_k is the effect of the *k*th genotype, and ε_{ijk} is the residual error with $\varepsilon_{ij} \sim N(0, \sigma^2_\varepsilon)$.

Milling quality was evaluated by the yield after milling (YAM), the percentage of head rice recovery (PHR), and the percentage of chalky grain (GC). For YAM and PHR, 100 g of rough rice was dried to 13% moisture, hulled with a Satake Rubber Roll Huller (Satake Engineering Co., Ltd., Tokyo, Japan), milled with a Satake Grain Testing Mill (Model TM 05C, abrasive roll #36, Satake Engineering Co., Ltd.), and separated into broken and whole kernels using a thickness grader (Model TWSM, Satake Engineering Co. Ltd.) with an indented cylinder (cylinder indent sizes of 4.75 mm). The weight of grain recovered after milling and separating was used to calculate the percentage of total milled rice or YAM. The percentage of whole kernels recovered after separating was used as the PHR. For GC, a subsample of 50 g of total milled rice was visually inspected by analysts to determine GC. According to industry standards, whole or broken kernels were considered to be chalky when the area of chalk (core, white back, or belly) was larger than half of the kernel area.

Principal Component Analysis and Population Structure Analyses

Population structure was analyzed via principal component analysis (PCA) and a model-based clustering algorithm. The PCA analyses were performed with the imputed marker score matrix in R statistical software (R Core Team, 2017) using the package *rrBLUP* (Endelman, 2011). Based on the PCA results, clustering of *indica* or *tropical japonica* individuals was implemented with ADMIXTURE software version 1.23 (Alexander et al., 2009). The number of populations (*k*) was selected according to two main criteria: first, the lowest cross-validation error across a range of *k* values (i.e., *k* = 1–10); second, an ad hoc correspondence with pedigree information. The resulting probabilities of belonging to groups from ADMIXTURE were then plotted with the *barplot* function in the R statistical software (R Core Team, 2017) to obtain stacked bar charts.

Genome-Wide Association Study, LD Decay, and Haplotype Analysis

Genome-wide association studies were performed with mixed models to correct for population structure and genetic relationships. The most common mixed models for GWAS were compared: naive, kinship (Parisseaux and Bernardo, 2004), and eigenvalue (Price et al., 2006; Malosetti et al., 2007). The best model was selected on the basis of quantile–quantile plots (i.e., Schweder and Spjotvoll plots; Schweder and Spjotvoll, 1982) (Supplemental File S2). The kinship was the selected model, with:

$$\boldsymbol{y} = \mathbf{X}\boldsymbol{\beta} + \mathbf{Z}\boldsymbol{u} + \boldsymbol{e}, \quad [2]$$

where $\boldsymbol{y}$ is the vector of phenotypic means, $\mathbf{X}$ is the molecular marker score matrix, β is the vector of marker allelic effects, $\mathbf{Z}$ is an incidence matrix, $\boldsymbol{u}$ is the vector of polygene background effects with $\text{Var}(\boldsymbol{u})$ being $2\mathbf{K}V_G$ ($\mathbf{K}$ is the matrix of kinship coefficients and V_G is the genetic variance), and ε is the residual error vector. A GWAS analysis for each rice subpopulation was performed in the R statistical software (R Core Team, 2017) with the *lmem.gwaser* package (Gutierrez et al., 2016). For QTL determination, the marker with the highest marker–trait association was chosen as an anchor and then, a sliding window of 1 Mb was used to identify all significant markers within that window. The window size was determined according to the LD decay in each chromosome (Supplemental File S3 and Supplemental File S4). A QTL was defined when three or more significant SNPs were found within the 1-Mb window, following Rosas et al. (2017). Given the level of genetic relatedness in our populations, markers in close proximity are in high LD, making it unlikely to have an isolated significant SNP. Therefore, isolated markers are more probably caused by genotyping or imputation error (Brandariz et al., 2016) than a true QTL. Choosing three markers for our threshold makes our analysis less likely to declare a false QTL. Linkage disequilibrium was computed as pairwise r^2 between all SNPs in the chromosome and then in a specific region, and limits between LD blocks were graphically assessed with the R package (R Core Team, 2017). The threshold level for calling a significant marker–trait associations was calculated by using a *p*-value corrected by multiple comparisons with the Li and Ji (2005) statistic at an α level of 0.05. The proportion of the total phenotypic variance explained (PVE) by each QTL was estimated by fitting a full multi-QTL model with all significant SNPs from all genomic regions involved for a trait in the *lme4* package (Bates et al., 2015) of R statistical software (R Core Team, 2017). Allelelic effects for each QTL were obtained with the *emmeans* package (Lenth, 2018) in R statistical software (R Core Team, 2017). Finally, the most prevalent haplotypes were identified with the *clusterhap* package (Quero et al., 2017) in R statistical software (R Core Team, 2017) and the phenotypic means for each haplotype were estimated (Supplemental File S5).

Identification of Candidate Genes

A literature survey and a genome annotation pipeline were used to search for putative causal candidate genes.

The numbers of genes located within a defined QTL were retrieved from the Michigan State University public gene annotation database (http://rice.plantbiology.msu.edu/downloads_gad.shtml, accessed 14 June 2018) via an in-house script (Supplemental File S6). The Plant Metabolic Network was used to assign a function to each gene (Zhang et al., 2010). OryzaCyc was used to search for plant metabolic pathway functionality. Gene function was further explored by studying the metabolic pathways where the encoded enzymes were involved. This was analyzed with the Kyoto Encyclopedia of Genes and Genomes (Kanehisa and Goto, 2000), which is a collection of pathway maps. The literature survey was focused on major genes involved in starch synthesis known as starch synthesis-related genes (SSRGs) (Zeng et al., 2017). The SSRGs include genes for ADP-glucose pyrophosphorylase, granule-bound starch synthase, starch synthase, branching enzyme, debranching enzyme, starch phosphorylase, disproportionating enzyme, and glucose 6-phosphate translocator. After identification of the candidate genes, we analyzed the presence of SNPs in its coding sequence in the Nipponbare reference genome (Michigan State University Nipponbare reference genome version 7.0). When a SNP was found within the coding sequence, the amino acid sequence of the encoded protein with both versions of the SNP was determined. To do this, Mega version 6 software was used (Tamura et al., 2013).

RESULTS

Population Structure and Phenotypic Variation

Two main subpopulations were observed in the PCA corresponding to the *indica* and *tropical japonica* subpopulations (Fig. 1a). The first two principal components explained more than 78.2% of the total genotypic variance. Within the *indica* subpopulation, two subgroups were identified with a model-based algorithm corresponding to the two distinct origins of lines coming from the breeding programs at the INIA or the Fondo Latinoamericano de Arroz de Riego (Fig. 1a). Five subgroups were identified within the *tropical japonica* subpopulation (Fig. 1a) on the basis of the clustering algorithm and pedigree information. The *tropical japonica* subpopulation is defined as a multiparent cross where the lines were derived from 12 parents, and each of the five subgroups was comprised of half-sib families. The *indica* subpopulation had lower GC on average, with smaller variance than the *tropical japonica* subpopulation (Fig. 1b), whereas estimates of YAM and PHR were similar in both subpopulations. In the *tropical japonica* subpopulation, the three grain quality traits were correlated: YAM and PHR were positively correlated, but GC was negatively correlated with YAM and PHR. On the other hand, no correlation among traits was observed for the *indica* subpopulation (Fig. 1b).

Quantitative Trait Loci Identified by GWAS

Genome-wide association studies for every targeted trait were performed separately for *indica* and *tropical japonica* because of the population structure. When different mixed models for GWAS were compared, the kinship model using the realized relationship matrix estimated from the marker data was the best model (Supplemental File S2). We therefore used this model to map QTL following the analytical framework outlined in Supplemental File S5. We identified a total of 22 putative QTL in the two subpopulations (Fig. 2). These QTL were identified with a multiple comparison test at a p-value threshold of 8.5×10^{-4} for *tropical japonica* and 1.3×10^{-3} for *indica* subpopulation, according to the calculated Li and Ji (2005) threshold. In the *indica* subpopulation, five putative QTL were identified for GC, one for YAM, and six for PHR (Supplemental File S7), whereas in *tropical japonica*, three QTL were identified for GC, five for YAM, and two for PHR (Supplemental File S8; Fig. 2). We did not find any QTL shared between the *indica* and *tropical japonica* subpopulations. There is a genomic region on chromosome 6 (26,894,513–29,480,530 bp) of *tropical japonica*, where three putative QTL mapped for all quality traits evaluated (qYAM.j.6.1, qPHR.j.6.1, and qGC.j.6.2). Markers on these QTL were in high LD (Fig. 3a). The PVE for each QTL was above 30%, which means all of them are large-effect QTL (Table 1). On the other hand, all QTL in the *indica* subpopulation had lower PVE and only two QTL had a PVE above 10% (qPHR.i.2.1 and qPHR.i.3.1).

Genomic Regions and Haplotype Analysis

Of the 22 marker–trait associations detected in this study, eight SSRGs (Zeng et al., 2017) were identified within or in the flanking regions of nine QTL (Table 2). By using a genome annotation approach, we also identified eight candidate genes in five putative QTL observed in our subpopulations (Supplemental File S9). Beside starch metabolism, these candidate genes are involved in cell wall formation and degradation. Our study provides hypothetical candidate genes that should be further studied to elucidate whether they have a functional role in grain quality.

Three putative QTL (qYAM.j.6.1, qPHR.j.6.1, and qGC.j.6.2) were colocated in a region on chromosome 6 in the *tropical japonica* subpopulation. We identified three candidate genes within the QTL region involved in starch metabolism and three involved in cell wall formation (Supplemental File S9). These genes include two α-glucosidases that are part of the first pathway of starch degradation. A functional mutation (genotyping-by-sequencing SNP S6_28101061; A > G) in one of the α-glucosidase genes, *LOC_Os06g46340*, alters the protein sequence (p.Glu45Gly) and is noteworthy because the derived allele codes for an amino acid belonging to a different group and would probably result in a conformational change in the protein product.

Besides these candidate genes, we found that one SSRG, specifically a starch branching enzyme I gene, *OsBEI* (*LOC_Os06g51084*; Ohdan et al., 2005) is located next to the QTL interval on chromosome 6. Rice has two branching enzyme families, BEI and BEII, coded by one (*OsBEI*) and two genes (*OsBEIIa* and *OsBEIIb*), respectively. *OsBEI* is the only BEI gene in rice and it is known to be involved in amylopectin structure (Ohdan et al., 2005). We detected two

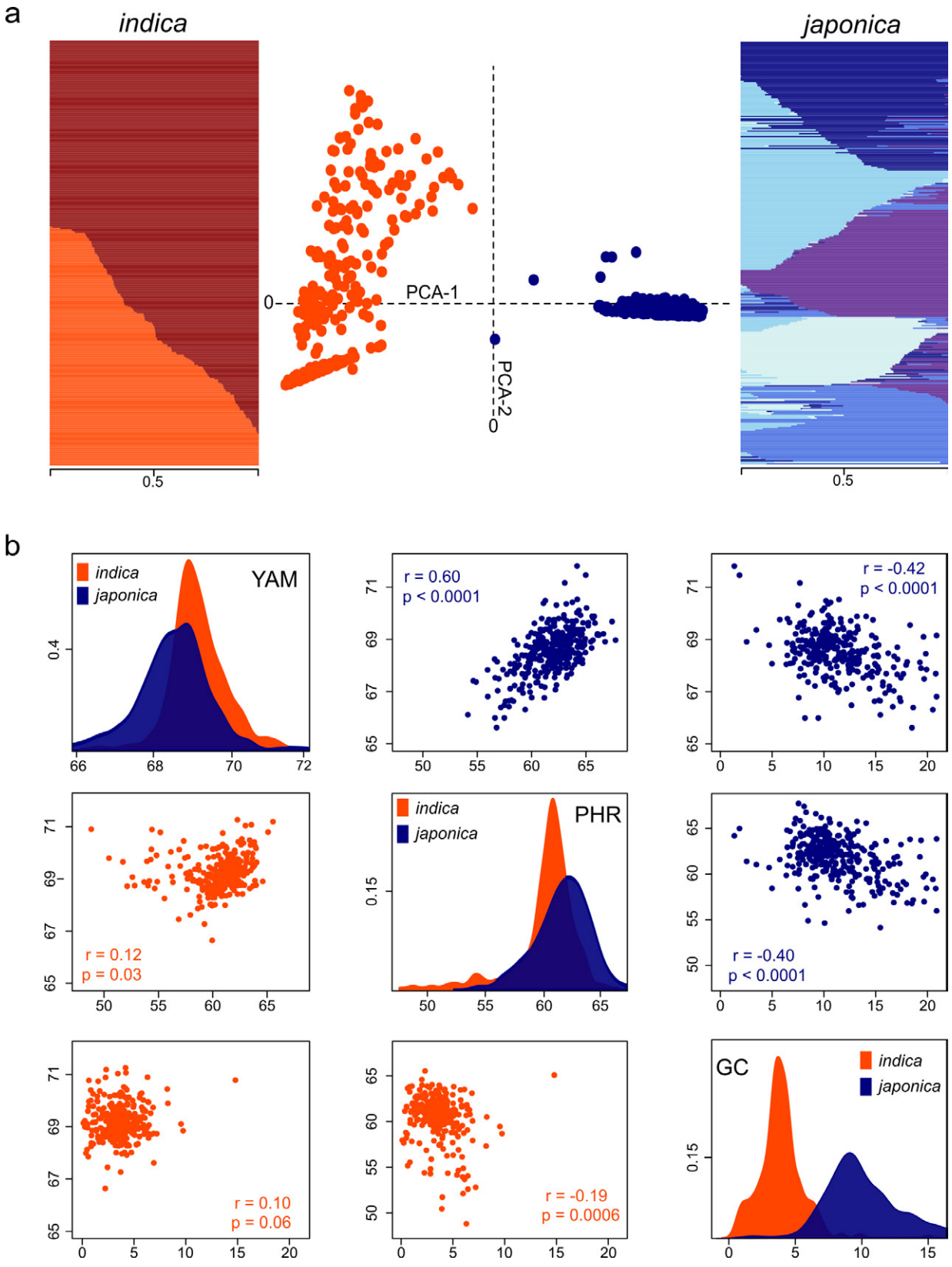

Figure 1. Genetic structure and phenotypic variation in locally adapted rice populations. (a) The central image shows the first two principal components separating *indica* (red, n = 326) and tropical japonica (blue, n = 311) individuals; the left-hand image shows the two genetic subgroups within *indica*; the right-hand image shows the five genetic subgroups within *tropical japonica*. (b) Scatterplot matrix for grain quality traits showing density plots for each trait [yield after milling (YAM), percentage of head rice recovery (PHR), and percentage of chalky grain (GC)] in the diagonal, scatterplots between traits for *tropical japonica* (blue, n = 311) above the diagonal, and scatterplots between traits for *indica* (red, n = 326) below the diagonal. Numbers inside the scatterplots indicate Pearson's correlation between pairs of traits and their *p*-values. Each scatterplot displays two variables with the *x* and *y* axes corresponding to the variables in the diagonal.

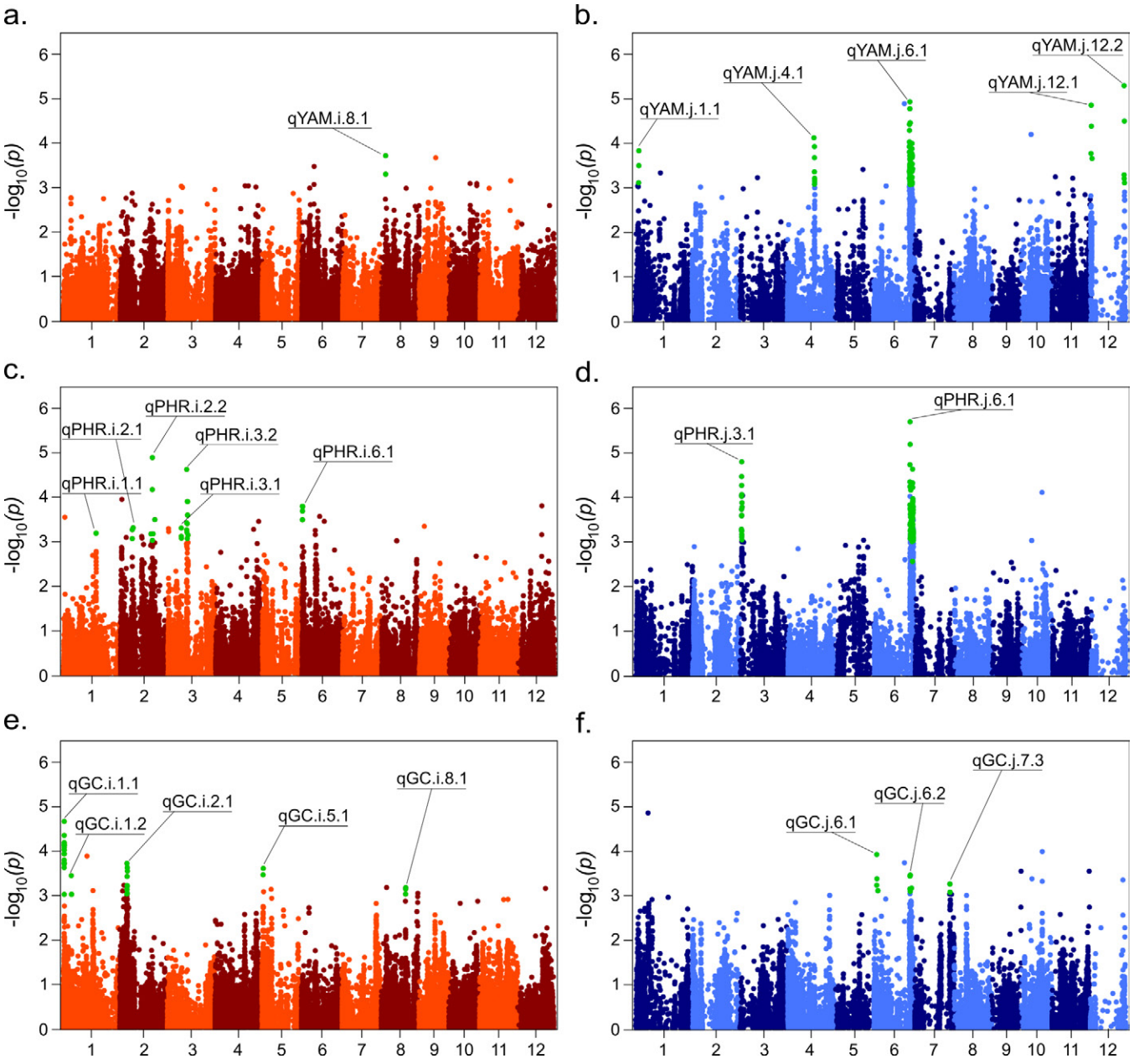

Figure 2. Genome-wide association study (GWAS) for rice physical grain quality in two breeding subpopulations. Manhattan plots of the *indica* subpopulation (red, n = 326) for yield after milling (YAM) (a), percentage of head rice recovery (PHR) (c), and percentage of chalky grain (GC) (e) and of the *tropical japonica* subpopulation (blue, n = 311) for YAM (b), PHR (d), and GC (f). The x-axis shows single nucleotide polymorphism (SNP) positions along chromosomes; the y-axis shows the –log10 of the P-value for each marker–trait association. Associations above the significance threshold [calculated via the method of Li and Ji (2005) with multiple test correction] are shown in green.

SNPs (S6_30900078 and S6_30900838) within the *OsBEI* gene that are in high LD with most of the significant SNPs located within the QTL (Fig. 3b), with an average r^2 of 0.63, 0.65 and 0.83 between *OsBEI* and qYAM.j.6.1, qPHR.j.6.1, and qGC.j.6.2, respectively. Furthermore, we observed three clearly differentiated haplotypes present in ~90% of the lines and a few minor recombinant haplotypes (data not shown). For YAM and PHR, the groups of individuals carrying the H1 and H2 haplotypes had significantly higher phenotypic means than H3, while for GC the groups of individuals carrying the H1 and H2 haplotype had significantly lower phenotypic means than H3 (Fig. 3b). For all traits, H1 and H2 were different from each other by only one SNP (S6_30900078), which is located within the *OsBEI* gene. Considering the phenotypic mean of theses haplotypes, this polymorphism had no effect on PHR and GC, but it had an effect on YAM (Fig. 3b).

Other SSRGd were found linked to be to QTL identified by GWAS in the *tropical japonica* subpopulation (Table 2). The SSRG *OsBEIIa* (*LOC_Os04g33460*) is located within the QTL qYAM.j.4.1 and all markers within the QTL are in perfect LD with one SNP located within the *OSBEIIa* gene (Fig. 4a). This QTL region has three major haplotypes with different phenotypic means (Fig. 4b).

Table 1. Proportion of the phenotypic variance explained (PVE) by each putative quantitative trait locus (QTL) identified from the genome-wide association study analysis of a large rice population in both *indica* (i) and *tropical japonica* (j) subpopulations showing the single nucleotide polymorphisms (SNP) with the most significant marker–trait associations.

QTL	SNP	PVE
qGC.i.1.1	S1_1066894	4.78
qGC.i.1.2	S1_6427540	4.49
qGC.i.2.1	S2_5409930	7.29
qGC.i.5.1	S5_1053773	6.30
qGC.i.8.1	S8_18577900	0.84
qPHR.i.1.1	S1_24735280	0.70
qPHR.i.2.1	S2_9639305	10.34
qPHR.i.2.2	S2_24210614	0.34
qPHR.i.3.1	S3_10247958	15.94
qPHR.i.3.2	S3_14353133	9.95
qPHR.i.6.1	S6_366796	1.81
qYAM.i.8.1	S8_2999273	7.18
qGC.j.6.1	S6_2140954	2.78
qGC.j.6.2	S6_27519265	35.27
qGC.j.7.1	S7_26562521	3.63
qYAM.j.1.1	S1_3059047	2.65
qYAM.j.4.1	S4_19985917	8.90
qYAM.j.6.1	S6_27313987	34.26
qYAM.j.12.1	S12_566928	7.89
qYAM.j.12.2	S12_25469756	8.46
qPHR.j.3.1	S3_1354379	5.63
qPHR.j.6.1	S6_27037310	37.40

Table 2. Putative candidate starch synthesis-related genes (SSRGs) that are located within or close to quantitative trait loci (QTL) identified from the genome-wide association study analysis of a large rice population in both *indica* and *tropical japonica* subpopulations.

QTL	Reference gene locus	SSRG name	SSRG product
qPHR.i.1.1	*LOC_Os01g44220*	*OsAGPL2*	ADP-glucose pyrophosphorylase large subunit 2
qPHR.i.6.1	*LOC_Os06g04200*	*OsGBSSI*	Granule-bound starch synthase I
qYAM.i.8.1	*LOC_Os08g09230*	*OsSSIIIa*	Starch synthase IIIa
qYAM.j.4.1	*LOC_Os04g33460*	*OsBEIIa*	Starch branching enzyme IIa
qGC.j.6.1	*LOC_Os06g06560*	*OsSSI*	Starch synthase I
qGC.j.6.2	*LOC_Os06g51084*	*OsBEI*	Starch branching enzyme I
qYAM.j.6.1	*LOC_Os06g51084*	*OsBEI*	Starch branching enzyme I
qPHR.j.6.1	*LOC_Os06g51084*	*OsBEI*	Starch branching enzyme I
qGC.j.7.1	*LOC_Os07g43390*	*OsDEP1*	Disproportionating enzyme I
qGC.j.7.1	*LOC_Os07g46790*	*OsDEP2*	Disproportionating enzyme II

On the other hand, the SSRG *OsSSI* (*LOC_Os06g06560*) is in perfect LD with the QTL qGC.j.6.1 (Supplemental File S10) and the only two disproportionation enzyme genes in rice genome, DP1 (*LOC_Os07g43390*) and DP2 (*LOC_Os07g46790*; Lu and Sharkey, 2004), flank the QTL qGC.j.7.1 (Table 2). All SNPs within this QTL are in complete LD with the SNPs flanking both genes (Fig. 4a). On the other hand, for qGC.j.7.1, there is a difference of ~2% of GC between the two major haplotypes (Fig. 4c).

We could identify candidate genes in two *indica* QTL (Supplemental File S9): a gene for a fructose-bisphospate aldolase (*LOC_Os01g02880*), which is associated with starch metabolism, in qGC.i.1.1 and a gene encoding an arabinofuranosidase (*LOC_Os02g10190*). In addition, in the QTL q.GC.i.2.1, one of the SNPs in this gene generates a mutation at position 845, where an alanine is changed to a threonine (p.Ala845Thr). Again, as occurred for *LOC_Os06g46340*, both amino acids belong to different groups.

DISCUSSION

By using *indica* and *tropical japonica* breeding populations and historical phenotypic data from 3 yr of replicated and balanced experiments on grain quality, we found enough diversity to map relevant quantitative traits for rice quality and to identify haplotypes with significant differences on rice quality traits. The use of breeding populations for GWAS has some advantages over the use of diverse populations, including immediate application to breeding programs (Kraakman et al., 2004) because it can identify loci that are segregating in the population (Langridge et al., 2001) and that have a reduced genetic background (Langridge et al., 2001) and QTL × environment interactions (Malosetti et al., 2004; Mathews et al., 2008; Gutiérrez et al., 2015). The use of larger structured populations might increase mapping resolution for detecting global QTL (McCouch et al., 2016). However, we decided against a global test with individuals from both subpopulations because: (i) when SNPs were called for all individuals, fewer SNPs that passed our data curation process were identified; (ii) most SNPs were in opposite phases, being monomorphic for one subpopulation and polymorphic for the other, reducing the power for marker–trait associations; (iii) the phenotype was associated with population structure at least for one of our traits (i.e., GC), which would also reduce the power of our statistical tests; and (iv) because of the general challenges of properly controlling for population structure. Therefore, we mapped within subpopulations.

Quality phenotypic traits were correlated in *tropical japonica*. This finding was consistent with previous studies where GC was associated with an increase in grain breakage and therefore a decrease in the percentage of head rice recovery (Lisle et al., 2000; Zhou et al., 2015). In the case of *indica* subpopulation, the low level of correlation among the phenotypic variables could be related to the most diverse grain morphology being found in this population. These findings point toward selection as one possible explanation for the strong correlation in *tropical japonica* instead of pleiotropy. Although a genomic region responsible for all traits was found in *tropical japonica*, the genetic mechanism behind it could be a series of linked genes maintained through selection.

We used genotyping by sequencing to identify more than 44,000 polymorphic SNPs in *tropical japonica* and more than 92,000 SNPs in *indica* (Supplemental File S11). This genotyping strategy generated a relatively high density of SNPs that were appropriate for association mapping and avoided

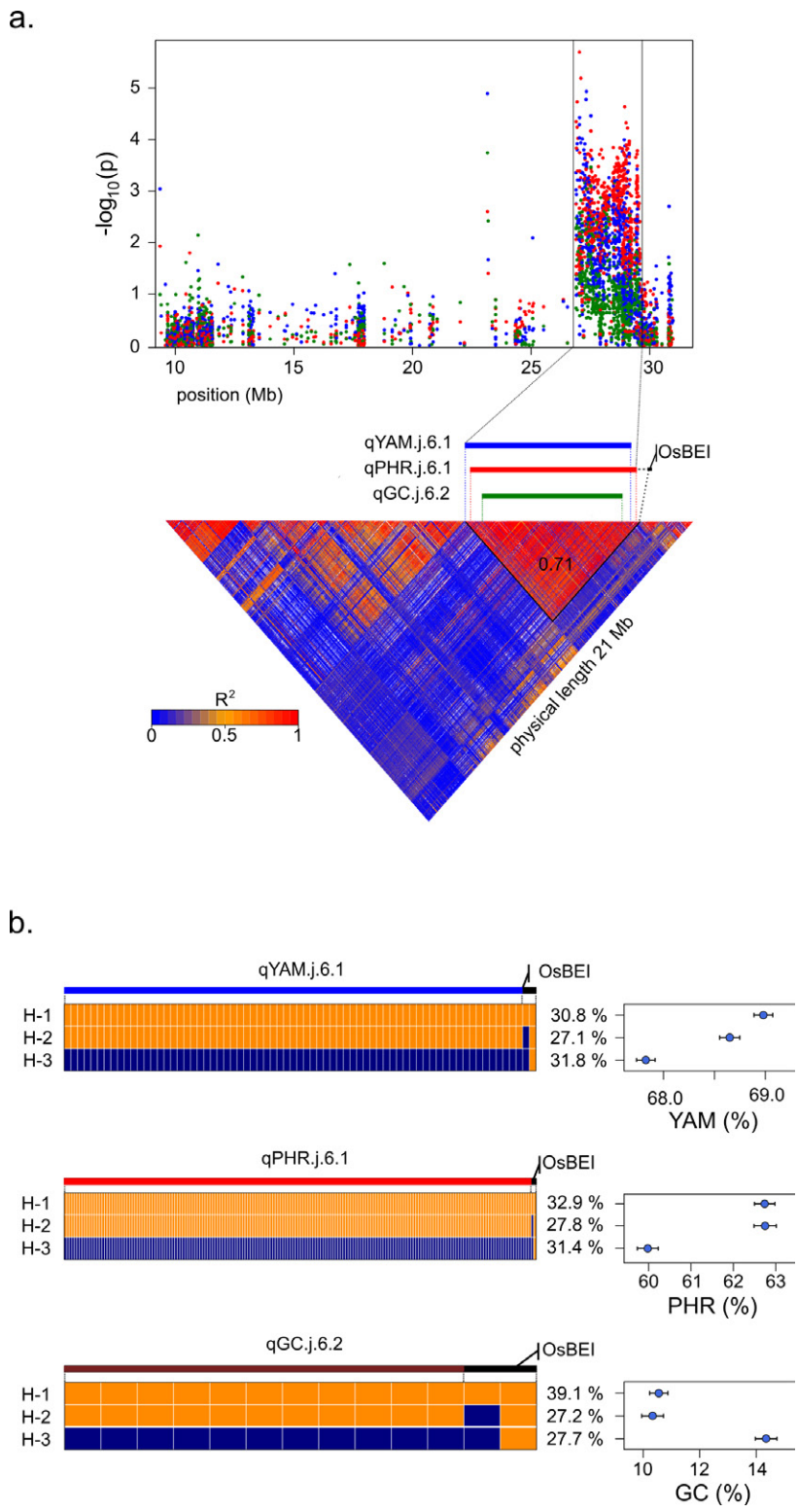

Figure 3. Genome-wide association study (GWAS) hits on chromosome 6 in the *tropical japonica* subpopulation in relation to *OsBEI*, a gene encoding Starch Branching Enzyme 1. (a) Manhattan plot for the three quality traits [yield after milling (YAM), represented in blue, percentage of head rice recovered (PHR) in red, and percentage of chalky grain (GC) in green] in the *tropical japonica* (n = 311) subpopulation showing significant marker–trait associations in the same region on chromosome 6. Linkage disequilibrium (LD) plot within the region showing the LD among the quantitative trait locus (QTL) region and the *OsBEI* gene is shown below the Manhattan plots. The number within the LD block is the average r^2 among all pairwise marker combinations within the window. (b) Predominant haplotypes, with the percentage of individuals carrying each haplotype. Haplotypes are defined by all significant single nucleotide polymorphisms (SNPs) for each trait within the QTL region and SNPs within and flanking the *OsBEI* gene. Each SNP allele is represented with a different color: orange or blue. At the right of each haplotype, a dot-plot showing the adjusted phenotypic means and SE for lines carrying each haplotype is shown.

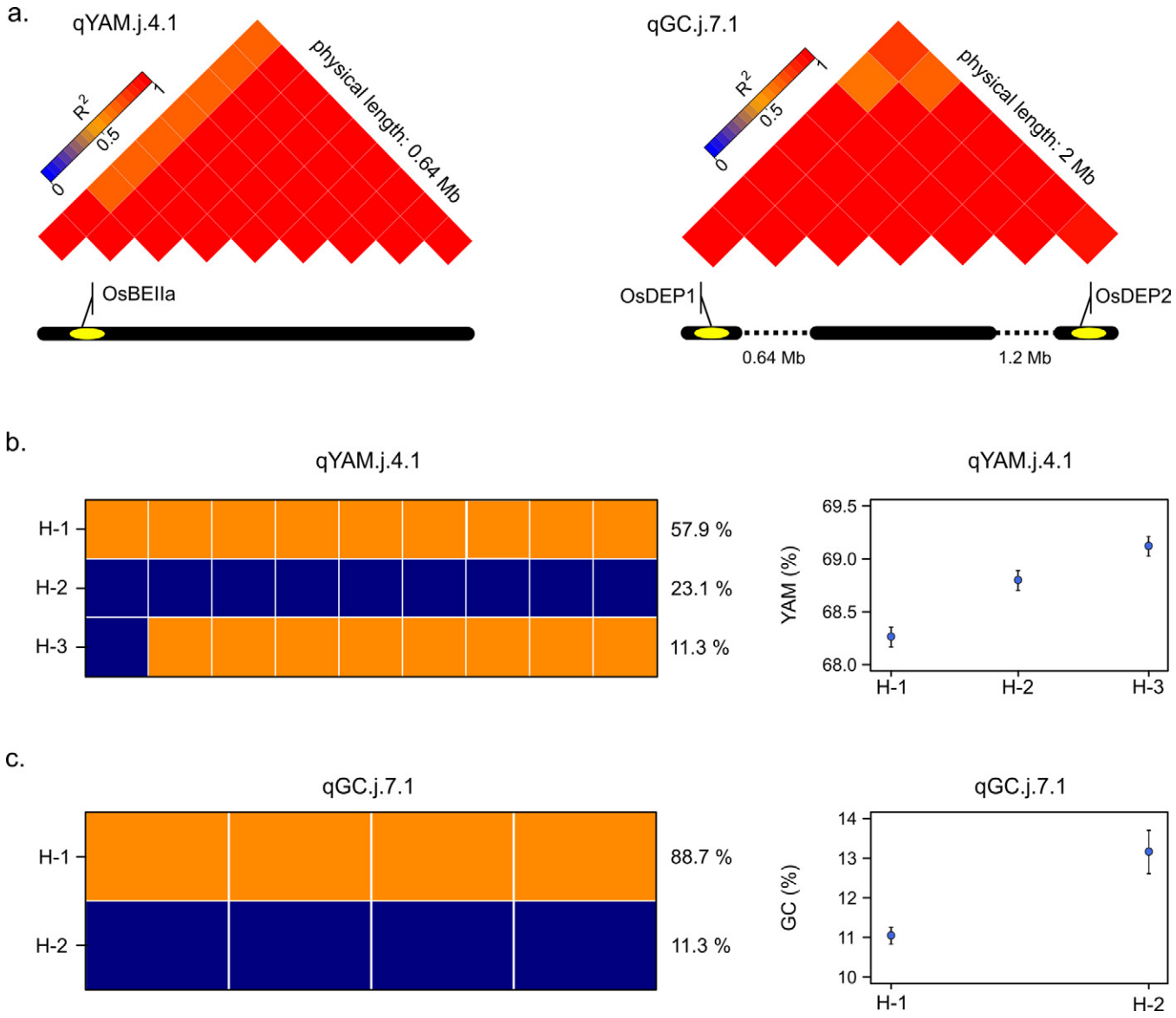

Figure 4. Genome-wide association study (GWAS) in the *tropical japonica* subpopulation in relation to starch synthesis-related genes (SSRGs). (a) Linkage disequilibrium (LD) plot across the qYAM.j.4.1 quantitative trait locus (QTL) showing the LD within the QTL region and single nucleotide polymorphisms (SNPs) located within the SSRG *OsBEIIa* (left) and the LD plot across the QTL qGC.j.7.1 showing the LD among the QTL region and SNPs located within the SSRG genes *DPEI* and *DPEII* (right). Predominant haplotypes with the percentage of individuals carrying each haplotype are shown for (b) qYAM.j.4.1 and (c) qGC.j.7.1. Haplotypes are defined by all significant SNPs within the QTL region. Each SNP allele is represented with a different color: orange or blue. At the right of each haplotype scheme, a dot-plot showing the adjusted phenotypic means and SE for lines carrying each of the haplotypes is shown.

the ascertainment bias that is inherent to the use of fixed genotyping arrays (Heslot et al., 2013). Combined with our analytical strategy that involved a combination of GWAS, LD determination, haplotype identification, and candidate gene identification, this provided good candidate QTL for marker-assisted selection strategies. With the high quality of genome annotation available for rice (National Agriculture and Food Research Organization, 2017), there are several studies that have successfully integrated genetic, genomic (Fitzgerald et al., 2009; Tian et al., 2009) and, in some cases, metabolomic (Heuberger et al., 2010; Yamakawa and Hakata, 2010; Calingacion et al., 2012; Chen et al., 2014; Okazaki and Saito, 2016) information to begin to define the molecular mechanisms underlying important grain quality traits such as grain chalkiness and milling properties. In this study, we identified genes involved in two cellular processes, starch metabolism and cell wall formation or degradation. Many previous studies have related starch content to rice grain quality traits (Su, 2000; Vandeputte and Delcour, 2004; Ashida et al., 2009; Bao, 2014; Lin et al., 2014; Zhao et al., 2015; Zeng et al., 2017), particularly with GC (Ashida et al., 2009) and PHR (Gallant et al., 1997; Patindol and Jabe-Wang, 2003; Yamakawa and Hakata, 2010). Here, we identified five SSRGs and four candidate genes involved in starch metabolism that were physically colocated with our QTL. Once these genotype–phenotype associations are validated, the SNPs will provide breeders

with a valuable tool for early generation selection for several economically valuable grain quality traits, similar to the use of the *waxy* SNP markers currently used for amylose content selection in rice (Kharabian-Masouleh et al., 2012).

In addition to starch content, rice grain quality has been associated with the polysaccharide composition of the cell wall in different grain tissues, such as the starchy endosperm, the aleurone layer, and the transfer cells (Burton and Fincher, 2014; Lin et al., 2014), all affecting grain consistency. The milling process removes the cell walls in the aleurone layer and therefore aleurone cell walls are associated with YAM performance (Burton and Fincher, 2014). In this study, we identified putative QTL with regions coding for three glycosyl hydrolase genes that are involved in heteroxylan backbound formation, modifications, and degradation (Strohmeier et al., 2004; Numan and Bhosle, 2006; Mitchell et al., 2007; Eklöf and Brumer, 2010) and an arabinofuranosidase gene. Arabinofuranose is one of the constituents of hemicellulose, the major component of the rice wall endosperm (Shibuya and Iwasaki, 1978; Shibuya and Nakane, 1984; Numan and Bhosle, 2006).

The candidate genes colocated with putative QTL identified in this work, especially the SSRGs, provide interesting targets for follow-up studies to enhance our understanding of the genetics of grain quality in rice. On the other hand, the results of this study can also improve the accuracy of the genomic selection models used to estimate breeding values and help implement a pragmatic genomic selection strategy in breeding programs.

CONCLUSIONS

In this work, we were able to find putative QTL associated with rice grain quality. The use of locally adapted germplasm with narrow genetic variance provided an opportunity to map subtle phenotypic differences that are likely to be overlooked with a more diverse germplasm panel. From the breeding perspective, the haplotypes provide an opportunity to examine whether substitution of alleles across one particular region of the QTL contributes positively or negatively to the mean performance of each trait. In addition, the use of a locally adapted population of elite breeding materials allows for immediate application in breeding programs, including marker-assisted introgression of favorable genomic regions conferring rice quality traits or targeted genome editing as the basis for future genetics experiments and breeding applications.

Supplemental Information

Supplemental File S1. Phenotypic means for YAM, PHR, and GC of each *indica* and *tropical japonica* rice lines. This is a table of adjusted phenotypic means for each line after experimental design and spatial corrections were performed.

Supplemental File S2. Quantile–quantile (QQ) plots for the GWAS model comparison. Three GWAS models were compared via QQ-plots of observed and expected *p*-values: naive, kinship, and eigen.

Supplemental File S3. Linkage disequilibrium decay for all chromosomes in the *indica* subpopulation.

Supplemental File S4. Linkage disequilibrium decay for all chromosomes in the *tropical japonica* subpopulation.

Supplemental File S5. Analytical framework for QTL and candidate gene identification. This is a description of the analytical procedure followed in this study from genotyping-by-sequencing and phenotypic data to the identification of QTL, haplotypes, and candidate genes.

Supplemental File S6. Annotated genes within QTL regions. This is a list of all genes retrieved from the Michigan State University public gene annotation database with an in-house script.

Supplemental File S7. Significant SNPs and QTL identified in *indica* subpopulation. *P*-values and chromosomal localization for all significant SNPs within QTL for YAM, PHR, and GC are shown. The QTL nomenclature specifies the trait, the subpopulation *indica*, the chromosome, and a correlative number.

Supplemental File S8. Significant SNPs and QTL identified in the *tropical japonica* subpopulation. *P*-values and chromosomal localization for all significant SNPs within QTL for YAM, PHR, and GC are shown. The QTL nomenclature specifies the trait, the subpopulation *japonica*, the chromosome, and a correlative number.

Supplemental File S9. Candidate genes involved in starch metabolism and cell wall formation found within or close to QTL identified through GWAS.

Supplemental File S10. Linkage disequilibrium and haplotype analysis for QTL in relation to SSRGs. For all QTL located near a SSRG, the possible LD between the QTL and SNP within or next to the genes was determined. The LD is expressed as the recombination rate. The haplotypes for the QTL genomic region and the phenotypic mean of lines carrying each haplotype in the mapping population are also shown.

Supplemental File S11. Summary of genotyping-by-sequencing (GBS) results, showing the total number of markers after each filter in the GBS pipeline was applied.

Conflict of Interest Disclosure

The authors declare that there is no conflict of interest.

ACKNOWLEDGMENTS

This work was funded by INIA (Project L2 AZ_12), Agencia Nacional de Investigación Agropecuaria (ANII-POS_NAC_2012_1_8560), and a Fulbright Fellowship and Beachell-Bourlag International PhD Scholarship to EM. We acknowledge Gonzalo Zorrilla, Marco Dalla Rizza, and Omar Borsani for their continuous support for this work. We thank the molecular biology laboratory group and the field team of INIA. We also thank the anonymous reviewers for their comments that substantially improved the manuscript.

REFERENCES

Alexander, D.H., J. Novembre, and K. Lange. 2009. Fast model-based estimation of ancestry in unrelated individuals. Genome Res. 19:1655–1664. doi:10.1101/gr.094052.109

Ashida, K., S. Lida, and T. Yasui. 2009. Morphological, physical, and chemical properties of grain and flour from chalky rice mutants. Cereal Chem. 86:225–231. doi:10.1094/CCHEM-86-2-0225

Bao, J. 2014. Genes and QTLs for rice grain quality improvement. In: J. Bao, editor, Rice—Germplasm, genetics and improvement. InTech, London, UK. p. 239–278.

Bates, D., M. Maechler, B. Bolker, and S. Walker. 2015. Fitting linear mixedeffects models using lme4. J. Stat. Softw. 67:1–48. doi:10.18637/jss.v067.i01

Begum, H., J.E. Spindel, A. Lalusin, T. Borromeo, G. Gregorio, J. Hernandez, et al. 2015. Genome-wide association mapping for yield and other agronomic traits in an elite breeding population of tropical rice (*Oryza sativa*). PLoS One 10(3):e0119873. doi:10.1371/journal.pone.0119873

Blanco, P., F. Molina, F. Pérez de Vida, S. Avila, A. Lavecchia, C. Marchesi, et al. 2004. INIA Olimar: Characterization and performance in season 2003–2004. (In Spanish) Arroz 38:40–48.

Blanco, P., F. Pérez de Vida, and M. Piriz. 1993. INIA Tacuarí: New early and high yielding rice variety. (In Spanish) Bol. Divulg. INIA 31:5–10.

Brachi, B., G.P. Morris, and J. Borevitz. 2011. Genome-wide association studies in plants: The missing heritability is in the field. Genome Biol. 12:232. doi:10.1186/gb-2011-12-10-232

Bradbury, P.J., Z. Zhang, D.E. Kroon, T.M. Casstevens, Y. Ramdoss, and E.S. Buckler. 2007. TASSEL: Software for association mapping of complex traits in diverse samples. Bioinformatics 23:2633–2635. doi:10.1093/bioinformatics/btm308

Brandariz, S.P., A. González Reymúndez, B. Lado, M. Malosetti, A.A.F. Garcia, M. Quincke, et al. 2016. Ascertainment bias from imputation methods evaluation in wheat. BMC Genomics 17(1):773. doi:10.1186/s12864-016-3120-5

Burton, R.A., and G.B. Fincher. 2014. Evolution and development of cell walls in cereal grains. Front. Plant Sci. 5:456–470. doi:10.3389/fpls.2014.00456

Calingacion, M.N., C. Boualaphanh, V.D. Daygon, R. Anacleto, R. Sackville, R.S. Hamilton, et al. 2012. A genomics and multi-platform metabolomics approach to identify new traits of rice quality in traditional and improved varieties. Metabolomics 8:771–783. doi:10.1007/s11306-011-0374-4

Chen, W., Y. Gao, W. Xie, L. Gong, K. Lu, W. Wang, et al. 2014. Genome-wide association analyses provide genetic and biochemical insights into natural variation in rice metabolism. Nat. Genet. 46:714–721. doi:10.1038/ng.3007

Eklöf, J.M., and H. Brumer. 2010. The *XTH* gene family: An update on enzyme structure, function, and phylogeny in xyloglucan remodeling. Plant Physiol. 153:456–466. doi:10.1104/pp.110.156844

Elshire, R.J., J.C. Glaubitz, Q. Sun, J.A. Poland, K. Kawamoto, E.S. Buckler, et al. 2011. A robust, simple genotyping-by-sequencing (GBS) approach for high diversity species. PLoS One 6:e19379. doi:10.1371/journal.pone.0019379

Endelman, J.B. 2011. Ridge regression and other kernels for genomic selection with R package rrBLUP. Plant Genome 4:250–255. doi:10.3835/plantgenome2011.08.0024

Famoso, A., K. Zhao, R.T. Clark, C.W. Tung, M.H. Wright, C. Bustamante, et al. 2011. Genetic architecture of aluminum tolerance in rice (*Oryza sativa*) determined through genome-wide association analysis and QTL mapping. PLoS Genet. 7(8):e1002221. doi:10.1371/journal.pgen.1002221

Fitzgerald, M.A., S.R. McCouch, and R.D. Hall. 2009. Not just a grain of rice: The quest for quality. Trends Plant Sci. 14:133–139. doi:10.1016/j.tplants.2008.12.004

Food and Agriculture Organization of the United Nations. 2009. Increasing crop production sustainably. The perspective of biological processes. Food and Agricultural Organization of the United Nations. http://www.fao.org/docrep/012/i1235e/i1235e00.htm (accessed 5 June 2018).

Gallant, D.J., B. Bouchet, and P.M. Baldwin. 1997. Microscopy of starch: Evidence of a new level of granule organization. Carbohydr. Polym. 32:177–191. doi:10.1016/S0144-8617(97)00008-8

Glaubitz, J.C., T.M. Casstevens, F. Lu, J. Harriman, R.J. Elshire, Q. Sun, et al. 2014. TASSEL-GBS: A high capacity genotyping by sequencing analysis pipeline. PLoS One 9(2):E90346 doi:10.1371/journal.pone.0090346

Godfray, C.H., J.R. Beddington, I.R. Crute, L. Haddad, D. Lawrence, J.F. Muir, et al. 2010. Food security: The challenge of feeding 9 billion people. Science 327:812–818. doi:10.1126/science.1185383

Gore, M.A., J.M. Chia, R.J. Elshire, Q. Sun, E.S. Ersoz, B.L. Hurwitz, et al. 2009. A first-generation haplotype map of maize. Science 326:1115–1117. doi:10.1126/science.1177837

Gutiérrez, L., S. Germán, S. Pereyra, P.M. Hayes, C.A. Pérez, F. Capettini, et al. 2015. Multi-environment multi-QTL association mapping identifies disease resistance QTL in barley germplasm from Latin America. Theor. Appl. Genet. 128:501–516.

Gutierrez, L., G. Quero, S. Fernandez, and S. Brandariz. 2016. lmem.gwaser: Linear mixed effects models for genome-wide association studies. R package version 0.1.0. https://CRAN.R-project.org/package=lmem.gwaser (accessed 17 Jan. 2017).

Heslot, N., J. Rutkoski, J. Poland, J.L. Jannink, and M.E. Sorrells. 2013. Impact of marker ascertainment bias on genomic selection accuracy and estimates of genetic diversity. PLoS One 8:e74612. doi:10.1371/journal.pone.0074612

Heuberger, A.L., M.R. Lewis, M.H. Chen, M.A. Brick, E.L. Leach, and E.P. Ryan. 2010. Metabolomic and functional genomic analyses reveal varietal differences in bioactive compounds of cooked rice. PLoS One 5:e12915. doi:10.1371/journal.pone.0012915

Hsiaoping, C. 2005. Rice is life: Scientific perspectives for the 21st century. In: K. Toriyama, K.L. Heong, and B. Hardy, editors, Proceedings of the World Rice Research Conference, Tokyo and Tsukuba, Japan. 4–7 Nov. 2004. IRRI, Philippines. p. 497–499.

Huang, X., X. Wei, T. Sang, Q. Zhao, Q. Feng, Y. Zhao, et al. 2010. Genome-wide association studies of 14 agronomic traits in rice landraces. Nat. Genet. 42:961–967. doi:10.1038/ng.695

Huang, X., Y. Zhao, X. Wei, C. Li, A. Wang, Q. Zhao, et al. 2012. Genome-wide association study of flowering time and grain yield traits in a worldwide collection of rice germplasm. Nat. Genet. 44:32–39. doi:10.1038/ng.1018

Instituto Nacional de Semillas. 2017. Registro nacional de cultivares y registro de propiedad de cultivares. Instituto Nacional de Semillas. http://www.inase.uy/EvaluacionRegistro/ (accessed 14 June 2018).

Jannink, J.L., M. Bink, and R. Jansen. 2001. Using complex plant pedigrees to map valuable genes. Trends Plant Sci. 6:337–342. doi:10.1016/S1360-1385(01)02017-9

Kanehisa, M., and S. Goto. 2000. KEGG: Kyoto Encyclopedia of Genes and Genomes. Nucleic Acids Res. 28:27–30. doi:10.1093/nar/28.1.27

Kharabian-Masouleh, A., D. Waters, R. Reinke, R. Ward, and R. Henry. 2012. SNP in starch biosynthesis genes associated with nutritional and functional properties of rice. Sci. Rep. 2:557–566. doi:10.1038/srep00557

Kraakman, A., R. Niks, P. Van den Berg, P. Stam, and F.A. Van Eeuwijk. 2004. Linkage disequilibrium mapping of yield and yield stability in modern spring barley cultivars. Genetics 168:435–446. doi:10.1534/genetics.104.026831

Kump, K.L., P.J. Bradbury, R.J. Wisser, E.S. Buckler, A.R. Belcher, and M.A. Oropeza-Rosas. 2011. Genome-wide association study of quantitative resistance to southern leaf blight in the maize nested association mapping population. Nat. Genet. 43:163–168. doi:10.1038/ng.747

Langmead, B., and S.L. Salzberg. 2012. Fast gapped-read alignment with Bowtie 2. Nat. Methods 9:357–359. doi:10.1038/nmeth.1923

Langridge, P., E.S. Lagudah, T.A. Holton, R. Appels, P.J. Sharp, and K.J. Chalmers. 2001. Trends in genetic and genome analyses in wheat: A review. Crop Pasture Sci. 52:1043–1077. doi:10.1071/AR01082

Lenth, R.V. 2018. Least-squares means: The R package lsmeans. J. Stat. Softw. 69:1–33. doi:10.18637/jss.v069.i01

Li, J., and L. Ji. 2005. Adjusting multiple testing in multilocus analyses using the eigenvalues of a correlation matrix. Heredity 95:221–227. doi:10.1038/sj.hdy.6800717

Lin, Z., X. Zhang, X. Yang, G. Li, S. Tang, S. Wang, et al. 2014. Proteomic analysis of proteins related to rice grain chalkiness using iTRAQ and a novel comparison system based on a notched-belly mutant with white-belly. BMC Plant Biol. 14:163–179. doi:10.1186/1471-2229-14-163

Lisle, A., M. Martin, and M. Fitzgerald. 2000. Chalky and translucent rice grains differ in starch composition and structure and cooking properties. Cereal Chem. 77:627–632. doi:10.1094/CCHEM.2000.77.5.627

Lu, Y., and T. Sharkey. 2004. The role of amylomaltase in maltose metabolism in the cytosol of photosynthetic cells. Planta. 218:466–473. doi:10.1007/s00425-003-1127-z

Mace, E.S., C.H. Hunt, and D.R. Jordan. 2013. Supermodels: Sorghum and maize provide mutual insight into the genetics of flowering time. Theor. Appl. Genet. 126:1377–1395. doi:10.1007/s00122-013-2059-z

Malosetti, M., D. Bustos-Korts, M.P. Boer, and F.A. van Eeuwijk. 2016. Predicting responses in multiple environments: Issues in relation to genotype× environment interactions. Crop Sci. 56(5):2210–2222. doi:10.2135/cropsci2015.05.0311

Malosetti, M., C. Van der Linden, B. Vosman, and F.A. Van Eeuwijk. 2007. A mixed-model approach to association mapping using pedigree information with an illustration of resistance to *Phytophthora infestans* in potato. Genetics 175:879–889. doi:10.1534/genetics.105.054932

Malosetti, M., J. Voltas, I. Romagosa, S.E. Ullrich, and F.A. Van Eeuwijk. 2004. Mixed models including environmental covariables for studying QTL by environment interaction. Euphytica 137:139–145. doi:10.1023/B:EUPH.0000040511.46388.ef

Mathews, K.L., M. Malosetti, S. Chapman, L. McIntyre, M. Reynolds, R. Shorter, et al. 2008. Multi-environment QTL mixed models for drought stress adaptation in wheat. Theor. Appl. Genet. 117(7):1077–1091. doi:10.1007/s00122-008-0846-8

Maurer, A., V. Draba, Y. Jiang, F. Schnaithmann, R. Sharma, E. Schumann, et al. 2015. Modeling the genetic architecture of flowering time in barley through nested association mapping. BMC Genomics 16:290. doi:10.1186/s12864-015-1459-7

McCouch, S.R., M.H. Wright, C.W. Tung, L.G. Maron, K.L. McNally, M. Fitzgerald, et al. 2016. Open access resources for genome wide association mapping in rice. Nat. Commun. 7:11346. doi:10.1038/ncomms11346

Mitchell, R., P. Dupree, and P. Shewry. 2007. A novel bioinformatics approach identifies candidate genes for the synthesis and feruloylation of arabinoxylan. Plant Physiol. 144:43–53. doi:10.1104/pp.106.094995

Mohanty, S. 2013. Rice facts. Trends in global rice consumption. Rice Today 12: 44–45.

Numan, M., and N. Bhosle. 2006. Alpha-*l*-arabinofuranosidases: The potential applications in biotechnology. J. Ind. Microbiol. Biotechnol. 33:247–260. doi:10.1007/s10295-005-0072-1

Ohdan, T., P.B. Francisco, T. Sawada, T. Hirose, T. Terao, H. Satoh, et al. 2005. Expression profiling of genes involved in starch synthesis in sink and source organs of rice. J. Exp. Bot. 56:3229–3244. doi:10.1093/jxb/eri292

Okazaki, Y., and K. Saito. 2016. Integrated metabolomics and phytochemical genomics approaches for studies on rice. Gigascience 5:11. doi:10.1186/s13742-016-0116-7

Parisseaux, B., and R. Bernardo. 2004. In silico mapping of quantitative trait loci in maize. Theor. Appl. Genet. 109:508–514. doi:10.1007/s00122-004-1666-0

Patindol, J., and Y. Jabe-Wang. 2003. Fine structures and physicochemical properties of starches from chalky and translucent rice kernels. J. Agric. Food Chem. 51:2777–2784. doi:10.1021/jf026101t

Price, A.L., N.J. Patterson, R.M. Plenge, M.E. Weinblatt, N.A. Shadick, and D. Reich. 2006. Principal components analysis corrects for stratification in genome-wide association studies. Nat. Genet. 38:904–909. doi:10.1038/ng1847

Quero, G., S. Simondi, V. Bonnecarrere, and L. Gutierrez. 2017. Clusterhap: Clustering genotypes in haplotypes. R package version 0.1.0. The R Foundation. https://CRAN.R-project.org/package=clusterhap (accessed 5 June 2018).

R Core Team. 2017. R: A language and environment for statistical computing. The R Foundation. https://www.R-project.org (accessed 5 June 2018).

Rosas, J.E., S. Martínez, P. Blanco, F. Pérez de Vida, V. Bonnecarrere, G. Mosquera, et al. 2017. Resistance to multiple temperate and tropical stem and sheath diseases of rice. Plant Genome 11:170029. doi:10.3835/plantgenome2017.03.0029

Schweder, T., and E. Spjotvoll. 1982. Plots of *P*-values to evaluate many tests simultaneously. Biometrika 69:493–502. doi:10.1093/biomet/69.3.493

Shibuya, N., and R. Nakane. 1984. Pectic polysaccharides of rice *Oryza sativa* cultivar norin-29 endosperm cell walls. Phytochemistry 23:1425–1429. doi:10.1016/S0031-9422(00)80479-3

Shibuya, N., and T. Iwasaki. 1978. Polysaccharides and glycoproteins in rice endosperm cell-wall. Agric. Biol. Chem. 42:2259–2266. doi: 10.1271/bbb1961.42.2259

Spindel, J., H. Begum, D. Akdemir, P. Virk, B. Collard, E. Redoña, et al. 2015. Genomic selection and association mapping in rice *(Oryza sativa)*: Effect of trait genetic architecture, training population composition, marker number and statistical model on accuracy of rice genomic selection in elite, tropical rice breeding lines. PLoS Genet. 11(2):e1004982. doi:10.1371/journal.pgen.1004982

Strohmeier, M., M. Hrmova, M. Fischer, A.J. Harvey, G.B. Fincher, and J. Pleiss. 2004. Molecular modeling of family GH16 glycoside hydrolases: Potential roles for xyloglucan transglucosylases/hydrolases in cell wall modification in the *Poaceae*. Protein Sci. 13:3200–3213. doi:10.1110/ps.04828404

Su, J. 2000. Starch synthesis and grain filling in rice. In: K. Gupta and N. Kaur, editors, Carbohydrate reserves in plants—Synthesis and regulation. Developments in Crop Sci. 26. Elsevier, Amsterdam. p. 107–124.

Swarts, K., H. Li, J.A. Romero Navarro, D. An, M.C. Romay, S. Hearne, et al. 2014. Novel methods to optimize genotypic imputation for low-coverage, next-generation sequence data in crop plants. Plant Genome 7:1–12. doi:10.3835/plantgenome2014.05.0023

Tamura, K., G. Stecher, D. Peterson, A. Filipski, and S. Kumar. 2013. MEGA6: Molecular evolutionary genetics analysis version 6.0. Mol. Biol. Evol. 30:2725–2729. doi:10.1093/molbev/mst197

National Agriculture and Food Research Organization. 2017. The rice annotation project. National Agriculture and Food Research Organization. http://rapdb.dna.affrc.go.jp (accessed 5 June 2018).

Tian, F., P.J. Bradbury, P.J. Brown, H. Hung, Q. Sun, S. Flint-Garcia, et al. 2011. Genome-wide association study of leaf architecture in the maize nested association mapping population. Nat. Genet. 43:159–162. doi:10.1038/ng.746

Tian, Z., Q. Qian, Q. Liu, M. Yan, X. Liu, and C. Yan, et al. 2009. Allelic diversities in rice starch biosynthesis lead to a diverse array of rice eating and cooking qualities. Proc. Natl. Acad. Sci. 106:21760–21765. doi:10.1073/pnas.0912396106

Vandeputte, G., and J. Delcour. 2004. From sucrose to starch granule to starch physical behaviour: A focus on rice starch. Carbohydr. Polym. 58:245–266. doi:10.1016/j.carbpol.2004.06.003

Yamakawa, H., and M. Hakata. 2010. Atlas of rice grain filling-related metabolism under high temperature: Joint analysis of metabolome and transcriptome demonstrated inhibition of starch accumulation and induction of amino acid accumulation. Plant Cell Physiol. 51:795–809. doi:10.1093/pcp/pcq034

Yan, W., J.N. Rutger, R.J. Bryant, H.E. Bockelman, R.G. Fjellstrom, M.H. Chen, et al. 2007. Development and evaluation of a core subset of the USDA rice germplasm collection. Crop Sci. 47:869–876. doi:10.2135/cropsci2006.07.0444

Yu, J., J. Holland, M. McMullen, and E. Buckler. 2008. Genetic design and statistical power of nested association mapping in maize. Genetics 178:539–551. doi:10.1534/genetics.107.074245

Yu, Y., R.A. Wing, and J. Li. 2013. Grain quality. In: Q. Zhang and R.A. Wing, editors, Genetics and genomics of rice. Springer, New York. p. 237–254.

Zader, A. 2011. Technologies of quality: The role of the Chinese state in guiding the market for rice. EASTS 5:461–477. doi:10.1215/18752160-1458155

Zeng, D., Z. Tian, Y. Rao, G. Dong, Y. Yang, L. Huang, et al. 2017. Rational design of high-yield and superior-quality rice. Nat. Plant. 3:17031. doi:10.1038/nplants.2017.31

Zhang, P., K. Dreher, A. Karthikeyan, A. Chi, A. Pujar, R. Caspi, et al. 2010. Creation of a genome-wide metabolic pathway database for *Populus trichocarpa* using a new approach for reconstruction and curation of metabolic pathways for plants. Plant Physiol. 153:1479–1491. doi:10.1104/pp.110.157396

Zhao, K., C.W. Tung, G.C. Eizenga, M.H. Wright, M.L. Ali, and A.H. Price. 2011. Genome-wide association mapping reveals a rich genetic architecture of complex traits in *Oryza sativa*. Nat. Commun. 2:467. doi:10.1038/ncomms1467

Zhao, X., L. Zhou, K. Ponce, and G. Ye. 2015. The usefulness of known genes/QTLs for grain quality traits in an *indica* population of diverse breeding lines tested using association analysis. Rice (N. Y.) 8:29–41. doi:10.1186/s12284-015-0064-3

Zhou, L., S. Liang, K. Ponce, S. Marundon, G. Ye, and X. Zhao. 2015. Factors affecting head rice and chalkiness in *indica* rice. Field Crops Res. 172:1–10. doi:10.1016/j.fcr.2014.12.004

Zhu, Z., F. Zhang, H. Hu, A. Bakshi, M.R. Robinson, J.E. Powell, et al. 2016. Integration of summary data from GWAS and eQTL studies predicts complex trait gene targets. Nat. Genet. 48:481–487. doi:10.1038/ng.3538

2.1.1 Material suplementario

El material suplementario del artículo precedente se encuentra en el siguiente enlace:https://dl.sciencesocieties.org/publications/tpg/articles/11/3/170076?highlight=&search-result=1

3. CAPÍTULO III: LA PARTICIÓN DE ENERGÍA EN EL PROCESO FOTOSINTÉTICO COMO FACTOR CLAVE DE LA EFICIENCIA DE USO DE RADIACIÓN.

En este trabajo se estudió la eficiencia en el uso de la radiación a nivel de planta, específicamente a nivel del proceso fotoquímico de la fotosíntesis. Para evaluar la EUR a nivel de planta en condiciones controladas es fundamental moderar las características del ambiente lumínico en el cual se desarrollan las plantas. Un ambiente lumínico queda definido por la intensidad de la luz y la calidad espectral de la misma. En este sentido, para obtener los resultados que se muestran en este trabajo, desarrollamos y construimos dos sistemas de iluminación en base LED para poder evaluar la EUR en diferentes ambientes lumínicos. Como se cuenta detalladamente en el artículo, los sistemas diseñados permiten reproducir con bastante aproximación el espectro solar en intensidad y calidad espectral así como sus variaciones a lo largo del día.

A partir de los sistemas antes mencionados se generaron cuatro ambientes lumínicos en los cuales se evaluaron los cuatro cultivares principales de arroz utilizados en el país. Además, en este estudio se identificaron las variables de la fluorescencia de clorofilas que permiten conocer la partición de energía durante el proceso fotoquímico de la fotosíntesis. Se pudo establecer que los parámetros de rendimiento cuántico permiten diferenciar el proceso fotoquímico propiamente dicho de los procesos de disipación del calor. Esto es importante porque permite establecer los niveles de regulación de la fotoinhibición en los diferentes genotipos de arroz. Los parámetros de rendimiento cuántico identificados en este trabajo son los que se utilizaron para fenotipar la población de mapeo caracterizada genéticamente en el artículo anterior.

3.1 LIGHT-USE EFICIENCY AND ENERGY PARTITIONING IN RICE IS CULTIVAR DEPENDENT.

Photosynthesis Research (2019) 140:51–63
https://doi.org/10.1007/s11120-018-0605-x

ORIGINAL ARTICLE

Light-use efficiency and energy partitioning in rice is cultivar dependent

Gastón Quero[1,2] · Victoria Bonnecarrère[2] · Sebastián Fernández[3] · Pedro Silva[1] · Sebastián Simondi[4] · Omar Borsani[1]

Received: 29 August 2018 / Accepted: 12 November 2018 / Published online: 17 November 2018

Abstract

One of the main limitations of rice yield in regions of high productive performance is the light-use efficiency (LUE). LUE can be determined at the whole-plant level or at the photosynthetic apparatus level (quantum yield). Both vary according to the intensity and spectral quality of light. The aim of this study was to analyze the cultivar dependence regarding LUE at the plant level and quantum yield using four rice cultivars and four light environments. To achieve this, two in-house Light Systems were developed: *Light System I* which generates white light environments (spectral quality of 400–700 nm band) and *Light System II* which generates a blue-red light environment (spectral quality of 400–500 nm and 600–700 nm bands). Light environment conditioned the LUE and quantum yield in PSII of all evaluated cultivars. In white environments, LUE decreased when light intensity duplicated, while in blue-red environments no differences on LUE were observed. Energy partition in PSII was determined by the quantum yield of three de-excitation processes using chlorophyll fluorescence parameters. For this purpose, a quenching analysis followed by a relaxation analysis was performed. The damage of PSII was only increased by low levels of energy in white environments, leading to a decrease in photochemical processes due to the closure of the reaction centers. In conclusion, all rice cultivars evaluated in this study were sensible to low levels of radiation, but the response was cultivar dependent. There was not a clear genotypic relation between LUE and quantum yield.

Keywords Energy dissipation · Quenching analyses · Relaxation analyses · Quantum yields

Introduction

Light is a critical environmental factor for plant growth and development (Monteith 1977; Devlin et al. 2007). Light intensity levels or photon flux density (PPFD) and the spectral quality directly affect energy conversion processes in plant cells (Campbell and Norman 1998; Murata et al. 2007;

Electronic supplementary material The online version of this article (https://doi.org/10.1007/s11120-018-0605-x) contains supplementary material, which is available to authorized users.

✉ Victoria Bonnecarrère
vbonnecarrere@inia.org.uy

Gastón Quero
gastonquero@fagro.edu.uy

Sebastián Fernández
sebfer@fing.edu.uy

Pedro Silva
psilvalerena@gmail.com

Sebastián Simondi
sebastian.simondi@uncu.edu.ar

Omar Borsani
oborsani@fagro.edu.uy

[1] Departamento de Biología Vegetal, Facultad de Agronomía, Universidad de la República, Garzón 809, Montevideo, Uruguay

[2] Instituto Nacional de Investigación Agropecuaria (INIA), Unidad de Biotecnología. Estación Experimental Wilson Ferreira Aldunate, Ruta 48, Km 10, Rincón del Colorado, 90200 Canelones, Uruguay

[3] Instituto de Ingeniería Eléctrica, Facultad de Ingeniería, Universidad de la República, Julio Herrera y Reissig 565, Montevideo, Uruguay

[4] Area de Matemática, Facultad de Ciencias Exactas y Naturales, Universidad Nacional de Cuyo (FCEN-UNCuyo), Padre Contreras 1300, Mendoza, Argentina

Nobel 2009). A widely accepted model states that the production of biomass is determined by the PPFD intercepted by the plant and by the conversion efficiency of radiation to carbohydrates during photosynthesis (Monteith 1972, 1977; Brestic et al. 2018). In plant physiology, the conversion efficiency of light energy to biomass production is known as light-use efficiency (LUE) (Medlyn 1998). At plant level, LUE can be estimated as the ratio between daily biomass and incident radiation (Monteith 1972, 1977; Sinclair and Horie 1989; Mitchell et al. 1998; Sinclair and Muchow 1999), whereas at the photosynthesis-apparatus level, LUE is known as quantum yield (Φ) or quantum efficiency (Skillman 2008; Gitelson and Gamon 2015).

In the photochemical stage of photosynthesis, quantum yield can be studied from the fluorescence emission of chlorophylls in photosystem II (PSII) (Genty et al. 1989; Baker 2008; Klughammer and Schreiber 2008; Lazár 2015). Chlorophyll emission can be determined using the pulse amplitude modulation (PAM) technique (Kalaji et al. 2014, 2017; Goltsev et al. 2016). PAM technique measures energy decay during the de-excitation of PSII chlorophylls, both in darkness and light (Baker 2008). Therefore, the methodology of saturating pulse can be used to estimate the quantum yield of PSII in a light-adapted leaf (quenching analysis) or during the PSII relaxation process that occurs in darkness after a period of light (relaxation analysis) (Krause and Jahns 2003; Ahn et al. 2009; Kasajima et al. 2009). The strategy of combining the quenching analysis with a subsequent relaxation analysis allows the energy that reaches PSII to be decomposed in five components.

The quenching analysis determines the quantum yields of PSII (Φ_{PSII}), non-photochemical quenching (Φ_{NPQ}) and basal energy dissipation (Φ_{NO}). The Φ_{PSII} is directly related to the rate of electron transfer in the PSII towards biochemical processes; Φ_{NPQ} reflects the quantum yield of regulatory light-induced non-photochemical quenching; and Φ_{NO} reflects the quantum yield of constitutive non-regulatory (basal or dark) non-photochemical dissipation processes (Genty et al. 1989; Kramer et al. 2004; Hendrickson et al. 2005; Klughammer and Schreiber 2008; Chen et al. 2012; Brestic et al. 2016). On the other hand, the relaxation analysis allows the Φ_{NPQ} parameter to be the decomposed in quantum yield of fast-relaxing non-photochemical quenching ($\Phi_{NPQfast}$) and quantum yield of slow-relaxing non-photochemical quenching ($\Phi_{NPQslow}$) (Kasajima et al. 2009). $\Phi_{NPQfast}$ is related to the regulated energy dissipation in PSII, whereas $\Phi_{NPQslow}$ is related to PSII damage caused by photoinhibition (Ahn et al. 2009; Kasajima et al. 2009).

Quantum yield determination enables the visualization of the energy partition in each stage of the photosynthesis. The structural stability of photosystems (PSs) has a direct effect on the quantum yield (Dall'Osto et al. 2015). If the energy absorbed surpasses the transfer capability of the PSs, photoinhibition processes may occur in both photosystem II (PSII) and photosystem I (PSI) (Klimov et al. 1990; Allakhverdiev et al. 2003; Müh et al. 2012; Derks et al. 2015). Photoinhibition processes are proportional to light intensity (Allakhverdiev and Murata 2004; Hakala et al. 2005; Murata et al. 2012; Campbell and Tyystjärvi 2012), to the inactivation and repair rate of PSs (Allakhverdiev et al. 2005, 2007; Murata et al. 2007), to the size and heterogeneity of PSII (Mehta et al. 2010), to the cyclic flow of electrons through PSI (Nishiyama et al. 2011; Murata and Nishiyama 2017), and to the PSII–PSI relation (Tikkanen and Aro 2012; Brestic et al. 2016; Tikkanen et al. 2014).

The energy partition analysis is important because it reveals the destination of the incident energy and allows us to differentiate photochemical and dissipation processes from photoinhibition processes (Zivcak et al. 2015, 2018). An interesting aspect of the study of energy partitioning by quantifying the quantum yield is that the sum of the returns is equal to 1 (Demmig-Adams et al. 1996; Kramer et al. 2004; Hendrickson et al. 2005). Therefore, each return represents a fraction of the light energy use in each process and their values can be directly compared. The energy partitioning analysis is complemented by the quantification of maximum quantum yield in light (Φ_{Po}) and darkness ($\Phi_{PSIIpot}$) and by the determination of the proportion of open reaction center in PSII (qL). Φ_{Po} and $\Phi_{PSIIpot}$ describe the stability and maximum capacity of PSII, respectively, while qL helps to understand the causes of differences in the quantum yield (Kramer et al. 2004; Kasajima et al. 2009; Lazár 2015).

Different light environments generate changes in photosynthesis due to differential responses of pigments to the wavelength spectrum. In addition, these different environments affect the photosystems' balance (Hogewoning et al. 2012) by modifying the quantum yield (Walters and Horton 1995) and LUE at plant and photosynthesis-apparatus levels (Evans 1987, 1996; Murchie and Horton 1998; Sinclair and Muchow 1999; Wagner et al. 2008; Terashima et al. 2009; Yamazaki 2010, Su et al. 2014; Ware et al. 2015). Establishing light intensity treatments is relatively simple since it is achieved by reducing irradiance through meshes of variable density (Murchie et al. 2002). However, specific spectral-quality treatments require working under fine controlled conditions. In that regard, artificial light-emitting diode (LED) systems allow different spectral combinations or light environments with variable light intensities. Thereby, the use of LEDs allows us to study the effects of the light-regime components on energy conversion processes (Nelson et al. 2005; Morrow 2008; Nelson and Bugbee 2014, 2015; Kozai 2013; Kozai et al. 2016).

Rice (*Oryza sativa* L.) is the main food source for nearly half the world's population, and its demand for 2050 is expected to increase by nearly 30% over the production levels of 2005–2007 (Alexandratos and Bruinsma 2012).

One of the main limitations of rice yield in regions of high productive performance is the LUE. The genetic diversity of rice is high, and selective breeding for LUE to improve its yield potential is very important (Yin and Struik 2017) and has been achieved by different authors (Murchie et al. 1999; Horton 2000; Zhu et al. 2008; Long et al. 2006; Hubbart et al. 2007; Liu and Sun 2013). Several works show the effect of the light environment on LUE and the acclimatization of the photosynthetic response of rice (Murchie and Horton 1997, 1998; Murchie et al. 2002; Yamazaki et al. 1999; Yamazaki 2010). However, studies relating the effect of light quality on LUE or photosynthesis are scarce (Matsuda et al. 2004, 2008; Yamazaki 2010). On the other hand, works focused on the effect of light quality generally do not reach adequate levels of irradiance (Wang et al. 2009; Berkovich et al. 2017).

The aim of this study was to analyze the cultivar dependence regarding LUE at whole-plant and photosynthetic apparatus levels in rice. In order to measure LUE at the photosynthetic apparatus level, energy partitioning was determined through the photochemical and non-photochemical quantum yield. The strategy used to analyze LUE in rice cultivars was the comparison of four rice cultivars in four light environments, differing on light quality and quantity. Rice cultivars were selected considering differences in subspecies, crop cycle, and average yield. In addition, we had to develop two in-house light systems to generate the light environments.

Materials and methods

Plant materials, growth conditions, and experimental design

Two cultivars of *O. sativa indica* subspecies (El Paso 144 and INIA Olimar) and two cultivars of *O. sativa tropical japonica* subspecies (INIA Parao and INIA Tacuarí), supplied by INIA's Rice Breeding Program, were grown in a custom-built growth room. They were maintained at 25 °C, 50–60% RH, and a 12/12-h dark/light cycle. Seeds were pre-germinated and selected by their uniformity in seedling development. One seedling was transferred to an individual cylinder pot of 850 mL. Growing shelves had a surface area of 0.5 m^2 (0.5 m × 1 m) and pots were 0.06 m in diameter × 0.45 m high, arranged with 0.1 m of separation between the centers of each pot (Supplementary Fig. S1).

Plants were grown in sand:vermiculite (1:1) and watered with Yoshida medium (Yoshida et al. 1976) every 3 days. Each pot represented one replication. There were three replications per treatment. A completely random design was applied for each assay. Analyses were performed on the newest expanded leaf in V5 stage (Counce et al. 2000). According to the author, this stage is defined as collar formation on leaf five of the main stem. Pots were arranged in such a way as to minimize the superposition of leaves in order to achieve a uniform incidence of light (Supplementary Fig. S1).

To measure LUE at the whole-plant level, the entire aerial part (five leaves) was harvested at the end of the growth period. All cultivars showed the same phenological state during the evaluated growth period.

Light treatments: photon flux density and spectral quality

To establish different light treatments, two light systems were built based on LED source lamps. These systems can control the quantity and quality of light. One of the systems (*Light System I*) was designed using white and blue LED lights which permit a radiation emission covering the entire PAR spectral range from 400 to 700 nm. The second light system (*Light System II*) was built using seven single-color LED light lamps. This system allowed us to decompose the spectrum in seven bands ranging from 400 to 700 nm. In this study, we only used bands of 400 and 700 nm. For both systems, the quantification of light-radiation intensities was established on the 400–700 nm range. For this purpose, the PAR spectral ranges were divided in three bands of 100 nm each (400–500 nm, 500–600 nm, and 600–700 nm).

The photoperiod described in materials and methods consisted of 12 h of light with an increment of the radiation in the first 6 h and a decrease in the radiation in the following 6 h. The levels and kinetics of radiation increase and decrease were set using as reference the measured levels of a sunny day of October in the geographical region of rice cultivation in Uruguay (33°13′51″S 54°22′56″W).

The spectrum and intensity of different light treatments were measured using a spectroradiometer (USB2000 + spectrometer, Ocean Optics, Duiven, The Netherlands) which was calibrated against a standard light source supplied by the equipment. The sensor of spectroradiometer was located where the closer leaf was, at 30 cm from the center of the light source. The mobility of the lighting systems allowed us to keep this distance during the entire plant-growth period. Spectroradiometer measures were registered as power by unit of area (μW nm^{-1} cm^{-2}). However, since LUE was measured as energy received by unit of area in a time interval (MJ m^{-2} d^{-1}), the spectroradiometer measurements in μW nm^{-1} cm^{-2} were converted to MJ m^{-2} d^{-1} as described in Supplementary Fig. S2.

On the other hand, for the determination of PPFD, the spectroradiometer measures in μW nm^{-1} cm^{-2} were converted to μmol m^{-2} s^{-1} as described in Supplementary Fig. S2.

Light-use efficiency measurements

Light-use efficiency was calculated as a ratio of the difference in the biomass of leaves between two consecutive harvests (B) divided by the total PAR incident irradiance (PAR_{inc}) in the respective period (Gitelson and Gamon 2015):

$$LUE = B/PAR_{inc},$$

where LUE is measured in g MJ^{-1}, B is the difference of dry weight at final harvest and initial harvest expressed in g m^{-2}, and PAR_{inc} is the incident radiation during all growth period (MJ m^{-2}).

Energy partitioning: quenching and relaxation analyses

The quantification of energy partition in PSII was determined by the quantum yield of three de-excitation processes using the chlorophyll's fluorescence parameters. A quenching analysis (light-adapted plants) was performed for this purpose, followed by a relaxation analysis (dark-adapted plants after light period) of PSII as proposed by Kasajima et al. (2009) and revised by Lazár (2015) (Fig. 1a).

This analysis is based on the idea that the sum of all the dissipative processes of the energy absorbed by PSII is equal to 1 (Demmig-Adams et al. 1996; Kramer et al. 2004; Hendrickson et al. 2004; Logan et al. 2014):

$$\Phi_{PSII} + \Phi_{NPQ} + \Phi_{NO} = 1,$$

where Φ_{PSII} is the quantum yield of PSII, Φ_{NPQ} is the non-photochemical quenching, and Φ_{NO} is the quantum yield of constitutive non-regulatory (basal or dark) non-photochemical dissipation processes.

The quenching analysis of Φ_{PSII} was calculated as Eq. [1] (Fig. 1b), (Genty et al. 1989; Baker 2008). Φ_{NPQ} and Φ_{NO} were calculated as Eq. [2] and [5], respectively (Fig. 1b) (Hendrickson et al. 2004; Klughammer and Schreiber 2008). In the relaxation analysis of PSII, the quantum yields of the fast and slow components of the non-photochemical

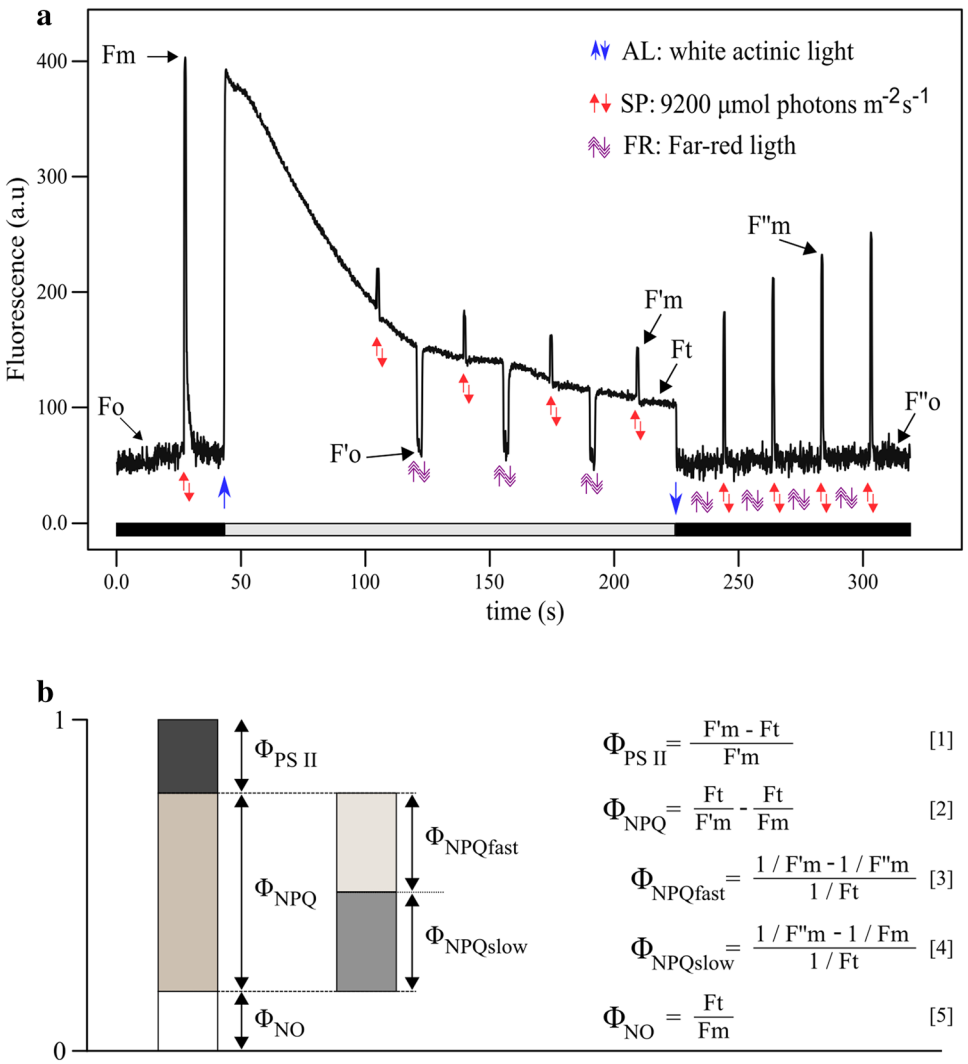

Fig. 1 Fluorescence quenching analysis followed by a relaxation analysis using modulated fluorescence. **a** A dark-adapted leaf is exposed to white actinic light (AL). Blue up and down arrows indicate that light is turned on or off, respectively. Red arrows indicate the position of saturating pulses (SP). Double head arrow indicates far red-light pulse (FR). F_o, F'_o, and F''_o represent minimum fluorescence in dark, light, and recovery phases, respectively. F(t) is the actual fluorescence for light-adapted states in the time t; F_m and F'_m represent maximum fluorescence in dark and light conditions, respectively. F''_m is the maximum fluorescence in dark condition during recovery. **b** Relationship between quantum yields and determining equations. Φ_{PSII} is the quantum yield of PSII [1], Φ_{NPQ} is the non-photochemical quenching [2], $\Phi_{NPQfast}$ is the quantum yield of fast-relaxing non-photochemical quenching [3], $\Phi_{NPQslow}$ is the quantum yield of slow-relaxing non-photochemical quenching slow component of the non-photochemical quenching [4], and Φ_{NO} is the quantum yield of constitutive non-regulatory (basal or dark) non-photochemical dissipation processes [5]

quenching $\Phi_{NPQfast}$ and $\Phi_{NPQslow}$ were calculated as Eq. [3] and Eq. [4], respectively (Fig. 1b) (Kasajima et al. 2009).

Fluorescence traces were obtained in vivo using a PAM Chl fluorometer (FMS1, Hansatech, King's Lynn, UK) after dark adaptation for 45 min at room temperature. White actinic light of 778 µmol m^{-2} s^{-1} was used during the adaptation to the light period. These measurements were made for the last completely expanded leaf (in the V5 stage, with a thickness of approximately 1 cm). Fluorescence measurement conditions were the same as plant-growth conditions.

The maximal quantum yield of PSII photochemistry for a dark-adapted state, Φ_{Po}, was calculated as (Kitajima and Butler 1975):

$$\Phi P_o = F_m - F_o/F_m = F_v/F_m.$$

The maximal quantum yield of PSII photochemistry for the light-adapted state, $\Phi_{PSII.pot}$, was calculated as (Oxborough and Baker 1997):

$$\Phi PSII.pot = F'_m - F'_o/F'_m = F'/F'_m.$$

The fraction of open PSII centers at the time t, qL, was calculated as (Kasajima et al. 2009):

$$qL = \left(1/F_t - 1/F'_m\right)/\left(1/F_o - 1/F'_m\right).$$

Determination of quantum yields in response to extreme actinic light intensities

To measure the response of PSII under high energy offer, we performed an experiment where the actinic light consisted of 255, and 2800 µmol m^{-2} s^{-1} actinic light intensities, separated by a dark recovery period of 45 min. The light spectrum of white actinic light and the curve of light intensity were set pursuant to the equipment manual. Details are shown in Supplementary Fig. S3.

Statistical analysis

Differences and interactions between cultivars and light conditions on the variances were tested using a two-way analysis of variance (ANOVA). Differences among the means were

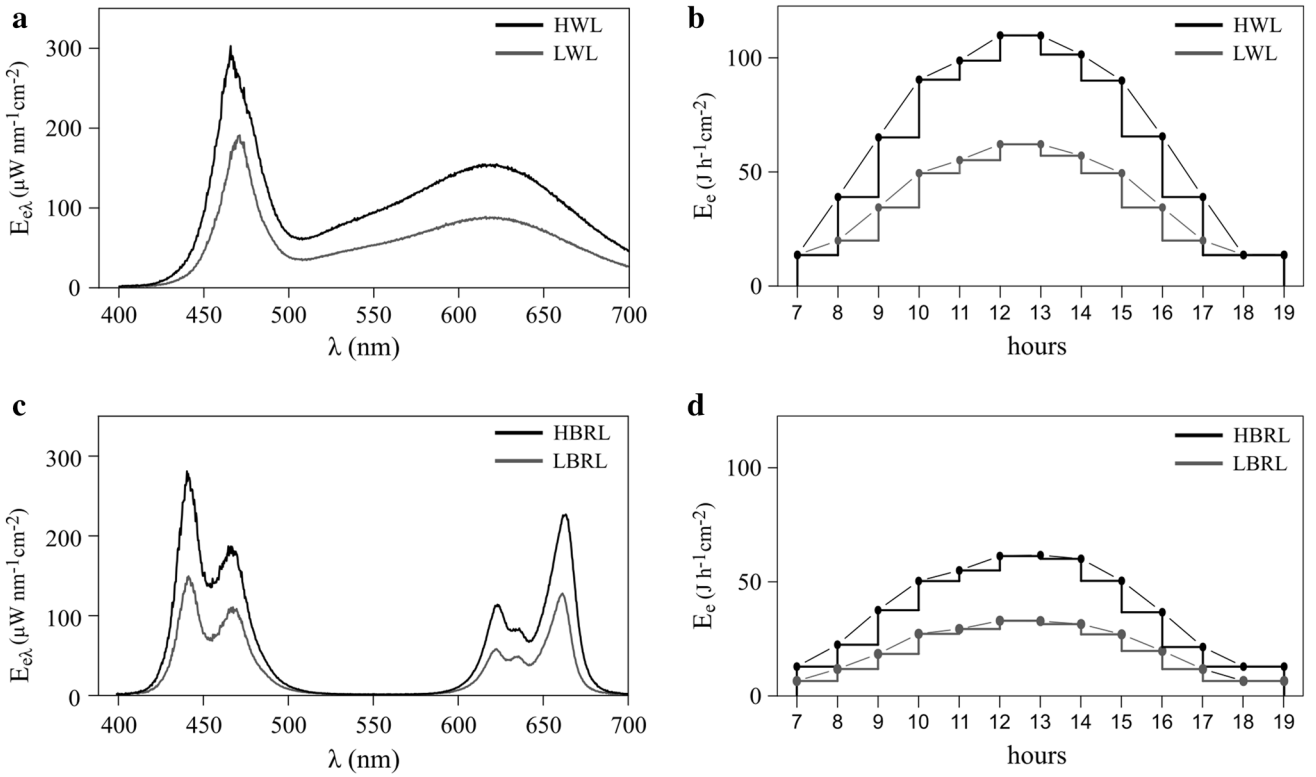

Fig. 2 Spectral distributions and energy accumulated at different light fluxes during a day applied to all light treatments. **a** Variation of Spectral Energy Flux (Eeλ) under white light spectral quality in a Low White Light (LWL) environment (841 µmol m^{-2} s^{-1}) and a High White Light (HWL) environment (1487 µmol m^{-2} s^{-1}). Environments were defined by using the maximum PPFD values (at 6 h of treatment) for white light spectral quality. **b** Variation of light intensity measured as Energy flux (Ee) in a 12-h cycle for LWL and HWL. **c** Variation of Spectral Energy Flux (Eeλ) under blue-red spectral quality in Low Blue-Red Light (LBRL) (427 µmol m^{-2} s^{-1}) environment and High Blue-Red Light (HBRL) (804 µmol m^{-2} s^{-1}) environment. Environments were defined by using the maximum PPFD values (at 6 h of treatment) for blue-red light spectral quality. **d** Variation of light intensity measured as Energy flux (Ee) for 12 h cycle for LBRL and HBRL

tested by orthogonal contrast analysis ($P < 0.05$). All statistical analyses were done in R using the stats package (R Core Team 2017). Contrast analyses were performed using the *emmeans* package (Russell 2018).

Results and discussion

Light environments used in this study

Two systems of LED-based lamps were developed in this study to evaluate the effect of light quantity and quality on rice plant development. The use of complementary spectral composition made it possible to establish four controlled light environments.

Light System I generated white light environments with a spectral-quality range from 400 to 700 nm (Fig. 2a). In this spectral quality, two maximum incident levels of light flux (at 6 h of treatment) were reached: 17.25 and 30.5 W m^{-2} (Fig. 2b). In terms of PPFD, those light environments reached a maximum of 841 and 1487 µmol m^{-2} s^{-1}, respectively. With these light fluxes, the incident energy accumulated throughout the period of 40–50 days was 150.4 and 285.6 MJ m^{-2}, respectively. These two light environments were defined as High White Light (HWL: 1487 µmol m^{-2} s^{-1}) and Low White Light (LWL: 841 µmol m^{-2} s^{-1}). HWL and LWL environments allowed us to evaluate LUE at high and low radiation while covering the entire spectrum of photosynthetically active radiation (PAR).

On the other hand, with *Light System II* it was possible to generate a light environment with the spectral quality generated only by the 400–500 nm and 600–700 nm bands, which cover part of the PAR radiation spectrum (Fig. 2c). In this spectral quality, two maximum light fluxes were fixed (at 6 h of treatment): 9.14 and 17.12 W m^{-2} (Fig. 2d). In terms of PPFD, the maximum were 427 and 804 µmol m^{-2} s^{-1}, respectively. These two light environments were defined as High Blue-Red Light (HBRL: 804 µmol m^{-2} s^{-1}) and Low Blue-Red Light (LBRL: 427 µmol m^{-2} s^{-1}). As with *Light System I*, having two light fluxes enabled different energy accumulation. The accumulated energy was 81.6 MJ m^{-2} in LBRL and 163.2 MJ m^{-2} in HBRL.

The decomposition of the spectral PAR in different bands allowed us to evaluate the energetic contribution of each band regarding the energy supplied by the total PAR radiation. In this work, the blue-red light treatments of *Light System II* were defined based on the energy in the blue (400–500 nm) and red (600–700 nm) bands of the white light spectrum of *Light System I* at each evaluated intensity.

From the measurements of the spectroradiometer, it was possible to estimate that 70% of the energy radiated by *Light System I* (HWL and LWL) came from the energy in blue (400–500 nm) and red (600–700 nm) bands. This

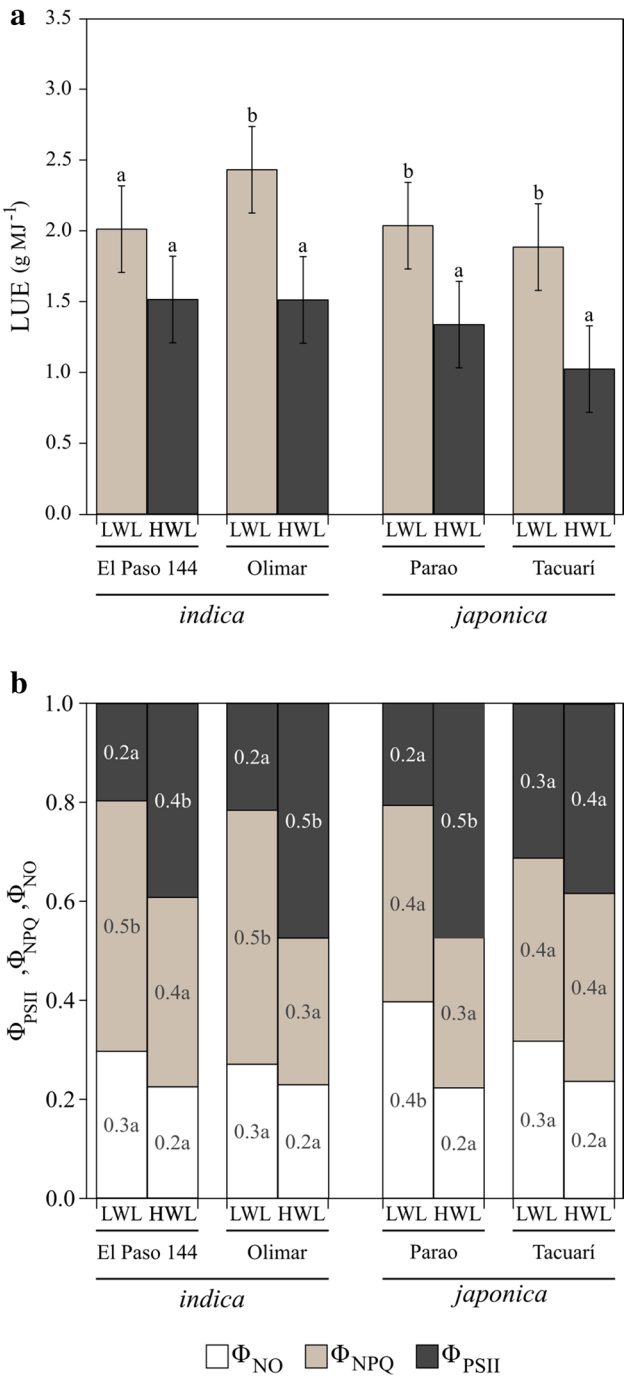

Fig. 3 Light-use efficiency and quantum yields of four rice cultivars in *Light System I*. **a** LUE of four rice cultivars grown under two light treatment, *LWL* Low White Light (841 µmol m^{-2} s^{-1}), and *HWL* High White Light intensity (1487 µmol m^{-2} s^{-1}). **b** Quantum yields of four rice cultivars grown under two light treatment, LWL and HWL. Φ_{PSII} is the quantum yield of PSII, Φ_{NPQ} is the non-photochemical quenching, and Φ_{NO} is the quantum yield of constitutive non-regulatory (basal or dark) non-photochemical dissipation processes. Different letters indicate significant differences by a contrasting analysis of each cultivar under different light treatments ($P \leq 0.05$)

result is consistent with Nelson and Bugbee (2014), who suggested a higher electrical efficiency and photon efficiency in blue and red wavelengths of LED systems.

It is important to mention that in addition to the four light environments generated for this study, the light systems developed in this work can be used to create other light environments with light quantity and quality handled independently.

Light-use efficiency and energy partitioning of rice cultivars under two light intensities of a visible full spectrum (*Light System I*)

The values of LUE obtained in both plant-growing environments generated in *Light System I* (LWL and HWL) varied from 1 to 2.5 g MJ^{-1}, as previously reported by Sinclair and Muchow (1999) and Mitchell et al. (1998). As it is expected, when light intensity increases (HWL), LUE decreases. These results are consistent with Horie and Sakuratani (1985), who described an increase in LUE under shading conditions. This was the case for all cultivars, except for El Paso 144, where no significant differences were observed in both environments (Fig. 3a). Therefore, LUE is dependent on the rice cultivar, which means light was handled differently by El Paso 144 as compared to Parao, INIA Olimar, and INIA Tacuarí.

The quenching and relaxation of PSII were studied to analyze the relation between LUE at the plant level and the energy partitioning at the photochemical level. Figure 3b shows the composition of the energy partitioning in its main components measured using an actinic light of 778 µmol m^{-2} s^{-1}. In a plant grown in LWL, 40–50% of the total energy was assigned to the Φ_{NPQ}, while in a plant grown in HWL, Φ_{NPQ} was 30–40% of the total energy. While there was no significant reduction of Φ_{NPQ} in Parao and INIA Tacuarí (*japonica* cultivars), El Paso 144 and INIA Olimar (*indica* cultivars) showed a decrease in this parameter.

On the other hand, Φ_{PSII} was significantly lower in plants grown in LWL for all cultivars except for INIA Tacuarí (Fig. 3b). A decrease in Φ_{PSII} in plants grown at low radiation was recorded for spring barley (*Hordeum vulgare L.*) (Zivcak et al. 2014) and for bread wheat (*Triticum aestivum L.*) (Zivcak et al. 2018).

This decrease in Φ_{PSII} occurs because the incident light energy cannot be transferred to the photochemical process (Šetlík et al. 1990; Keren et al. 1997; Nishiyama et al. 2006; Takahashi and Murata 2005; Murata et al. 2007; Müh et al. 2012). The growth of plants in low light-intensity conditions could lead to an alteration in the size and heterogeneity of PSII (Evans 1987; Mehta et al. 2010; Hogewoning et al. 2012). Hence, the incident energy must be dissipated as heat. In the case of El Paso 144 and INIA Olimar cultivars grown in LWL, heat is dissipated in a regulated way (expressed as Φ_{NPQ}), as opposed to an unregulated way (expressed as Φ_{NO}). In both environments, Φ_{NO} did not vary significantly for either cultivar. Since Φ_{NO} is the component of non-photochemical quenching which describes unregulated heat dissipation, it could be an indicator of PSII damage (Klughammer and Schreiber 2008).

In LWL, the Parao cultivar shows high Φ_{NO} in relation to the other two components (Fig. 3b). This relation changes in HWL, where proportions are consistent with the other three cultivars. On the other hand, Parao's Φ_{NPQ} remains the same in both environments and Φ_{PSII} increases in HWL. These results show that Parao is affected by low radiation conditions.

In the case of INIA Tacuarí, quantum yields do not change significantly in both light environments, indicating that for this cultivar energy partitioning does not change in relation to light intensity (Fig. 3b).

It is worth noting that despite the genetic similarities, *japonica* cultivars had different behaviors in both light environments. Plant growth in low radiation conditions did not allow the development of dissipation mechanisms in Parao, while there was no effect on INIA Tacuarí. In fact, plants of INIA Tacuarí were insensitive to both light environments generated in *Light System I*. Regarding *indica* cultivars, both cultivars behaved in the same way. Comparing HWL and

Table 1 Parameters of the quenching and relaxation analyses in *Light System I*

Cultivars	Light treatments	Dark. adap	Quenching analysis		Relaxation analysis	
		Φ_{Po}	$\Phi_{PSII.pot}$	qL	$\Phi_{NPQ.slow}$	$\Phi_{NPQ.fast}$
El Paso 144	LWL	0.85a	0.68a	0.12a	0.18b	0.33a
	HWL	0.87a	0.70a	0.30b	0.10a	0.28a
INIA Olimar	LWL	0.87a	0.70a	0.12a	0.16b	0.35a
	HWL	0.87a	0.74a	0.32b	0.10a	0.21a
Parao	LWL	0.86a	0.75a	0.09a	0.18b	0.22a
	HWL	0.86a	0.72a	0.39b	0.09a	0.21a
INIA Tacuarí	LWL	0.89a	0.78a	0.12a	0.14a	0.23a
	HWL	0.89a	0.75a	0.22a	0.11a	0.27a

LWL, Φ_{PSII} was higher in HWL while Φ_{NPQ} was lower and Φ_{NO} remained unchanged. According to these results, while in INIA Tacuarí, El Paso 144, and INIA Olimar the surplus energy is dissipated in a regulated way (e.g., xanthophyll cycle), in Parao the surplus energy is not processed by the non-harmful mechanisms of dissipation. In this work, we demonstrated that light intensity differentially affects LUE at the whole-plant level and the energy partitioning in all rice cultivars.

It is important to mention that the actinic light used for estimating quantum yield parameters in HWL and LWL was the same (778 µmol m^{-2} s^{-1}). Therefore, all the differences observed could be associated with a difference in the photosynthetic apparatus generated during plant development under two distinct light environments, and not with an instantaneous response of PSII to changes in the incident light. Nevertheless, contrary to what is expected, we could not find a relation between LUE at the whole-plant level and the observed energy partitioning. This relation was reported by Einhorn et al. (2004) and Krause et al. (2006).

The quenching analysis of all cultivars showed no difference of Φ_{Po} and $\Phi_{PSII.pot}$, either for dark-adapted and light-adapted states, in plants grown in both environments (Table 1). On the other hand, there were differences in the fraction of opened PSII centers (qL). In all cultivars except INIA Tacuarí, qL was lower in LWL compared with HWL (Table 1). This result confirms the previous finding regarding the insensitiveness of the INIA Tacuarí cultivar to different light intensities of *Light System I*. INIA Tacuarí's photosynthetic machinery is the same in both conditions. In all cases, qL value was consistent with the energy partitioning expressed as quantum yield.

Table 1 shows that PSII response could be determined by the fraction of open reaction centers instead of the maximum quantum yields. Namely, the ability to use energy in photochemistry was not given by the maximum photochemical capacity of the PSII but by the number of open reaction centers which is dependent on the growth light environment and the rice cultivar. The relaxation analysis showed that $\Phi_{NPQslow}$ was lower in HWL than LWL, except for INIA Tacuarí where no change was observed. On the other hand, $\Phi_{NPQfast}$ did not change in all cultivars and light environments.

$\Phi_{NPQslow}$ variation is associated with Φ_{NPQ} variation, and therefore $\Phi_{NPQslow}$ is the Φ_{NPQ} component which responds to the difference among cultivars and light environments. In Parao, this component represents 46% of Φ_{NPQ}, confirming the sensitivity of Parao to low radiation environments. $\Phi_{NPQslow}$, being directly related to PSII damage, is an indicator of photoinhibition. Photoinhibition may represent a negative regulation of the photosynthetic apparatus in response to excess light when more light energy is harvested than

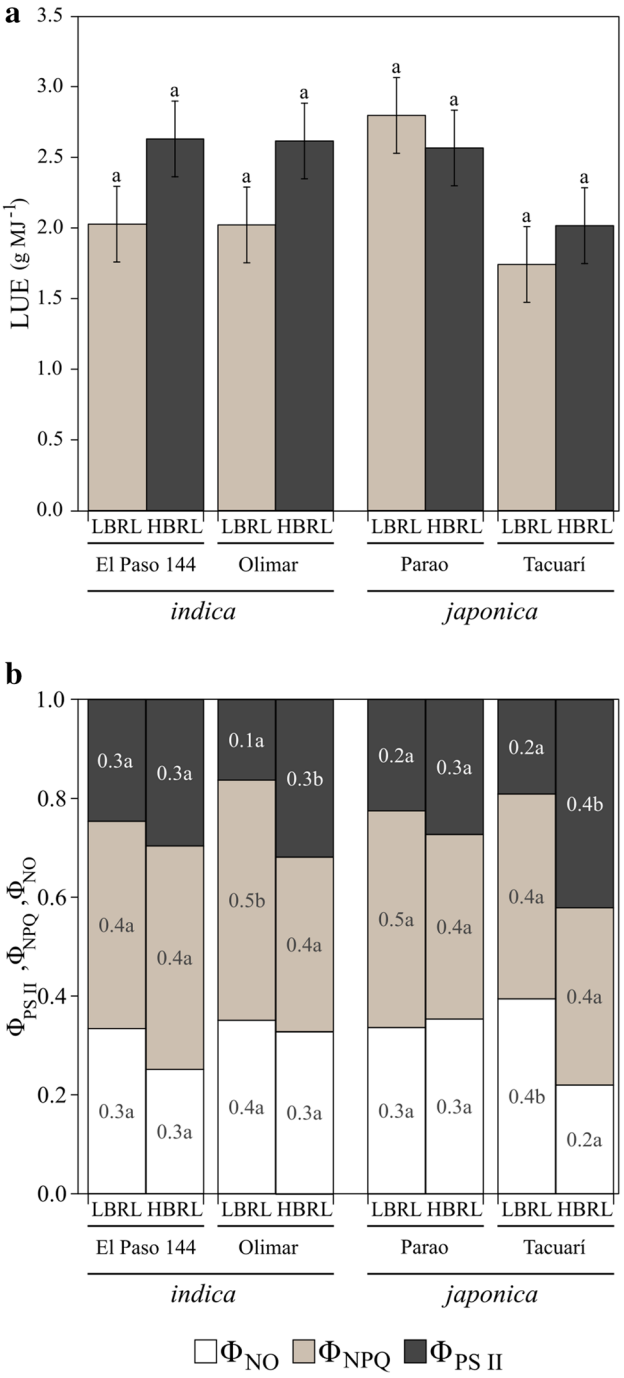

Fig. 4 Light-use efficiency and quantum yields of four rice cultivars in *Light System II*. **a** LUE of rice plants grown under two quality light treatments. *LBRL* Low Blue-Red Light (427 µmol m^{-2} s^{-1}) and *HBRL* High Blue-Red Light (804 µmol m^{-2} s^{-1}). **b** Complementary quantum yields. Φ_{PSII} is the quantum yield of photochemical energy conversion and n Φ_{NPQ} is the quantum yield for dissipation by down-regulation and Φ_{NO} is the quantum yield of other non-photochemical losses. Different letters indicate significant differences by a contrasting analysis of each cultivar under different light treatments $P \leq 0.05$

can be used by the chloroplast for the fixation of carbon dioxide (Adams et al. 2013). The excess of light is defined as a function of the energy flux in relation to the photosynthetic apparatus development and not to the absolute value of energy flux. In this sense, plants grown in LWL would present a less developed photosynthetic apparatus in relation to the available energy.

It is interesting to note that $\Phi_{NPQslow}$ variation between environments is inverse to qL. This is the first work which describes the relation between qL and $\Phi_{NPQslow}$ in rice, notwithstanding several studies showing the relation between qL and Φ_{NPQ} (Krause and Weis 1991; Kramer et al. 2004; Krause and Jahns 2004; Baker 2008; Kasajima et al. 2009).

Light-use efficiency and energy partitioning of rice cultivars under two light intensities composed by blue and red spectrum (*Light System II*)

In the case of light environments generated in *Light System II*, the values of LUE varied from 1.7 to 2.7 g MJ^{-1}. However, for all cultivars, there was not a significant difference between LBRL and HBRL (Fig. 4a). Contrary to *Light System I*, the increase in light intensity did not decrease LUE.

The range of variation of LUE at the whole-plant level was the same as for the white light environments and those reported in the literature for rice (Mitchell et al. 1998; Sinclair and Muchow 1999). This result indicates that at the whole-plant level LUE does not change with different light quality conditions.

Analyses of different components of quantum yield showed significant variation in INIA Tacuarí and INIA Olimar cultivars (Fig. 4b). An increase of Φ_{PSII} was observed in INIA Olimar and INIA Tacuarí in response to light intensity. In the case of INIA Tacuarí, the increase of Φ_{PSII} derived mainly from a decrease in Φ_{NO}, while in INIA Olimar the increase of Φ_{PSII} derived mainly from a decrease in Φ_{NPQ}. Compared to *Light System I*, these results show a differential impact of light intensity on energy control of these cultivars.

As in *Light System I*, the quenching analysis showed no difference of $\Phi_{PSII.pot}$ for all cultivars in both light environments (Table 2). However, there were differences in Φ_{Po} in HBRL for El Paso 144 and INIA Tacuarí. In the case of qL, the light treatment only had an effect in INIA Tacuarí, where a higher proportion of open reaction centers of PSII were observed in HBRL. In all cultivars, except El Paso 144, $\Phi_{NPQ.slow}$ is higher at lower radiation due to impediments for the energy to dissipate through photochemical processes (Table 2).

In INIA Olimar, changes in Φ_{PSII} are related to the $\Phi_{NPQ.slow}$ component of the Φ_{NPQ}; that is, the decrease in the quantum yield of the photochemical process is due to photoinhibition and it is not related to the fraction of open reaction centers of the PSII (qL). On the contrary, in INIA Tacuarí, photoinhibition affects the proportion of open reaction centers of the PSII (qL). As in *Light System I*, Parao shows higher PSII damage under low energy flux, although this damage did not affect Φ_{PSII}.

It is worth noting that in this light system there are no differences at the whole-plant level between light environments and between cultivars. However, there are differences at the photosynthetic apparatus level, evidencing an unclear relationship between both levels of analysis.

Quantum yields under two actinic white light intensities

In order to evaluate the dissipation processes of PSII under increased excitation light intensities, two points of actinic light were set with PAM (255 and 2800 µmol m^{-2} s^{-1}). This analysis was only performed on plants grown in the HWL and HBRL environments.

According to the results shown in Fig. 5, at a low level of actinic light intensity (255 µmol m^{-2} s^{-1}) energy is mainly used for phytochemical processes in all cultivars (regardless of the subspecies to which they belong). In fact, under this condition, approximately 70% of the energy is related to the parameter Φ_{PSII} and harmless dissipation processes are below 10%. When actinic light intensities increase more than

Table 2 Parameters of the quenching and relaxation analyses in *Light System II*

Cultivars	Light treatments	Dark.adap	Quenching analysis		Relaxation analysis	
		Φ_{Po}	$\Phi_{PSII.pot}$	qL	$\Phi_{NPQ.slow}$	$\Phi_{NPQ.fast}$
El Paso 144	LBRL	0.86a	0.73a	0.12a	0.15a	0.27a
	HBRL	0.88b	0.73a	0.16a	0.10a	0.35a
INIA Olimar	LBRL	0.86a	0.71a	0.08a	0.20b	0.28a
	HBRL	0.87a	0.76a	0.15a	0.08a	0.27a
Parao	LBRL	0.88a	0.76 a	0.09 a	0.19b	0.25a
	HBRL	0.88a	0.78a	0.11a	0.07a	0.30a
INIA Tacuarí	LBRL	0.86a	0.75a	0.09a	0.19b	0.22a
	HBRL	0.89b	0.75a	0.25b	0.08a	0.28a

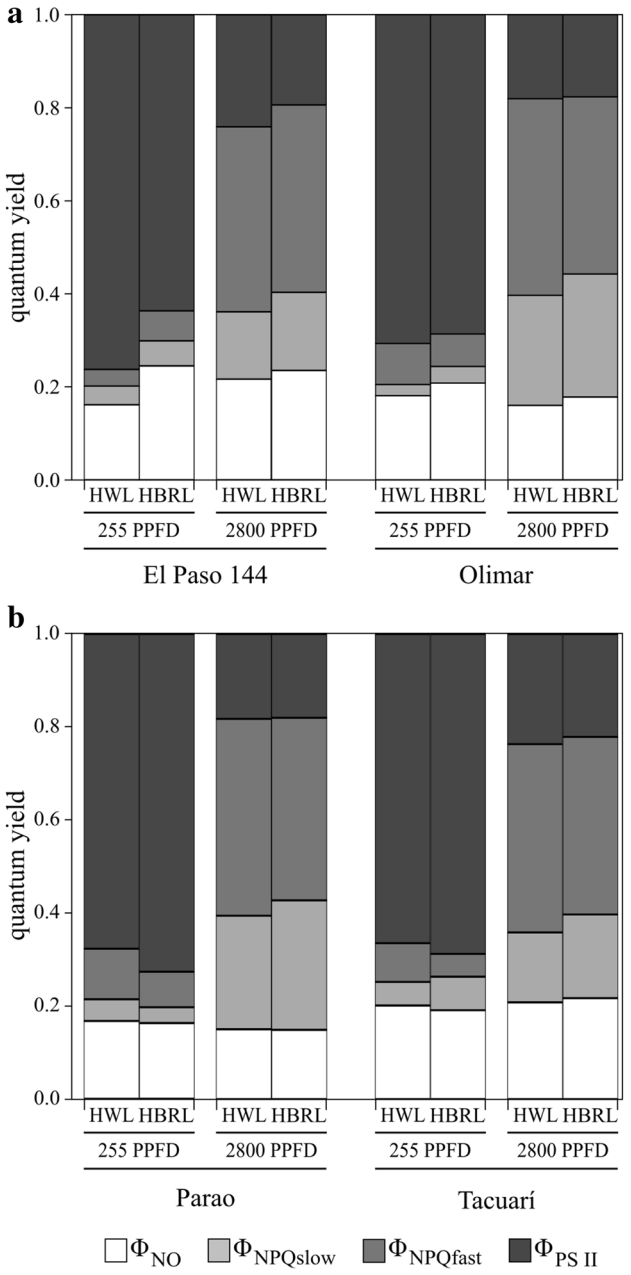

Fig. 5 Quantum yields in response to extreme actinic light intensities. **a** *Indica* rice cultivars grown under high irradiation conditions and **b** *japonica* rice cultivars grown under high irradiation conditions. HWL means high white light and HBRL means high blue-red light. Φ_{PSII} is the quantum yield of photochemical energy conversion; $\Phi_{NPQfast}$ is the quantum yield of fast-relaxing non-photochemical quenching; $\Phi_{NPQslow}$ is the quantum yield of slow-relaxing non-photochemical quenching and Φ_{NO} is the quantum yield of other non-photochemical losses. All quantum yield parameters were calculated using equations described in Fig. 1

tenfold (2800 µmol m^{-2} s^{-1}), energy is mostly dissipated through harmless mechanisms such as $\Phi_{NPQfast}$. This parameter explains the destination of 40% of the energy under said condition. Interestingly, this response is not affected by the quality neither by the quantity of the light to which the plants were subjected during their growth period. In addition, the basal dissipation mechanisms are among 15–20% in both actinic light intensity conditions. These results are consistent with those reported by Ishida et al. (2011).

This experiment shows the relevance of the actinic light intensities in which the photochemical process is being evaluated. Extreme actinic light intensities make it impossible to observe differences among light environments or among cultivars.

Conclusions

Light-use efficiency values found in this study are very similar to those reported in the literature. In all the analyzed rice cultivars, the decrease in LUE in relation to light intensity depends on the light spectral quality. On the other hand, LUE is different among the analyzed cultivars in different environments. These differences present opportunities to select for breeding programs those cultivars that are more efficient in the use of light.

At the level of the photosynthetic apparatus, it was observed that both the growth light environment and the cultivar condition the partition of energy in the PSII. In white light environments, low levels of energy increase the damage of PSII and lead to a decrease in photochemical processes due to the closure of the reaction centers. The rice cultivars evaluated in this study are sensitive to low levels of radiation. In this regard, Parao proved to be the cultivar most affected by low light energy. In contrast, quantum yields in INIA Tacuarí are independent of the amount of incident energy.

Energy partition in PSII depends on the energy levels and spectral quality. Doubling the irradiance energy in blue and red environments does not generate the same response as doubling the energy in white environments. In this sense, considering the intensity of the actinic light when evaluating the energy partition is crucial to finding differential responses among cultivars.

Acknowledgements We would like to acknowledge the Agencia Nacional de Investigación e Innovación (ANII) which funded the Doctoral Scholarship of Gaston Quero (POS_NAC_2012_1_8560). This research was also funded by an INIA Project named "Desarrollo de una plataforma de fenotipado como base para la mejora de la tolerancia a estrés ambiental de cultivos y ajuste de modelos de simulación" (L4_10_1_AZ_BT_GT1_8850), and by Grupo Comisión Sectorial de Investigación Científica (CSIC I+D 418).

Compliance with ethical standards

Conflict of interest The authors declare that they have no conflict of interest.

References

Adams WW, Muller O, Cohu CM, Demmig-Adams B (2013) May photoinhibition be a consequence, rather than a cause, of limited plant productivity? Photosynth Res 117:31–44. https://doi.org/10.1007/s11120-013-9849-7

Ahn TK, Avenson TJ, Peers G, Li Z, Dall'Osto L, Bassi R et al (2009) Investigating energy partitioning during photosynthesis using an expanded quantum yield convention. Chem Phys 357:151–158. https://doi.org/10.1016/j.chemphys.2008.12.003

Alexandratos N, Bruinsma J (2012) World agriculture towards 2030/2050: the 2012 revision. FAO, Rome

Allakhverdiev SI, Murata N (2004) Environmental stress inhibits the synthesis de novo of proteins involved in the photodamage-repair cycle of photosystem II in Synechocystis sp. PCC 6803. Biochim Biophys Acta 1657:23–32. https://doi.org/10.1016/j.bbabio.2004.03.003

Allakhverdiev SI, Mohanty P, Murata N (2003) Dissection of photodamage at low temperature and repair in darkness suggests the existence of an intermediate form of photodamaged photosystem II. Biochemistry 421:14277–14283. https://doi.org/10.1021/bi035205

Allakhverdiev SI, Tsvetkova N, Mohanty P, Szalontai B, Byoung YM, Debreczeny M, Murata N (2005) Irreversible photoinhibition of photosystem II is caused by exposure of Synechocystis cells to strong light for a prolonged period. Biochim Biophys Acta 1708:342–351. https://doi.org/10.1016/j.bbabio.2005.05.006

Allakhverdiev SI, Los DA, Mohanty P, Nishiyama Y, Murata N (2007) Glycinebetaine alleviates the inhibitory effect of moderate heat stress on the repair of photosystem II during photoinhibition. Biochim Biophys Acta 1767:1363–1371. https://doi.org/10.1016/j.bbabio.2007.10.005

Baker NR (2008) Chlorophyll fluorescence: a probe of photosynthesis in vivo. Annu Rev Plant Biol 59:89–113. https://doi.org/10.1146/annurev.arplant.59.032607.092759

Berkovich YA, Konovalova IO, Smolyanina SO, Erokhin AN, Avercheva OV, Bassarskaya EM, Tarakanov IG (2017) LED crop illumination inside space greenhouses. Reach Rev Hum Sp Explor 6:11–24. https://doi.org/10.1016/j.reach.2017.06.001

Brestic M, Zivcak M, Kunderlikova K, Allakhverdiev SI (2016) High temperature specifically affects the photoprotective responses of chlorophyll b-deficient wheat mutant lines. Photosynth Res 130:251–266. https://doi.org/10.1007/s11120-016-0249-7

Brestic M, Zivcak M, Hauptvogel P, Misheva S, Kocheva K, Yang X, Allakhverdiev SI (2018) Wheat plant selection for high yields entailed improvement of leaf anatomical and biochemical traits including tolerance to non-optimal temperature conditions. Photosynth Res 136:245–255. https://doi.org/10.1007/s11120-018-0486-z

Campbell G, Norman J (1998) An introduction to environmental biophysics. Springer, New York. https://doi.org/10.1007/978-1-4612-1626-1

Campbell DA, Tyystjärvi E (2012) Parameterization of photosystem II photoinactivation and repair. Biochim Biophys Acta 1817:258–265. https://doi.org/10.1016/j.bbabio.2011.04.010

Chen C, Zhang D, Li P, Ma F (2012) Partitioning of absorbed light energy differed between the sun-exposed side and the shaded side of apple fruits under high light conditions. Plant Physiol Biochem 60:12–17. https://doi.org/10.1016/j.plaphy.2012.07.016

Counce PA, Keisling TC, Mitchell J (2000) A uniform, objective and adaptive system for expressing rice development. Crop Sci 40:436–443. https://doi.org/10.2135/cropsci2000.402436x

Dall'Osto L, Bressan M, Bassi R (2015) Biogenesis of light harvesting proteins. Biochim Biophys Acta 1847:861–871. https://doi.org/10.1016/j.bbabio.2015.02.009

Demmig-Adams B, Adams WW III, Barker DH, Logan BA, Bowling DR, Verhoeven AS (1996) Using chlorophyll fluorescence to assess the fraction of absorbed light allocated to thermal dissipation of excess excitation. Physiol Plant 98:253–264. https://doi.org/10.1034/j.1399-3054.1996.980206.x

Derks A, Schaven K, Bruce D (2015) Diverse mechanisms for photoprotection in photosynthesis. Dynamic regulation of photosystem II excitation in response to rapid environmental change. Biochim Biophys Acta 1847:468–485. https://doi.org/10.1016/j.bbabio.2015.02.008

Devlin PF, Christie JM, Terry MJ (2007) Many hands make light work. J Exp Bot 58:3071–3077. https://doi.org/10.1093/jxb/erm251

Einhorn KS, Rosenqvist E, Leverenz JW (2004) Photoinhibition in seedlings of Fraxinus and Fagus under natural light conditions: implications for forest regeneration? Oecologia 140:241–251. https://doi.org/10.1007/s00442-004-1591-6

Evans JR (1987) The relationship between electron transport components and photosynthetic capacity in pea leaves grown at different irradiances. Aust J Plant Physiol 14:157–170. https://doi.org/10.1071/PP9870157

Evans JR (1996) Developmental constrains on photosynthesis: effects of light and nutrition. In: Baker N (ed.) Photosynthesis and the environment. Kluwer Academic Publishers, Dordrecht, pp 281–304. https://doi.org/10.1007/0-306-48135-9

Genty B, Briantais J, Baker NR (1989) The relationship between the quantum yield of photosynthetic electron transport and quenching of chlorophyll fluorescence. Biochim Biophys Acta 990:87–92. https://doi.org/10.1016/S0304-4165(89)80016-9

Gitelson AA, Gamon JA (2015) The need for a common basis for defining light-use efficiency: implications for productivity estimation. Remote Sens Environ 156:196–201. https://doi.org/10.1016/j.rse.2014.09.017

Goltsev VN, Kalaji HM, Paunov M, Bąba W, Horaczek T, Mojski J, Allakhverdiev SI (2016) Variable chlorophyll fluorescence and its use for assessing physiological condition of plant photosynthetic apparatus. Russ J Plant Physiol 63:869–893. https://doi.org/10.1134/S1021443716050058

Hakala M, Tuominen I. Keränen M, Tyystjärvi T, Tyystjärvi E (2005) Evidence for the role of the oxygen-evolving manganese complex in photoinhibition of photosystem II. Biochim Biophys Acta 1706:68–80. https://doi.org/10.1016/j.bbabio.2004.09.001

Hendrickson L, Furbank RT, Chow WS (2004) A simple alternative approach to assessing the fate of absorbed light energy using chlorophyll fluorescence. Photosynth Res 82:73–81. https://doi.org/10.1023/B:PRES.0000040446.87305.f4

Hendrickson L, Förster B, Pogson BJ, Wah SC (2005) A simple chlorophyll fluorescence parameter that correlates with the rate coefficient of photoinactivation of photosystem II. Photosynth Res 84:43–49. https://doi.org/10.1007/s11120-004-6430-4

Hogewoning SW, Wientjes E, Douwstra P, Trouwborst G, van Ieperen W, Croce R, Harbinson J (2012) Photosynthetic quantum yield dynamics: from photosystems to leaves. Plant Cell 24:1921–1935. https://doi.org/10.1105/tpc.112.097972

Horie T, Sakuratani T (1985) Studies on crop-weather relationship model in rice. 1. Relation between absorbed solar radiation by the crop and dry matter production. J Agric Meteorol 40:331–342. https://doi.org/10.2480/agrmet.40.331

Horton P (2000) Prospects for crop improvement through the genetic manipulation of photosynthesis: morphological and biochemical aspects of light capture. J Exp Bot 51:475–485

Hubbart S, Peng S, Horton P, Chen Y, Murchie EH (2007) Trends in leaf photosynthesis in historical rice varieties developed in the

Philippines since 1966. J Exp Bot 58:3429–3438. https://doi.org/10.1093/jxb/erm192
Ishida S, Morita KI, Kishine M, Takabayashi A, Murakami R, Takeda S et al (2011) Allocation of absorbed light energy in PSII to thermal dissipations in the presence or absence of PsbS subunits of rice. Plant Cell Physiol 52:1822–1831. https://doi.org/10.1093/pcp/pcr119
Kalaji HM, Schansker G, Ladle RJ, Goltsev V et al (2014) Frequently asked questions about in vivo chlorophyll fluorescence: practical issues. Photosynth Res 122:121–158. https://doi.org/10.1007/s11120-014-0024-6
Kalaji HM, Schansker G, Brestic M, Bussotti F, Calatayud A, Ferroni L, Bąba W et al (2017) Frequently asked questions about chlorophyll fluorescence, the sequel. Photosynth Res 132:13–66. https://doi.org/10.1007/s11120-016-0318-y
Kasajima I, Takahara K, Kawai-Yamada M, Uchimiya H (2009) Estimation of the relative sizes of rate constants for chlorophyll de-excitation processes through comparison of inverse fluorescence intensities. Plant Cell Physiol 50:1600–1616. https://doi.org/10.1093/pcp/pcp102
Keren N, Berg A, van Kan PJM, Levanon H, Ohad I (1997) Mechanism of photosystem II photoinactivation and D1 protein degradation at low light: the role of back electron flow. Proc Natl Acad Sci USA 94:1579–1584. https://doi.org/10.1073/pnas.94.4.1579
Kitajima M, Butler WL (1975) Quenching of chlorophyll fluorescence and primary photochemistry in chloroplasts by dibromothymoquinone. Biochim Biophys Acta 376:105–115. https://doi.org/10.1016/0005-2728(75)90209-1
Klimov VV, Shafiev MA, Allakhverdiev SI (1990) Photoinactivation of the reactivation capacity of photosystem II in pea subchloroplast particles after a complete removal of manganese. Photosynth Res 23:59–65. https://doi.org/10.1007/BF00030063
Klughammer C, Schreiber U (2008) Complementary PS II quantum yields calculated from simple fluorescence parameters measured by PAM fluorometry and the saturation pulse method. PAM Appl Notes 1:27–35
Kozai T (2013) Resource use efficiency of closed plant production system with artificial light: concept, estimation and application to plant factory. Proc Jpn Acad Ser B 89:447–461. https://doi.org/10.2183/pjab.89.447
Kozai T, Kazuhiro F, Runkle ES (2016) LED Lighting for urban agriculture. Springer, New York. https://doi.org/10.1007/978-981-10-1848-0
Kramer DM, Johnson G, Kiirats O, Edwards GE (2004) New fluorescence parameters for the determination of QA redox state and excitation energy fluxes. Photosynth Res 79:209–218. https://doi.org/10.1023/B:PRES.0000015391.99477.0d
Krause H, Jahns P (2003) Pulse amplitude modulated chlorophyll fluorometry and its application in plant science. In: Green B, Parson W (eds) Light-harvesting antennas, Kluwer Academic Publ, Dordrecht, pp 373–399. https://doi.org/10.1007/978-94-017-2087-8
Krause H, Jahns P (2004) Non-photochemical energy dissipation determined by chlorophyll fluorescence quenching: characterization and function. In: Papageorgiou GC, Govindjee (eds) Chlorophyll a fluorescence: a signature of photosynthesis. Springer, Dordrecht, pp 463–495. https://doi.org/10.1007/978-1-4020-3218-9
Krause H, Weis E (1991) Chlorophyll fluorescence and photosynthesis: the basics. Annu Rev Plant Physiol Plant Mol Biol 42:313–349. https://doi.org/10.1146/annurev.pp.42.060191.001525
Krause H, Gallé A, Virgo A, García M, Bucic P, Jahns P, Winter K (2006) High-light stress does not impair biomass accumulation of sun-acclimated tropical tree seedlings (*Calophyllum longifolium* Willd. and *Tectona grandis* L. f.). Plant Biol 8:31–41. https://doi.org/10.1055/s-2005-872901
Lazár D (2015) Parameters of photosynthetic energy partitioning. J Plant Physiol 175:131–147. https://doi.org/10.1016/j.jplph.2014.10.021
Liu Z, Sun N (2013) Enhancing photosynthetic CO_2 use efficiency in rice: approaches and challenges. Acta Physiol Plant 35:1001–1009. https://doi.org/10.1007/s11738-012-1171-z
Logan BA, Demmig-adams B, Adams W III, Bilger W (2014) Context, quantification, and measurement guide for non-photochemical quenching of chlorophyll fluorescence. In: Demmig-Adams B et al (ed) Non-photochemical quenching and energy dissipation in plants, algae and cyanobacteria. Springer, Dordrecht, pp 187–201. https://doi.org/10.1007/978-94-017-9032-1
Long SP, Zhu X, Naidu SL, Ort DR (2006) Can improvement in photosynthesis increase crop yields? Plant Cell Environ 29:315–330. https://doi.org/10.1111/j.1365-3040.2005.01493.x
Matsuda R, Ohashi-kaneko K, Fujiwara K, Goto E, Kurata K (2004) Photosynthetic characteristics of rice leaves grown under red light with or without supplemental blue light. Plant Cell Physiol 45:1870–1874. https://doi.org/10.1093/pcp/pch203
Matsuda R, Ohashi-Kaneko K, Fujiwara K, Kurata K (2008) Effects of blue light deficiency on acclimation of light energy partitioning in PSII and CO_2 assimilation capacity to high irradiance in spinach leaves. Plant Cell Physiol 49:664–670. https://doi.org/10.1093/pcp/pcn041
Medlyn BE (1998) Physiological basis of the light use efficiency model. Tree Physiol 18:167–176
Mehta P, Allakhverdiev SI, Jajoo A (2010) Characterization of photosystem II heterogeneity in response to high salt stress in wheat leaves (*Triticum aestivum*). Photosynth Res 105:249–255. https://doi.org/10.1007/s11120-010-9588-y
Mitchell PL, Sheehy JE, Woodward FI (1998) Potential yields and the efficiency of radiation use in rice. IRRI 32:1–63
Monteith JL (1972) Solar radiation and productivity in tropical ecosystems. J Appl Ecol 9:747–766. https://doi.org/10.2307/2401901
Monteith J (1977) Climate and the efficiency of crop production in Britain. Philos Trans R Soc Lond 281:277–294. https://doi.org/10.1098/rstb.1977.0140
Morrow RC (2008) LED lighting in horticulture. HortScience 43:1947–1950
Müh F, Glöckner C, Hellmich J, Zouni A (2012) Light-induced quinone reduction in photosystem II. Biochim Biophys Acta 1817:44–65. https://doi.org/10.1016/j.bbabio.2011.05.021
Murata N, Nishiyama Y (2017) ATP is a driving force in the repair of photosystem II during photoinhibition. Plant Cell Environ 41:285–299. https://doi.org/10.1111/pce.13108
Murata N, Takahashi S, Nishiyama Y, Allakhverdiev SI (2007) Photoinhibition of photosystem II under environmental stress. Biochim Biophys Acta 1767:414–421. https://doi.org/10.1016/j.bbabio.2006.11.019
Murata N, Allakhverdiev SI, Nishiyama Y (2012) The mechanism of photoinhibition in vivo: re-evaluation of the roles of catalase, α-tocopherol, non-photochemical quenching, and electron transport. Biochim Biophys Acta 1817:1127–1133. https://doi.org/10.1016/j.bbabio.2012.02.020
Murchie EH, Horton P (1997) Acclimation of photosynthesis to irradiance and spectral quality in British plant species: chlorophyll content, photosynthetic capacity and habitat preference. Plant Cell Environ 20:438–448. https://doi.org/10.1046/j.1365-3040.1997.d01-95.x
Murchie EH, Horton P (1998) Contrasting patterns of photosynthetic acclimation to the light environment are dependent on the differential expression of the responses to altered irradiance and

spectral quality. Plant Cell Environ 21:139–148. https://doi.org/10.1046/j.1365-3040.1998.00262.x
Murchie EH, Chen Y, Hubbart S, Peng S, Horton P (1999) Interactions between senescence and leaf orientation determine in situ patterns of photosynthesis and photoinhibition in field grown rice 1. Plant Physiol 119:553–563. https://doi.org/10.1104/pp.119.2.553
Murchie EH, Hubbart S, Chen Y, Peng S, Horton P (2002) Acclimation of rice photosynthesis to irradiance under field conditions. Plant Physiol 130:1999–2010. https://doi.org/10.1104/pp.011098.protein
Nelson JA, Bugbee B (2014) Economic analysis of greenhouse lighting: light emitting diodes vs. high intensity discharge fixtures. PLoS ONE. https://doi.org/10.1371/journal.pone.0099010
Nelson JA, Bugbee B (2015) Analysis of environmental effects on leaf temperature under sunlight, high pressure sodium and light emitting diodes. PLoS ONE 10:1–13. https://doi.org/10.1371/journal.pone.0138930
Nelson M, Dempster WF, Silverstone S, Alling A, Allen JP, Van Thillo M (2005) Crop yield and light/energy efficiency in a closed ecological system: laboratory biosphere experiments with wheat and sweet potato. Adv Sp Res 35:1539–1543. https://doi.org/10.1016/j.asr.2005.01.016
Nishiyama Y, Allakhverdiev SI, Murata N (2006) A new paradigm for the action of reactive oxygen species in the photoinhibition of photosystem II. Biochim Biophys Acta 1757:742–749. https://doi.org/10.1016/j.bbabio.2006.05.013
Nishiyama Y, Allakhverdiev SI, Murata N (2011) Protein synthesis is the primary target of reactive oxygen species in the photoinhibition of photosystem II. Physiol Plant 142:35–46. https://doi.org/10.1111/j.1399-3054.2011.01457.x
Nobel PS (2009) Physicochemical and environmental plant physiology. Academic Press, Cambridge. https://doi.org/10.1016/B978-0-12-374143-1.00001-6
Oxborough K, Baker NR (1997) Resolving chlorophyll a fluorescence of photosynthetic efficiency into photochemical components—calculation of qP and Fv/Fm without measuring Fo. Photosynth Res 54:135–142
R Core Team (2017) R: a language and environment for statistical computing. The R Foundation. https://www.R-project.org. Accessed 5 June 2018
Russell L (2018) emmeans: estimated marginal means, aka least-squares means. R package version 1.2.1. https://CRAN.R-project.org/package=emmeans
Šetlík I, Allakhverdiev SI, Nedbal L, Šetlíková E, Klimov VV (1990) Three types of photosystem II photoinactivation-I. Damaging processes on the acceptor side. Photosynth Res 23:39–48. https://doi.org/10.1007/BF00030061
Sinclair TR, Horie T (1989) Leaf nitrogen, photosynthesis, and crop radiation use efficiency: a review. Crop Sci 29:90–98. https://doi.org/10.2135/cropsci1989.0011183X002900010023x
Sinclair TR, Muchow RC (1999) Radiation use efficiency. Adv Agron 65:215–265. https://doi.org/10.1016/S0065-2113(08)60914-1
Skillman JB (2008) Quantum yield variation across the three pathways of photosynthesis: not yet out of the dark. J Exp Bot 59:1647–1661. https://doi.org/10.1093/jxb/ern029
Su N, Wu Q, Shen Z, Xia K, Cui J (2014) Effects of light quality on the chloroplastic ultrastructure and photosynthetic characteristics of cucumber seedlings. Plant Growth Regul 73:227–235. https://doi.org/10.1007/s10725-013-9883-7
Takahashi S, Murata N (2005) Interruption of the Calvin cycle inhibits the repair of photosystem II from photodamage. Biochim Biophys Acta 1708:352–361. https://doi.org/10.1016/j.bbabio.2005.04.003
Terashima I, Fujita T, Inoue T, Chow WS, Oguchi R (2009) Green light drives leaf photosynthesis more efficiently than red light in strong white light: revisiting the enigmatic question of why leaves are green. Plant Cell Physiol 50:684–697. https://doi.org/10.1093/pcp/pcp034
Tikkanen M, Aro EM (2012) Thylakoid protein phosphorylation in dynamic regulation of photosystem II in higher plants. Biochim Biophys Acta 1817:232–238. https://doi.org/10.1016/j.bbabio.2011.05.005
Tikkanen M, Mekala NR, Aro EM (2014) Photosystem II photoinhibition-repair cycle protects Photosystem i from irreversible damage. Biochim Biophys Acta 1837:210–215. https://doi.org/10.1016/j.bbabio.2013.10.001
Wagner R, Dietzel L, Bräutigam K, Fischer W, Pfannschmidt T (2008) The long-term response to fluctuating light quality is an important and distinct light acclimation mechanism that supports survival of Arabidopsis thaliana under low light conditions. Planta 228:573–587. https://doi.org/10.1007/s00425-008-0760-y
Walters RG, Horton P (1995) Acclimation of *Arabidopsis thaliana* to the light environment: changes in photosynthetic function. Planta 197:306–312. https://doi.org/10.1007/BF00202652
Wang H, Gu M, Cui J, Shi K, Zhou Y, Yu J (2009) Effects of light quality on CO_2 assimilation, chlorophyll-fluorescence quenching, expression of Calvin cycle genes and carbohydrate accumulation in Cucumis sativus. J Photochem Photobiol B Biol 96:30–37. https://doi.org/10.1016/j.jphotobiol.2009.03.010
Ware MA, Belgio E, Ruban AV (2015) Photoprotective capacity of non-photochemical quenching in plants acclimated to different light intensities. Photosynth Res 126:261–274. https://doi.org/10.1007/s11120-015-0102-4
Yamazaki JY (2010) Is light quality involved in the regulation of the photosynthetic apparatus in attached rice leaves? Photosynth Res 105:63–71. https://doi.org/10.1007/s11120-010-9567-3
Yamazaki JY, Kamimura Y, Okada M, Sugimura Y (1999) Changes in photosynthetic characteristics and photosystem stoichiometries in the lower leaves in rice seedlings. Plant Sci 148:155–163. https://doi.org/10.1016/S0168-9452(99)00132-6
Yin X, Struik PC (2017) Can increased leaf photosynthesis be converted into higher crop mass production? A simulation study for rice using the crop model GECROS. J Exp Bot 68:2345–2360. https://doi.org/10.1093/jxb/erx085
Yoshida S, Forno D, Cock JH, Gomez KA (1976) Laboratory manual for physiological studies of rice, (3rd edn). International Rice Research Institute, Los Baños
Zhu XG, Long SP, Ort DR (2008) What is the maximum efficiency with which photosynthesis can convert solar energy into biomass? Curr Opin Biotechnol 19:153–159. https://doi.org/10.1016/j.copbio.2008.02.004
Zivcak M, Brestic M, Kalaji HM. Govindjee (2014) Photosynthetic responses of sun- and shade-grown barley leaves to high light: is the lower PSII connectivity in shade leaves associated with protection against excess of light? Photosynth Res 119:339–354. https://doi.org/10.1007/s11120-014-9969-8
Zivcak M, Brestic M, Kunderlikova K, Sytar O, Allakhverdiev SI (2015) Repetitive light pulse-induced photoinhibition of photosystem I severely affects CO_2 assimilation and photoprotection in wheat leaves. Photosynth Res 126:449–463. https://doi.org/10.1007/s11120-015-0121-1
Zivcak M, Brestic M, Botyanszka L, Chen YE, Allakhverdiev SI (2018) Phenotyping of isogenic chlorophyll-less bread and durum wheat mutant lines in relation to photoprotection and photosynthetic capacity. Photosynth Res 0:1–13. https://doi.org/10.1007/s11120-018-0559-z

3.1.1 Material suplementario

El material suplementario del artículo precedente se encuentra en el siguiente enlace: https://link.springer.com/article/10.1007%2Fs11120-018-0605-x

4. CAPÍTULO IV: IDENTIFICACIÓN DE REGIONES DEL GENOMA ASOCIADOS CON LA PARTICIÓN DE LA ENERGIA EN LA FOTOSÍNTESIS

En este artículo utilizamos una estrategia de mapeo asociativo de genoma completo (GWAS) para de identificación de loci (QTL) asociados a rasgos de partición de energía durante la fase fotoquímica de la fotosíntesis. Además en este trabajo, establecimos una estrategia analítica para la definición cuantitativa de la calidad espectral de la luz actínica incidente con la cual realizamos las mediciones de partición de energía en el fotosistema II. Para generar el ambiente lumínico en el cual crecieron las plantas se utilizó el sistema en base LED de luz blanca desarrollado en Quero et al. (2019) (ver capítulo II de esta tesis). Las condiciones de temperatura, humedad, intensidad y la calidad espectral de la luz (ambiente HWL) utilizada para evaluar la población de mapeo se describe en Quero et al. (2019) (ver capítulo II de esta tesis).

Como población de mapeo para el análisis de GWAS se utilizó una sub-muestra de 152 líneas de las 324 líneas de subgrupo *indica* evaluadas para rasgos de calidad en Quero et al. (2018) (ver capítulo III de esta tesis). Para el análisis de la estructura genética de la población y para el análisis de GWAS se utilizaron los algoritmos y paquetes de R desarrollados en Quero et al. (2018).

La estrategia experimental y analítica utilizada en este trabajo permitió, a través de una estrategia de GWAS, identificar genes asociados a los principales parámetros que definen el rendimiento cuántico del PSII en arroz. Nuestro trabajo muestra la asociación entre los complejos antena de los fotosistema y el rendimiento cuántico potencial del PSII, así como la relacion de regiones que codifican para proteínas vinculadas con PSI en las distribución de energía durante el proceso fotoquímico de la fotosíntesis. Más estudios son necesarios para establecer claramente el mecanismo de acción de la calidad espectral de la luz sobre el PSI y como esto define la partición de energía del PSII.

4.1 GENETIC ARCHITECTURE OF PHOTOSYNTHESIS ENERGY PARTITIONING AS REVEALED BY A GENOME-WIDE ASSOCIATION APPROACH

Photosynthesis Research
https://doi.org/10.1007/s11120-020-00721-2

ORIGINAL ARTICLE

Genetic architecture of photosynthesis energy partitioning as revealed by a genome-wide association approach

Gastón Quero[1] · Victoria Bonnecarrère[2] · Sebastián Simondi[3] · Jorge Santos[4] · Sebastián Fernández[5] · Lucía Gutierrez[6,7] · Silvia Garaycochea[2] · Omar Borsani[1]

Received: 11 October 2019 / Accepted: 10 February 2020

Abstract

The photosynthesis process is determined by the intensity level and spectral quality of the light; therefore, leaves need to adapt to a changing environment. The incident energy absorbed can exceed the sink capability of the photosystems, and, in this context, photoinhibition may occur in both photosystem II (PSII) and photosystem I (PSI). Quantum yield parameters analyses reveal how the energy is managed. These parameters are genotype-dependent, and this genotypic variability is a good opportunity to apply mapping association strategies to identify genomic regions associated with photosynthesis energy partitioning. An experimental and mathematical approach is proposed for the determination of an index which estimates the energy per photon flux for each spectral bandwidth (Δ_λ) of the light incident (QI index). Based on the QI, the spectral quality of the plant growth, environmental lighting, and the actinic light of PAM were quantitatively very similar which allowed an accurate phenotyping strategy of a rice population. A total of 143 genomic single regions associated with at least one trait of chlorophyll fluorescence were identified. Moreover, chromosome 5 gathers most of these regions indicating the importance of this chromosome in the genetic regulation of the photochemistry process. Through a GWAS strategy, 32 genes of rice genome associated with the main parameters of the photochemistry process of photosynthesis in rice were identified. Association between light-harvesting complexes and the potential quantum yield of PSII, as well as the relationship between coding regions for PSI-linked proteins in energy distribution during the photochemical process of photosynthesis is analyzed.

Keywords Actinic light · Candidate genes · GWAS · Quantum yields

Introduction

The photosynthesis process is determined by the intensity level and spectral quality of the light (Jones and Kok 1966; McCree 1971; Allakhverdiev and Murata 2004; Zavafer et al. 2015b; Landi et al. 2020). Both parameters, jointly referred to as light environment, determine the energy conversion processes in plant cells (DeLucia et al. 1996; Campbell and Norman 1998; Murata et al. 2007; Nobel 2009; Brodersen and Vogelmann 2010; Smith et al. 2017). If the energy absorbed exceeds the sink capability of the photosystems, photoinhibition may occur in both photosystem II (PSII) and photosystem I (PSI) (Klimov et al. 1990; Allakhverdiev et al. 2003; Allakhverdiev and Murata 2004; Hakala et al. 2005; Miyake et al. 2009; Müh et al. 2012; Campbell and Tyystjärvi 2012; Murata et al. 2012; Derks et al. 2015).

In addition, as mentioned by Quero et al. (2019), photoinhibition is the result of different variables, such as the inactivation and repair rate of PSII and PSI (Allakhverdiev et al. 2005, 2007; Murata et al. 2007), the size and heterogeneity of PSII (Mehta et al. 2010; Albanese et al. 2016), the cyclic flow of electrons through PSI (Nishiyama et al. 2011; Murata and Nishiyama 2017), and the PSII–PSI relation (Tikkanen and Aro 2012; Tikkanen et al. 2014; Brestic et al. 2016).

On the other hand, photoinhibition is wavelength-dependent (Jones and Kok 1966; Ohnishi et al. 2005; Terashima et al. 2009; Takahashi et al. 2010; Vass 2012; Schreiber et al. 2012; Schreiber and Klughammer 2013; Zavafer et al. 2015b, 2017; Lysenko et al. 2018). The absorption of light by the manganese in the oxygen-evolving complex (OEC)

Electronic supplementary material The online version of this article (https://doi.org/10.1007/s11120-020-00721-2) contains supplementary material, which is available to authorized users.

✉ Gastón Quero
gastonquero@fagro.edu.uy

Extended author information available on the last page of the article

Published online: 18 February 2020

induces photoinhibition processes (Takahashi et al. 2010; Schreiber and Klughammer 2013; He et al. 2015; Zavafer et al. 2015a). The effect on manganese cluster is associated with the light spectral quality (Hakala et al. 2005; Oguchi et al. 2011a, b; Zavafer et al. 2017).

The effect of photoinhibitory processes in PSII could be measured through the determination of the PSII energy partitioning (Lazár 2015), revealing the destination of the incident energy and allowing the differentiation of photochemical and dissipation processes (Zivcak et al. 2015, 2018; Quero et al. 2019). Energy partitioning is estimated by quantum yield parameters (Dall'Osto et al. 2015). One way of measuring quantum yield parameters is through the determination of chlorophyll fluorescence emission in PSII (Genty et al. 1989; Baker 2008; Klughammer and Schereiber 2008; Lazár 2015). Chlorophyll emission can be determined using the pulse amplitude modulation (PAM) technique (Kalaji et al. 2014, 2017; Goltsev et al. 2016).

The following quantum yield parameters can be estimated: (i) the quantum yields of PSII (Φ_{PSII}), (ii) the quantum yields of non-photochemical quenching (Φ_{NPQ}), and (iii) the quantum yields of the basal energy dissipation (Φ_{NO}). Φ_{PSII} is directly related to the rate of electron transfer in PSII toward biochemical processes, Φ_{NPQ} reflects the quantum yield of regulatory light-induced non-photochemical quenching, and Φ_{NO} reflects the quantum yield of constitutive non-regulatory (basal or dark) non-photochemical energy dissipation processes (Genty et al. 1989; Krause and Jahns 2003; Kramer et al. 2004; Hendrickson et al. 2005; Klughammer and Schreiber 2008; Ahn et al. 2009; Kasajima et al. 2009; Chen et al. 2012; Brestic et al. 2016). The energy partitioning analysis is complemented by the quantification of maximum quantum yield in darkness (Φ_{Po}) and in light ($\Phi_{PSIIpot}$), and the determination of the proportion of open reaction center at the time t in PSII (qL) (Kasajima et al. 2009) and coefficient of photochemical quenching based on the ''puddle'' model (qP) (Zivcak et al. 2014). Φ_{Po} and $\Phi_{PSIIpot}$ describe the stability and maximum capacity of PSII in darkness and in light, respectively, while qL and qP helps to understand the causes of differences in the quantum yield (Kramer et al. 2004; Kasajima et al. 2009; Lazár 2015). In addition to the indirect parameters mentioned above, the inclusion of direct fluorescence parameters complements the analysis of PSII energy partitioning. These direct parameters, such as F_o and F'_o, represent minimal fluorescence from dark- and light-adapted leaf, respectively (Baker 2008); F_t is the actual fluorescence for light-adapted states in t (time) (Lazár 2015); F_m and F'_m represent maximal fluorescence from dark- and light-adapted leaf, respectively (Baker 2008). Considering the effect of light on photoinhibition, and therefore on quantum yield parameters, it is critical when evaluating photosynthesis processes to know the photosynthetic photon flux density (PPFD) and spectral quality of the environmental lighting wherein the plants grow and the actinic light is used in chlorophyll fluorescence determination (Pfündel et al. 2008; Oguchi et al. 2011a, b; Schreiber and Klughammer 2013; Kalaji et al. 2014; Laisk et al. 2014; He et al. 2015; Zavafer et al. 2015b; Lysenko et al. 2018; Pfündel et al. 2018; Su 2019; Zheng et al. 2019). Chlorophyll fluorescence studies can only be compared when using the same actinic light during the process. According to Oguchi et al. (2011a), the light spectral quality used for fluorescence studies can lead to an over- or underestimation of the chlorophyll fluorescence parameters. Thus, the results are dependent on the experimental method (Terashima et al 2009; He et al. 2015; Zavafer et al 2015b). Currently, conventional fluorometers for the application of PAM techniques are equipped with monochromatic actinic light or white actinic light (Schreiber and Klughammer 2013; Kalaji et al. 2014, 2017). In general, studies that use monochromatic equipment quantitatively report both PPFD and spectral quality levels (Oguchi et al. 2011a, b; Schreiber and Klughammer 2013; Hamdani et al. 2019; Zheng et al. 2019; Schreiber et al. 2019). However, in those studies using equipment that emit white actinic light, PPFD can be described quantitatively, but spectral distribution can only be described qualitatively in a specific spectral range (visible or white light) (Havurinne and Tyystjärvi 2017; Quero et al. 2019). This is a problem since the same PPFD of white light can be generated by different spectral compositions between 400 and 700 nm (approx.) (Sager and McFarlane 1997; Terashima et al. 2009; Zavafer et al 2015b). For this reason, it is necessary to quantitatively describe the spectral quality of the white actinic light used in the chlorophyll fluorescence emission studies.

As reported by Quero et al. (2019) in rice (*Oryza sativa* L.), the quantum yield parameters are genotype-dependent. Therefore, diverse populations can be used to identify the regions responsible for the quantum yield parameters. Genome-wide association studies (GWAS) have successfully identified genomic regions associated with complex traits in rice using diverse genotypic panels or breeding populations with narrow variability (Kraakman et al. 2004; Gore et al. 2009; Bergelson and Roux 2010; Huang et al. 2010, 2012; Famoso et al. 2011; Zhao et al. 2011; Chen et al. 2014; McCouch et al. 2016; Zhu et al. 2016; Quero et al. 2018). Furthermore, QTL and candidate genes associated with chlorophyll fluorescence parameters and photoinhibition have been identified in several spp. through GWAS (Hao et al. 2012; Ortiz et al. 2017; Herritt et al. 2018; Rapacz et al. 2019). QTL and candidate genes associated with Φ_{NPQ} were identified in rice using biparental populations (Gu et al. 2012; Hu et al. 2009; Kasajima et al. 2011). Moreover, Gu et al. (2012) and Hu et al. (2009) found QTL in association with Φ_{PSII} and chlorophyll fluorescence parameters, respectively.

Recently, Wang et al. (2017), using a combination of GWAS and biparental populations, identified genes that regulate photoprotection mechanisms in rice.

The aim of this study was to identify genomic regions and candidate genes related with the energy partitioning process through the association among genotypic variability and direct and indirect chlorophyll fluorescence parameters in a rice breeding population. To achieve the objective and to allow for the comparison with other mapping studies, a quantitative description of the actinic light spectral quality of chlorophyll fluorescence is proposed.

Materials and methods

Plant materials

A total of 154 genotypes from the National Rice Breeding Program Population (hereinafter Rice population) of the National Institute of Agricultural Research (INIA) were used as GWAS population. The evaluated population included 152 advanced inbred lines and two cultivars of *indica* subspecies: El Paso 144 (Yan et al. 2007) and INIA Olimar (Blanco et al. 2004).

Seeds were pre-germinated and selected by uniformity in seedling development. After 5 days, one seedling was transferred to an individual cylinder pot of 850 ml. Plants were grown in a custom-built growth room at 25 °C, 50–60% RH and a 12/12 h darkness/light cycle.

Experimental design

Plants were grown in sand:vermiculite (1:1) and watered with Yoshida medium (Yoshida et al. 1976) every three days. To phenotype all rice advanced inbred line, three assays were performed using a partially replicated design (PREP) (Cullis et al. 2006), with replicated genotypes arranged in all alpha resoluble incomplete block design with four checks. In each assay, three advanced inbred lines and four checks were evaluated with three replications, while all remaining lines were evaluated with only one replication per assay. Each pot containing one plant represented one experimental unit or replicate. Pots were arranged in such a way as to minimize the superposition of leaves to achieve a uniform incidence of light (ESM_1). Analyses were performed on the newest expanded leaf in the V5 stage (Counce et al. 2000) (ESM_1). According to the author, this stage is defined as collar formation on leaf 5 of the main stem. Conditions during fluorescence measurement are identical to plant growing conditions. All the advance inbred lines showed the same phenological state during the evaluated growth period.

Light environment

Environmental lighting wherein the plants were grown was generated by a light system based on LED source (Quero et al. 2019). The system was designed using white and blue LED lights which allow a radiation emission with the spectral quality range from 400 to 700 nm (Fig. 1a), also the system control quantity and quality of light. Maximum PPFD with this spectral quality was 1427 µmol photons m^{-2} s^{-1}

a

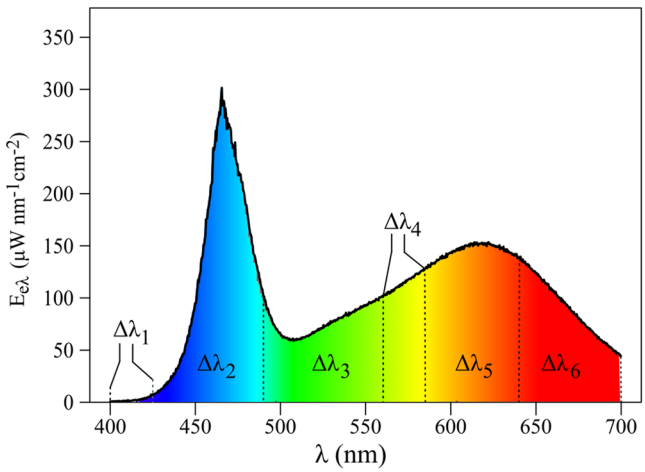

b

Δλ (nm)	PPFD (µmol $m^{-2}s^{-1}$)	E_e (J $m^{-2}s^{-1}$)	QI (J $µmol^{-1}$)	QI %
$Δλ_1$	1.93	0.55	0.29	21.4
$Δλ_2$	341.64	87.64	0.26	19.1
$Δλ_3$	240.70	54.64	0.23	16.7
$Δλ_4$	136.05	28.42	0.21	15.0
$Δλ_5$	409.12	79.91	0.20	15.0
$Δλ_6$	297.75	53.64	0.17	13.0
400 -700	1427.1	304.83	1.35	100

Fig. 1 Light environment: photon flux density and spectral quality. **a** Spectral energy flux (1427.1 µmol photons m^{-2} s^{-1}) of light environment emitted by light system, based on LED source. $E_{eλ}$ is the spectral energy flux. **b** Quantification of energy in each spectral bandwidth. λ is the specific wavelength. $Δ_λ$ is $λ_i - λ_{i-1}$, $Δ_{λ_1}$ (400–425), $Δ_{λ_2}$ (425–490), $Δ_{λ_3}$ (490–560), $Δ_{λ_4}$ (560–585), $Δ_{λ_5}$ (585–640), $Δ_{λ_6}$ (640–700), E_e is energy flux, PPFD is photosynthetic photon flux density, QI = E_e $PPFD^{-1}$ is energy by photon flux density or the percentage of E_e $PPFD^{-1}$ among the total

reached at "noon". The photoperiod described previously consisted of 12 h of light with an increment of the radiation in the first 6 h and a decrease in the radiation in the next 6 h. Level and kinetic of increase and decrease of radiation were settled using as reference the measured levels of a sunny day of October in the geographical region of rice cultivation in Uruguay (33° 13′ 51″ S 54° 22′ 56″ W).

Quantitative description of spectral quality of incident light

Light environment: photon flux density and spectral quality

The spectrum and intensity of light environment were measured using a spectroradiometer (USB2000 + spectrometer, Ocean Optics, Duiven, The Netherlands) which was calibrated against a standard light source supplied by the equipment. The sensor of spectroradiometer was localized at 30 cm from the center of the light source, where the closer leaf is (ESM_1). Spectroradiometer measures were registered as spectral energy flux ($E_{e\lambda}$), quantified as power by a unit of area (μW nm^{-1} cm^{-2}). Estimation of energy flux (E_e) and photosynthetic photon flux density (PPFD) in each spectral bandwidths (Δ_λ) was performed by numerical integration.

The integration analysis allowed the estimation of $E_{e\lambda}$ in each specific wavelength in the complete interval of visible light spectrum (400–740 nm) (Fig. 1). The spectral bandwidths (Δ_λ) were defined as described by Nobel (2009). Calculation of E_e and PPFD values for each Δ_λ and the unit conversion is describe in details in Supplementary Material (ESM_2).

Actinic light: photon flux density and spectral quality

The photon flux density and spectral quality of the white actinic light emitted by the PAM Chlorophyll fluorometer (FMS1, Hansatech, King's Lynn, UK) was performed as is described for Light environment. The sensor of the spectroradiometer was located at the end of the PAM's optic fiber, such as the leaf's adaxial surface when performing measurements (ESM_3). Spectroradiometer measures were registered as spectral energy flux ($E_{e\lambda}$), quantified as power by a unit of area (μW nm^{-1} cm^{-2}). Unlike the strategy used in the analysis of environmental lighting, in this case first, a non-lineal squares adjustment was performed with the data of the spectroradiometer which generated the function $f(\lambda)$ (ESM_2).

The function $f(\lambda)$ was used to model $E_{e\lambda}$ in the complete interval of visible light spectrum of PAM Chlorophyll fluorimeter utilized (Fig. 2a). Integration of $f(\lambda)$ gives us an estimation of $E_{e\lambda}$ in each wavelength (Δ_λ) in the interval between 400 and 740 nm. The spectral bandwidths (Δ_λ) were defined as described by Nobel (2009). Estimation of energy flux (E_e) and photosynthetic photon flux density (PPFD) in each spectral bandwidth (Δ_λ) was performed by analytically integrating the function, $f(\lambda)$, mentioned above (ESM_2).

With the main goal being the full characterization of the light spectrum in each wavelength interval of both light sources, QI is proposed as an index by establishing the ratio between E_{ei} and $PPFD_{ei}$ ($QI = E_{ei}\ PPFD_{ei}^{-1}$). Two main features are fully condensed in the QI index, namely the number of photons and their associated energy. We can observe from Figs. 1b and 2b that different values from this coefficient are computed for each wavelength interval and, the relative contribution (in percentage) to the total energy is also provided. A comparison of the values of these coefficients and the shape of the irradiance curve (Figs. 1a, 2a) clearly show in detail the energy available in any portion of the light spectrum.

Phenotyping of Rice population

Chlorophyll fluorescence parameters

The Rice population was phenotyped for direct chlorophyll fluorescence parameters, such as F_o, F'_o, F_t, F_m and F'_m. F_o and F'_o represent Minimal fluorescence from dark- and light-adapted leaf, respectively (Baker 2008); F_t is the actual fluorescence for light-adapted states in the time t (Lazar 2015); F_m and F'_m represent Maximal fluorescence from dark- and light-adapted leaf, respectively (Baker 2008).

Fluorescence parameter was obtained in vivo using a PAM Chlorophyll fluorometer (FMS1, Hansatech, King's Lynn, UK) after 45 min of dark adaptation at room temperature (ESM_1). A defined spectrum actinic light of 1503 μmol m^{-2} s^{-1} was used during the period of adaptation to light (200 s). For F_m and F'_m determination, a saturating pulse light of 9200 μmol photons m^{-2} s^{-1} was used.

The maximal quantum yield of PSII photochemistry for a dark-adapted state, Φ_{Po}, was calculated as follows(Kitajima and Butler 1975):

$$\Phi_{Po} = F_m - F_o F_m^{-1} = F_v F_m^{-1}$$

The maximal quantum yield of PSII photochemistry for the light-adapted state, $\Phi_{PSIIpot}$, was calculated as follows(Oxborough and Baker 1997):

$$\Phi_{PSIIpot} = F'_m - F'_o F'^{-1}_m = F'_v F'^{-1}_m$$

The fraction of open PSII centers at the time t, qL, was calculated as follows(Kasajima et al. 2009):

$$qL = F_t^{-1} - F'^{-1}_m)(F_o^{-1} - F'^{-1}_m)^{-1}$$

a

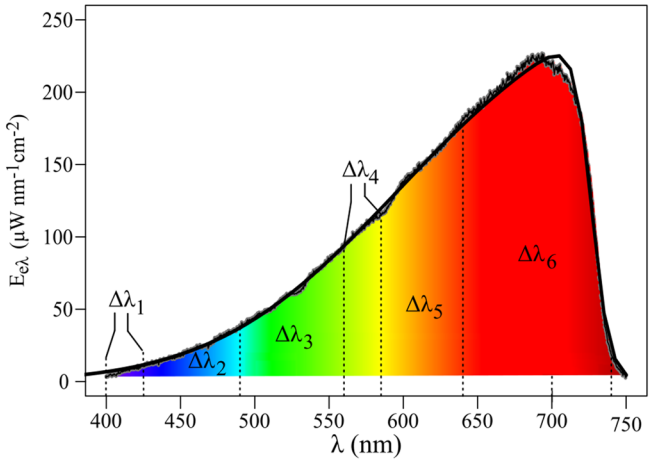

b

Δλ (nm)	PPFD (μmol m^{-2}s^{-1})	E_e (J m^{-2}s^{-1})	QI (J μmol^{-1})	QI %
$\Delta\lambda_1$	6.3	1.8	0.28	21.1
$\Delta\lambda_2$	57.0	14.7	0.26	19.1
$\Delta\lambda_3$	196.7	44.4	0.23	16.7
$\Delta\lambda_4$	125.5	26.2	0.21	15.5
$\Delta\lambda_5$	423.2	82.4	0.19	14.4
$\Delta\lambda_6$	694.3	123.8	0.17	13.2
400 -740	1503	293.3	1.35	100

c

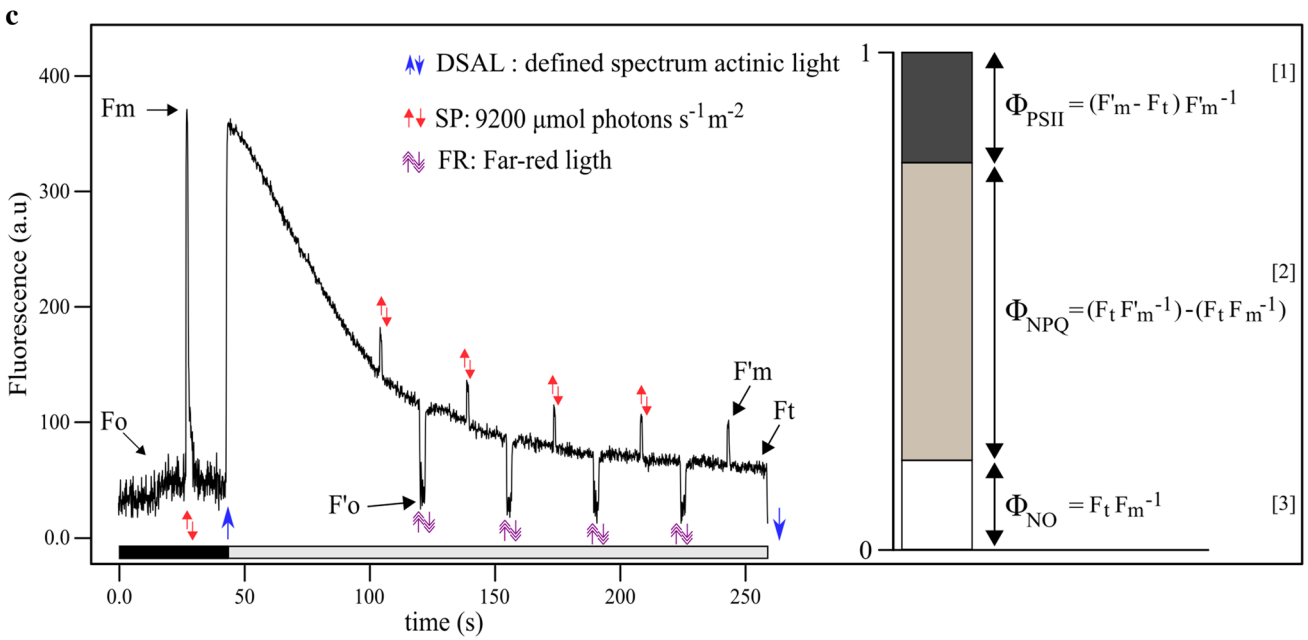

Fig. 2 Spectrum actinic light used for fluorescence quenching analysis. **a** Spectral energy flux (1503 μmol photons m^{-2} s^{-1}) of a defined spectrum actinic light (DSAL) emitted by the pulse amplitude modulation (PAM) Chlorophyll fluorometer. $E_{e\lambda}$ is the spectral energy flux; $f(\lambda)$ is the function used to quantify $E_{e\lambda}$ in each spectral bandwidth. **b** Quantification of energy in each spectral bandwidth. λ is the specific wavelength. $\Delta\lambda$ is $\lambda_i - \lambda_{i-1}$, Δ_{λ_1} (400–425), Δ_{λ_2} (425–490), Δ_{λ_3} (490–560), Δ_{λ_4} (560–585), Δ_{λ_5} (585–640), Δ_{λ_6} (640–740), E_e is energy flux, PPFD is photosynthetic photon flux density, QI = E_e PPFD^{-1} is energy by photon flux density or the percentage of E_e PPFD^{-1} among the total. **c** Fluorescence quenching analysis using modulated fluorescence. A dark-adapted leaf is exposed to a DSAL. Blue up and down arrows indicate that light is turned on or off, respectively. Red arrows indicate the position of saturating pulses (SP). A double head arrow indicates far red light pulse (FR). F_o and F'_o represent Minimal fluorescence from dark- and light-adapted leaf, respectively; F_t is the actual fluorescence for light-adapted states in the time t; F_m and F'_m represent Maximal fluorescence from dark- and light-adapted leaf, respectively. The relationship between quantum yields and determining equations is shown on the right. Φ_{PSII} is the quantum yield of PSII, Φ_{NPQ} is the quantum yield of non-photochemical quenching, and Φ_{NO} is the quantum yield of constitutive non-regulatory (basal or dark) non-photochemical dissipation processes

The coefficient of photochemical quenching (qP) was calculated as follows(Zivcak et al. 2014):

$$qP = \left(F'_m - F_t\right)\left(F'_m - F_o\right)^{-1}$$

Energy partitioning: quenching analyses

Quantification of energy partition in the PSII was determined by the quantum yield of three de-excitation processes using the chlorophyll fluorescence parameters. For this objective,

a quenching analysis (light-adapted plants) was performed (Fig. 2c). In this analysis, all process of energy absorbed by PSII are equal to 1 (Demmig-Adams et al. 1996; Kramer et al. 2004; Hendrickson et al. 2004; Logan et al. 2014):

$$\Phi_{PSII} + \Phi_{NPQ} + \Phi_{NO} = 1,$$

where Φ_{PSII} is the quantum yields of PSII, Φ_{NPQ} is the quantum yields of non-photochemical quenching, and Φ_{NO} is the quantum yield of constitutive non-regulatory (basal or dark) non-photochemical dissipation processes. The quenching analysis of Φ_{PSII} was calculated as Eq. 1 (Fig. 2c) (Genty et al. 1989; Baker 2008). Φ_{NPQ} and Φ_{NO} were calculated as Eqs. 2 and 3, respectively (Fig. 2c) (Hendrickson et al. 2004; Klughammer and Schreiber 2008).

Genotyping of Rice population

The Rice population was genotyped using a Genotyping-by-sequencing (GBS) strategy. DNA was extracted from young leaf tissue using Qiagen DNeasy kit. DNA samples were submitted in 96-well plates, digested with the restriction enzyme ApeKI and pools of 96 barcoded samples libraries were prepared using the protocol described by Elshire et al. (2011). GBS library construction and sequencing were done at the Biotechnology Resource Center of Cornell University. A GA Ilumina Sequencer was used. A total of 400 Gb of sequence data of 100 base read length (genome coverage) of 0.6 × were obtained. Single-nucleotide polymorphisms (SNP) were called from fastq files via the TASSEL version 3.0 genotyping-by-sequencing pipeline (Glaubitz et al. 2014). Alignment with the Michigan State University Nipponbare reference genome version 7.0 (https://rice.plantbiology.msu.edu/pub/data/Eukaryotic_Projects/o_sativa/annotation_dbs/pseudomolecules/version_7.0/, accessed 10 august 2019) was performed with Bowtie version 2 (Langmead and Salzberg 2012). To obtain the final SNP matrix, SNPs with over 50% missing data were removed from the analysis, as well as monomorphic SNPs and SNPs with a minor allele frequency under 1%. A matrix of 38,272 SNPs was used to perform the GWAS analyses.

Statistical analyses

Multivariate characterization of Rice population

To characterize the Rice population, phenotypic and genotypic data were analyzed according to the analytical pipeline described in ESM_4.

The multivariate characterization of the Rice population was accomplished by means of some exploratory analysis and visualization tools. First, the correlation and grouping of the photosynthesis variables was evaluated with a Principal Component Analysis (PCA) and a K-means clustering algorithm. A PCA of all standardized photosynthesis variables (F_o, F'_o, F_t, F_m, F'_m, Φ_{PSII}, Φ_{NPQ}, Φ_{NO}, Φ_{Po}, $\Phi_{PSIIpot}$, qL and qP) was conducted using the *PCA* function of the *FactoMineR* (Lê et al. 2008) package in R Statistical Software (R Core Team 2018). Photosynthesis variables were classified in groups, based on the coordinates of the PCA, using the *k*-means clustering algorithm to define the optimal number of *k*-groups, using the function *k-means* of the *stats* package in R Statistical Software (R Core Team 2018). Second, genotypes were clustered in groups based the PCA of all the photosynthetic variables using a hierarchical clustering algorithm (HCPC). Genotypes were grouped based on similarity from the Euclidean distance using the Ward method and the number of groups was determined by the highest relative loss in inertia using the function *HCPC* of the *FactoMineR* (Lê et al. 2008) package in R Statistical Software (R Core Team 2018). Third, genotypes were clustered in groups based the PCA of the genotypic variables using a hierarchical clustering algorithm (HCPC) similar to the cluster based on photosynthesis variables. Finally, a correspondence analysis (CA) was performed from the contingency tables of the HCPC analysis from genotypic and the photosynthesis variables. The correspondence analysis was performed to visualize the relationship between the two grouping strategies (i.e., based on molecular markers and based on photosynthesis variables).The CA was conducted using the *CA* function of the *FactoMineR* (Lê et al. 2008) package in R Statistical Software (R Core Team 2018).

The total contribution (c_{total}) of each variable to each dimension (Dim1 and Dim2) of the PCA analysis was calculated as follows:

$$c_{total} = \left(c_1 eig_1 + c_2 eig_2\right)\left(eig_1 + eig_2\right)^{-1}$$

where c_1 and c_2 are the contributions of the variable on Dim1 and Dim2, respectively, and eig_1 and eig_2 are the eigenvalues of Dim1 and Dim1, respectively (Kassambara 2017).

Adjustment of phenotypic means

Best linear unbiased estimators (BLUEs) for each advanced inbred line were obtained with mixed models to include experimental design components using the following model:

$$y_{ij} = \mu + \alpha_i + \beta_j + \varepsilon_{ij}$$

where y_{ij} is the response variable, μ is the overall mean or intercept, α_i a random variable associated with the *i*th assay with $\alpha_i \sim N(0, \sigma^2_A)$, β_j is the effect of the *j*th advanced inbred line, and ε_{ij} is the residual error with $\varepsilon_{ij} \sim N(0, \sigma^2_\varepsilon)$. The model was adjusted in the R statistical software using the *lme4* package (Bates et al. 2015) in R Statistical Software (R Core Team 2018). The BLUEs were estimated using the

emmeans package (Russell 2019) in the R statistical software (R Core Team 2018). In all cases, BLUEs were further used as genotypic values for the GWAS analysis.

Statistical models for GWAS

The most common mixed models for GWAS were compared: naïve, kinship (Parisseaux and Bernardo 2004), and eigenvalue (Price et al. 2006; Malosetti et al. 2007). The best model was selected based on quantile–quantile plots (Schweder and Spjøtvoll 1982) (ESM_5). The GWAS analysis was performed in the R statistical software (R Core Team 2018) with the *lmem.gwaser* package (Gutierrez et al. 2016).

The eigenvalue was the selected model:

$$y = X\beta + Zu + \varepsilon,$$

where y is the vector of phenotypic means, X is the molecular marker score matrix, β is the vector of marker allelic effects, Z is an incidence matrix, u is the vector of polygene background effects with Var (u) being $2QV_G$ (Q is the matrix of PCA scores coefficients and V_G is the genetic variance), and ε is the residual error vector.

For QTL determination, the marker with the highest marker–trait association was chosen as an anchor and then, a sliding window of 1 Mb was used to identify all significant markers within that window. The window size was determined according to the linkage disequilibrium (LD) decay in each chromosome reported by Quero et al. (2018). Given the level of genetic relatedness in Rice population, markers in close proximity are in high LD, making it unlikely to have an isolated significant SNP. The threshold level for calling significant marker–trait associations was calculated using a p value corrected by multiple comparisons with the Li and Ji (2005) statistic at a 0.05 α level.

Identification of candidate genes within associated genomic regions

The total genes located within a QTL region were manually retrieved from the Michigan State University public gene annotation database (https://rice.plantbiology.msu.edu/downloads_gad.shtml, accessed 1 July 2019). The gene ontology annotation was used to filter photosynthesis-related genes. The following words were used as filters in the gene ontology database: photosynthesis, chloroplast, thylakoid, and chlorophyll.

Results

Strategy for the quantitative determination of spectral quality of incident light

Experimental and mathematical approaches proposed by this study led to the identification of QI. This index estimates the energy per photon flux for each spectral bandwidth (Δ_λ) of the light incident (Figs. 1, 2b). Based on QI, the spectral quality of the plant growth, environmental lighting, and the actinic light of PAM were quantitatively very similar (Figs. 1b, 2b). In both spectra, the blue light fraction represented by the Δ_{λ_1} and Δ_{λ_2} (400–425, 425–490, respectively) represent almost the 40% of the total energy by photon flux in all wavelength intervals; meanwhile, the red light fraction (Δ_{λ_6}, 640–740 nm) represent less than 15% of the total. On the other hand, it is important to mention that in both spectra more than 50% of the total QI in the analyzed spectral band refers to blue light and green light fractions of visible light (Figs. 1, 2).

Energy partitioning is variable among rice advanced inbred lines

Of all the evaluated PSII energy partition processes, the energy dissipation in a regulated manner was the highest, represented as Φ_{NPQ}. The average value of Φ_{NPQ} was 0.57, within a range of 0.44 to 0.69 (Fig. 3a). After regulated heat dissipation, the most important energy sink were the unregulated dissipative processes or Φ_{NO}. The Φ_{NO} had an average value of 0.24, with a distribution that goes from 0.12 to 0.4 (Fig. 3a). Finally, photochemical processes are those which consume less energy in PSII, represented as Φ_{PSII}, with an average value of 0.19 within a range of 0.1 and 0.33 (Fig. 3a). Therefore, in this Rice population, approximately 80% of the energy that reaches the PSII is dissipated as heat ($\Phi_{NPQ} + \Phi_{NO}$) and only 20% is used in the photochemical processes (Φ_{PSII}). Nevertheless, when analyzing the quantum yield values of each advanced inbred line that make up the mapping population individually, a decrease in Φ_{PSII} is not the result of the same proportional variation in Φ_{NPQ} in regard to Φ_{NO}. Hence, the energy partition in rice is genotype-dependent (Fig. 3b).

Rice population is structured at genotypic and phenotypic level

The PCA of all fluorescence variables shows that about 72% of the variation is explained by the first two dimensions (PC1 and PC2) (Fig. 4a). About 51% of the variation is explained by PC1 and about 21% of the variation is

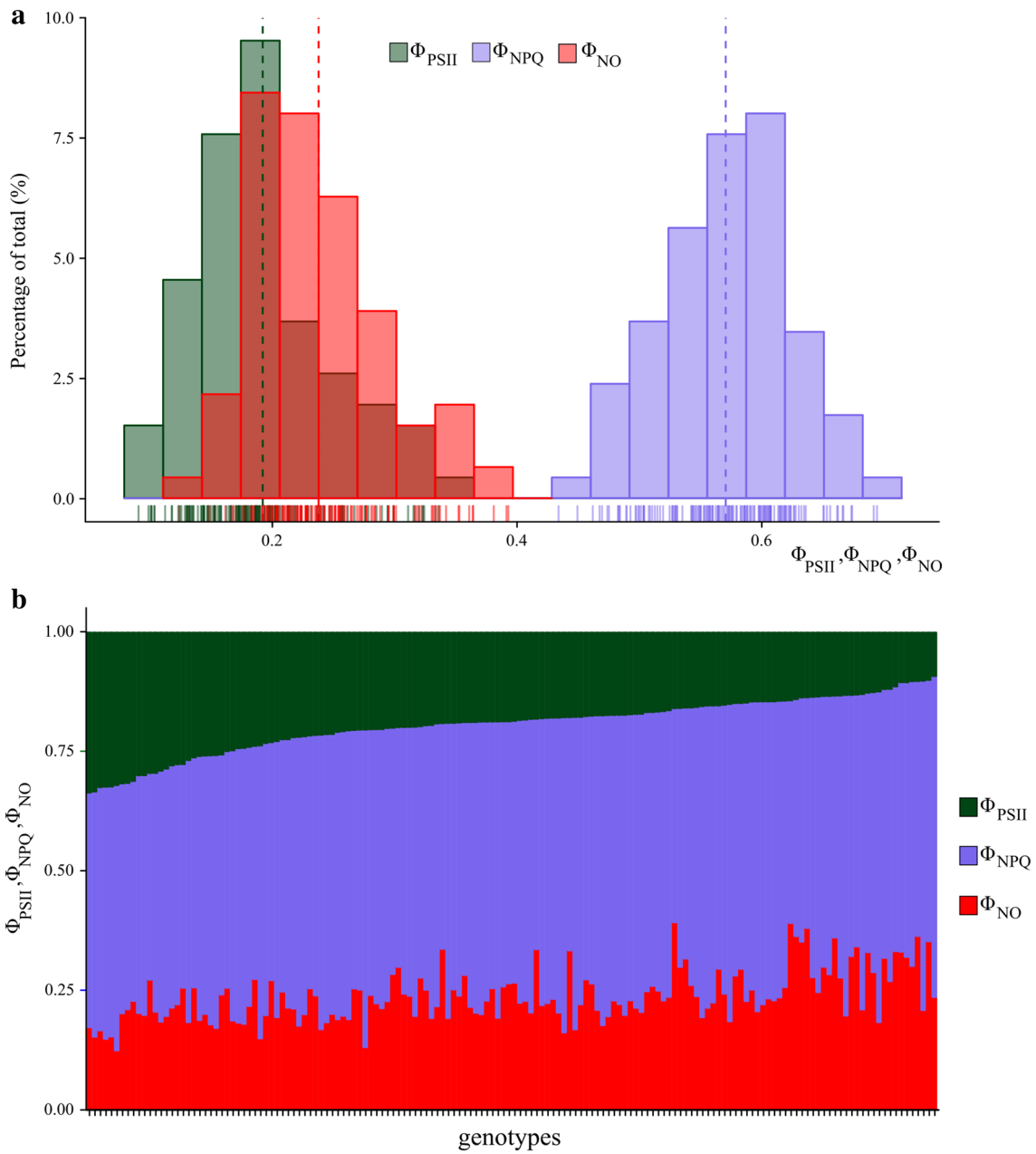

Fig. 3 Quantum yield parameters in the Rice population. **a** Frequency distribution of Φ_{PSII}, Φ_{NPQ}, and Φ_{NO} in the Rice population. **b** Energy partition of each advanced inbred line from the Rice population. Φ_{PSII} is the quantum yields of PSII, Φ_{NPQ} is the quantum yields of non-photochemical quenching, and Φ_{NO} is the quantum yields of basal energy dissipation

explained by PC2 (Fig. 4a). The percentages of variation for the remaining dimensions are shown in ESM_6. The total contribution of energy partitioning parameters of PSII to the variation explained by PC1 and PC2 was 24%. Each parameter contributes approximately 8% (Φ_{PSII} = 7.8%, Φ_{NPQ} = 7.9% and Φ_{NO} = 8.3%) to the total variation. In PC1, the variables which explain the majority percentage of the variance is the actual fluorescence for light-adapted states in t (F_t). The energy partitioning parameters of PSII with more relevance in this component is the Φ_{NO} (Fig. 4a and ESM_6). Respect to PC2 the variable with more incidence on this dimension is the Φ_{NPQ} (Fig. 4a and ESM_6).

The k-means clustering algorithm generated three clusters of fluorescence variables. It is relevant to note that in each of these clusters there is a quantum yield parameter. Cluster 1 (k_1) consists of six of the twelve fluorescence parameters evaluated (Φ_{NO}, $\Phi_{PSIIpot}$, F'_o, F_o, F'_m and F_t); cluster 2 (k_2) consists of three indirect parameters (Φ_{PSII}, qP and qL); and

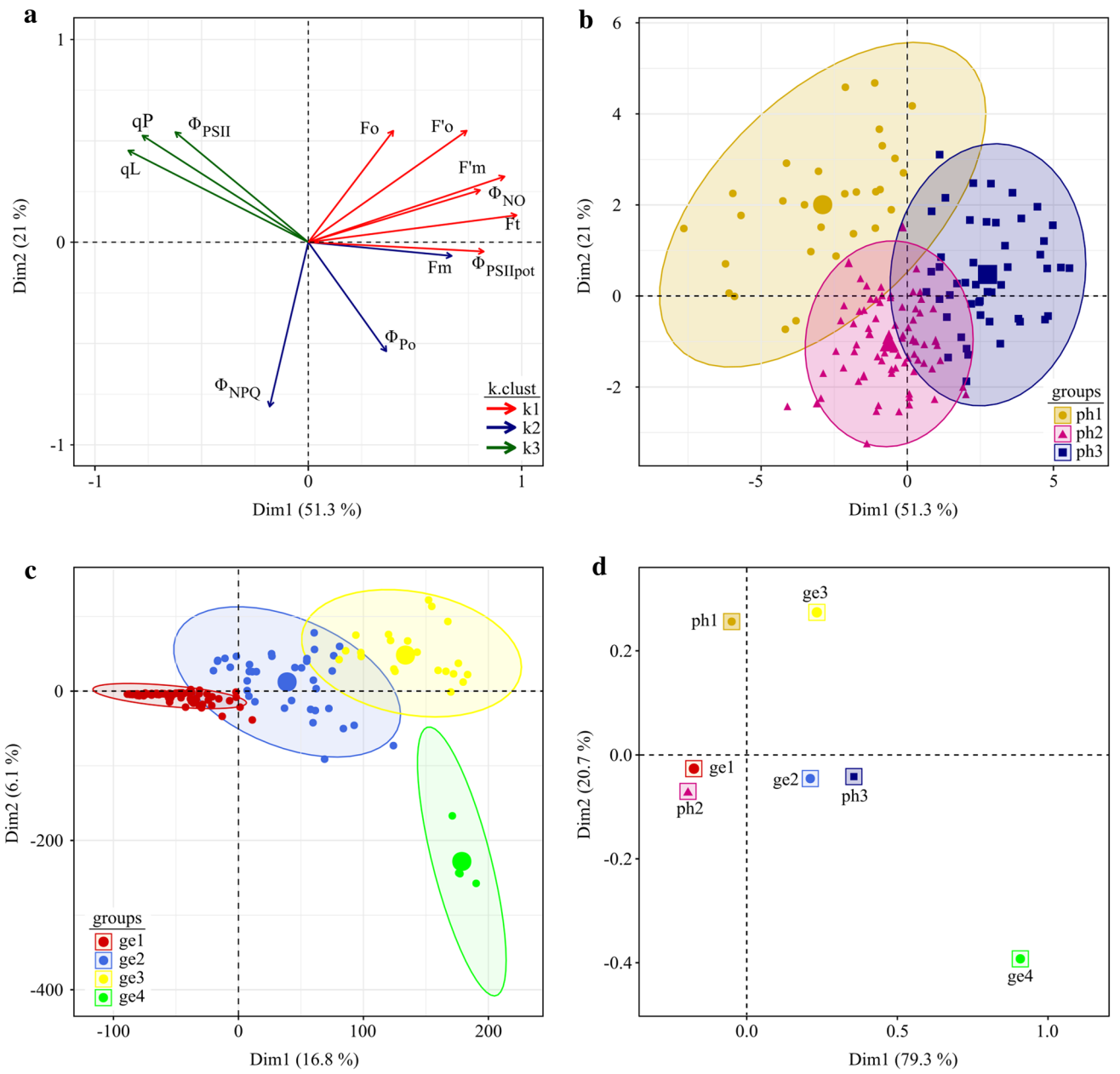

Fig. 4 Phenotypic and Genetic structure in Rice population. **a** Principal component analysis (PCA) for all fluorescence parameters. k_1, k_2, and k_3 groups were obtained by a *k*-means clustering algorithm. **b** Population structure calculated from all fluorescence parameters. ph_1, ph_2, and ph_3 groups were obtained by hierarchical clustering on principal component ($HCPC_{pheno}$). **c** Population structure calculated from genotypic data (molecular markers). ge_1, ge_2, ge_3, and ge_4 groups were obtained by $HCPC_{geno}$. **d** Correspondence analysis of the contingency table between groups based on phenotype and groups based on genotype

cluster 3 (k_3) consists of three parameters (Φ_{NPQ}, Φ_{Po} and F_m).

The HCPC analysis of the photochemical variables ($HCPC_{pheno}$) showed that, the mapping population can be separated into three main groups (Fig. 4b). The first group (ph_1) consists of 29 advanced inbred lines, a group 2 (ph_2) of 78 advanced inbred lines and a group 3 (ph_3) of 47 advanced inbred lines. Although the overlapping of ellipses shows that some lines could belong to one cluster or another, it is important to note that this strategy can be used to identify lines that are completely different when using all fluorescence variables analyzed together. In other words, the contrasting lines are those that are outside the intersection zones.

The genetic structure of the Rice population was determined by PCA analysis using 38,272 SNP. About 22.9%

of the variation is explained by the first two PC axis: 16.8% of the variation is explained by the PC1 (Dim1) and 6.1% by the PC2 (Dim2) (Fig. 4c). The HCPC analysis ($HCPC_{geno}$) identified four main groups (Fig. 4c). The first group (ge_1) consists of 92 advanced inbred lines, group 2 (ge_2) of 37 advanced inbred lines, group 3 (ge_3) of 21

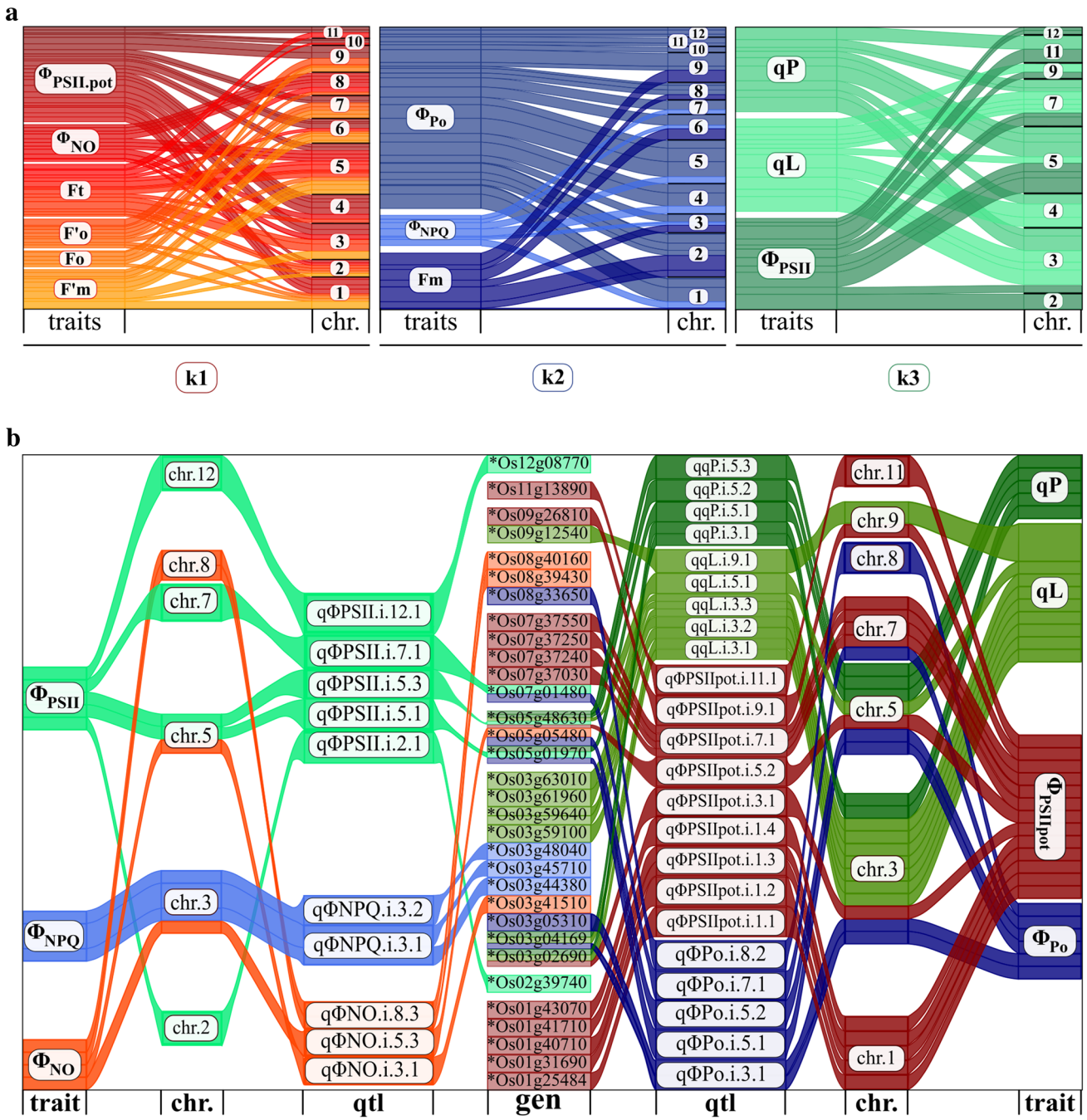

Fig. 5 Genetic architecture of photochemical processes. **a** Quantitative trait loci (QTL) associated with chlorophyll fluorescence parameters arranged according to phenotyping cluster groups: from left to right, cluster 1 (k_1), cluster 2 (k_2), and cluster 3 (k_3). **b** QTL and candidate genes associated with indirect parameters of chlorophyll fluorescence. Quantum yield parameters are shown on the left of the figure, and complementary indirect parameters on the right. On the left and right side the chr. column indicates the chromosomes in which are the QTL identified for each trait. In the central column are the identification of the genes that are in the region of the respective QTL. Φ_{PSII} is the quantum yields of PSII, Φ_{NPQ} is the quantum yields of the non-photochemical quenching, Φ_{NO} is the quantum yields of the basal energy dissipation, Φ_{Po} is the maximum quantum yield of PSII photochemistry for a dark-adapted state, $\Phi_{PSII.pot}$ is the maximum quantum yield of PSII photochemistry for the light-adapted state, qL is the fraction of open PSII centers at the time t, and qP is the coefficient of photochemical quenching.*LOC. The id of the genes corresponds to Michigan State University Nipponbare reference genome version 7

advanced inbred lines, and group 4 (ge_4) of 4 advanced inbred lines.

The correspondence analysis between $HCPC_{pheno}$ and $HCPC_{geno}$ groups showed the following correspondence: ge_1 with ph_2, and ge_2 with ph_3. The relation between ge_3 and ph_1 is not clear. Finally, ge_4 was not associated with any group of the phenotypic structure (Fig. 4d). Phenotypic values (PC1 score) of these three associations are shown in ESM_6.

Rice genomic regions associated with chlorophyll fluorescence parameters

After the comparison of different mixed models for all fluorescence parameters, the eigenvalue model was selected based on QQ-plot (ESM_5). As expected for quantitative traits, a total of 143 QTL were identified (ESM_7). Genetic architecture of the fluorescence parameters evaluated in the Rice population is shown in Fig. 5.

For traits of k_1, ten QTL were identified for F'_m, five for F_o, nine for F'_o, fifteen for F_t, eleven for Φ_{NO}, and 24 for $\Phi_{PSIIpot}$ (Fig. 5a, ESM_7 and 8). For traits of k_2, seven QTL were identified for Fm, seven for Φ_{NPQ}, and twenty five for Φ_{Po} (Fig. 5b, ESM_7 and 9). For traits of k_3, eleven QTL were identified for Φ_{PSII}, eleven for qL, and nine for qP (Fig. 5c, ESM_7 and 10).

Shared QTL were found among photosynthesis traits (Table 1). Common QTL are those found in the same chromosomic regions, regardless of the size of genomic overlapping. For k_1 traits, 46 QTL were identified for more than one trait the only chromosome where there are no shared QTL is chromosome 11 (Table 1 and ESM_11). For the same cluster, in chromosome 5, there are 19 QTL in the same genomic region (Fig. 5a and ESM_11). Nine of these shared QTL are in an interval of 2 Mb between positions 26,477,010–28,446,984 (ESM_11). For k_2 traits, 5 QTL were identified in the same regions for Φ_{NPQ} and F_m (Table 1). These shared QTL are in chromosomes 1, 2, 5, 6, and 8 (Fig. 5a and ESM_11). On the other hand, for k_3 18 QTL were identified for more than one trait (Table 1). The shared QTL are in chromosomes 3, 4, 5, 7, 9, and 11 (Fig. 5a and ESM_11). For the k_3, in chromosome 5 there are 6 QTL in the same genomic region (Fig. 5a and ESM_8). It is worth noting that in chromosome 5 there are 22 QTL shared between k_1 and k_3, and 4 QTL shared between k_2 and k_3 (Table 1). Finally, in chromosomes 2, 3, 5, 7, and 8 there are shared QTL genomic regions for traits belonging to different clusters (Table 1 and ESM_11). Respect to energy partitioning parameters, QTL for Φ_{PSII} and Φ_{NO} were found in chromosomes 3 and 5 (Table 1 and ESM_11). However, no shared QTL of Φ_{NPQ} and Φ_{NO} or Φ_{PSII} were identified. The only shared QTL were found with Φ_{NO} and the rest of the fluorescence parameters with the exception of F_o and Φ_{NPQ}.

Rice candidate genes associated with energy partitioning parameters

To prioritize the selection of candidate genes, the work was focused on genes associated with quantum yield values (Φ_{PSII}, Φ_{NPQ}, Φ_{NO}) and indirect parameters associated with them ($\Phi_{PSIIpot}$, Φ_{Po}, qP and qL). Of all the annotated

Table 1 Number of genomic regions associated and shared among photosynthesis traits

	k_1						k_2			k_3		
	Φ_{NO}	$\Phi_{PSIIpot}$	F_t	F'_m	F'_o	F_o	Φ_{NPQ}	Φ_{po}	F_m	Φ_{PSII}	qP	qL
Φ_{NO}												
$\Phi_{PSIIpot}$	3											
F_t	7	8										
F'_m	2	4	9									
F'_o	2	2	1	3								
F_o		1			4							
Φ_{NPQ}												
Φ_{po}	3					1	1					
F_m	2						5					
Φ_{PSII}	2	1	3					2				
qP	3	4	5		1			2	6	6		
qL	1	3	2		1				4	4	8	

genes within the associated genomic region, 32 genes were selected. Initial analysis included the words photosynthesis, chloroplast, thylakoid and chlorophyll as filters for the browsing in the gene ontology database (Table 2).

Five genes were located in QTL associated with Φ_{PSII} (chr. 5, chr. 7 and chr. 12), two genes associated with Φ_{NPQ} (chr. 3), three genes associated with Φ_{NO} (chr. 3, chr. 5 and chr. 8), five genes associated with Φ_{Po} (chr. 3, chr. 5, chr. 7 and chr. 8), nine genes associated with $\Phi_{PSIIpot}$ (chr. 1, chr. 3, chr. 5, chr. 7, chr. 9 and chr. 11), five genes associated with qL (chr. 1, chr. 3, chr. 5 and chr. 9), and four genes associated with qP (chr. 3 and chr. 5). In chromosome 5, candidate genes associated with almost all traits measured in this study were found, except with Φ_{NPQ} (Fig. 5b).

In this work, from the 32 candidate genes selected, 22 of them are related to the electron transfer chain in the thylakoid membrane, while the remaining ten genes are associated with chlorophyll catabolism and chloroplast development. From the first group of 22 genes, seven refer to the antenna complex (LOC_Os01g40710, LOC_Os07g37240, LOC_Os07g37550, LOC_Os09g12540, LOC_Os09g26810, LOC_Os11g13890), one to the cytochrome

Table 2 Candidate genes associated and shared by photosynthetic parameters

Chr	QTL	Gene ID	Gene location (bp)	Gene product name*2
Chr. 1	$q\Phi_{PSIIpot.i.1.1}$	LOC_Os01g25484	14,446,910–14,453,474	Ferredoxin–nitrite reductase
	$q\Phi_{PSIIpot.i.1.2}$	LOC_Os01g31690	17,349,311–17,350,816	Oxygen-evolving enhancer protein 1
	$q\Phi_{PSIIpot.i.1.3}$	LOC_Os01g40710	23,003,671–23,005,010	High light inducible protein
	$q\Phi_{PSIIpot.i.1.3}$	LOC_Os01g41710	23,607,348–23,608,583	Chlorophyll a/b binding protein
	$q\Phi_{PSIIpot.i.1.4}$	LOC_Os01g43070	24,572,982–24,576,293	PsbP-related thylakoid lumenal protein 4
Chr. 2	$q\Phi_{PSII.i.2.1}$	LOC_Os02g39740	24,000,931–24,003,192	psaB translation factor
Chr. 3	qΦPSIIpot.i.3.1, qqP.i.3.1, qqL.i.3.1	LOC_Os03g02690	1,004,394–1,007,269	Dihydrodipicolinate reductase
	qΦPSIIpot.i.3.1, qqP.i.3.1, qqL.i.3.1	LOC_Os03g04169	1,909,201–1,919,541	ATP phosphoribosyltransferase, chloroplastic
	$q\Phi_{Po.i.3.1}$	LOC_Os03g05310	2,576,496–2,580,452	Pheophorbide a oxygenase
	$q\Phi_{NO.i.3.1}$	LOC_Os03g41510	23,086,275–23,090,306	Oxidoreductase
	$q\Phi_{NPQ.i.3.1}$	LOC_Os03g44380	24,959,107–24,961,777	9-cis-epoxycarotenoid dioxygenase 1 chloroplastic
	$q\Phi_{NPQ.i.3.1}$	LOC_Os03g45710	25,800,415–25,801,331	2Fe–2S iron–sulfur cluster binding domain containing protein
	$q\Phi_{NPQ.i.3.2}$	LOC_Os03g48040	27,309,857–27,312,904	2Fe–2S iron–sulfur cluster binding domain containing protein
	$qqL_{.i.3.2}$	LOC_Os03g59100	33,645,110–33,647,519	Pheophorbide a oxygenase
	$qqL_{.i.3.2,}$ $qqL_{.i.3.3}$	LOC_Os03g59640	33,955,198–33,961,962	Magnesium-chelatase subunit chlD
	$qqL_{.i.3.3}$	LOC_Os03g61960	35,122,440–35,124,356	2Fe–2S iron–sulfur cluster binding domain containing protein
	$qqL_{.i.3.3}$	LOC_Os03g63010	35,625,601–35,629,619	Plastid terminal oxidase
Chr. 5	qΦPo.i.5.1, qΦPSII.i.5.1 $qqP_{.i.5.1}$	LOC_Os05g01970	552,021–554,342	NAD dependent epimerase/dehydratase family protein
	qΦPo.i.5.2	LOC_Os05g05480	2,725,695–2,733,753	Putative Deg protease homologue, expressed
	$q\Phi_{NO.i.5.3}$, $q\Phi_{PSIIpot.i.5.2}$, $q\Phi_{PSII.i.5.3}$, $qqL_{.i.5.1}$, $qqP_{.i.5.2}$, $qqP_{.i.5.3}$	LOC_Os05g48630	26,477,010–28,446,984	Photosystem I reaction center subunit VI
Chr. 7	qΦPo.i.7.1, qΦPSII.i.7.1	LOC_Os07g01480	306,009–307,555	Photosystem II oxygen-evolving complex protein PsbQ family protein
	$q\Phi_{PSIIpot.i.7.1}$	LOC_Os07g37030	22,184,376–22,187,030	Cytochrome b6-f complex iron–sulfur subunit
	$q\Phi_{PSIIpot.i.7.1}$	LOC_Os07g37240	22,317,936–22,316,268	Chlorophyll a/b binding protein
	$q\Phi_{PSIIpot.i.7.1}$	LOC_Os07g37250	22,323,191–22,319,007	Thylakoid formation
	$q\Phi_{PSIIpot.i.7.1}$	LOC_Os07g37550	22,487,421–22,488,766	Chlorophyll a/b binding protein
Chr. 8	$q\Phi_{PSIIpot.i.8.3}$	LOC_Os08g33650	21,014,458–21,018,732	Similar to photosystem II protein I
	$q\Phi_{PSIIpot.i.8.3}$	LOC_Os08g39430	24,935,696–24,936,427	Thylakoid lumen protein
	$q\Phi_{PSIIpot.i.8.3}$	LOC_Os08g40160	25,416,106–25,418,793	Thylakoid lumen protein
Chr. 9	$qqL_{.i.9.1}$	LOC_Os09g12540	7,185,218–7,188,146	Chlorophyll a/b binding protein
	$q\Phi_{PSIIpot.i.9.1}$	LOC_Os09g26810	16,287,916–16,290,862	Chlorophyll a/b binding protein
Chr. 11	$q\Phi_{PSIIpot.i.11.1}$	LOC_Os11g13890	7,659,682–7,662,281	Chlorophyll a/b binding protein
Chr. 12	$q\Phi_{PSII.i.12.1}$	LOC_Os12g08770	4,506,723–4,507,879	Photosystem I reaction center subunit N

b6-f complex iron–sulfur subunit (LOC_Os07g37030), eight to PSI (LOC_Os03g02690, LOC_Os01g25484, LOC_Os03g45710, LOC_Os03g48040, LOC_Os03g61960, LOC_Os05g48630, LOC_Os12g08770, LOC_Os02g39740), and six to PSII (LOC_Os08g33650, LOC_Os01g43070, LOC_Os08g39430, LOC_Os08g40160, LOC_Os01g31690, LOC_Os07g01480).

On the other hand, five of these genes were found in QTL shared among traits. Such is the case of genes LOC_Os03g02690 and LOC_Os03g04169, located in QTL associated with $\Phi_{PSIIpot}$, qP and qL (qΦPSIIpot.i.3.1, qqP.i.3.1 and qqL.i.3.1). The gene LOC_Os05g01970 is located in QTL qΦPo.i.5.1, qΦPSII.i.5.1 and qqP.i.5.1, associated with Φ_{Po}, Φ_{PSII} and qP, respectively. The gene LOC_Os05g48630 is in qΦNO.i.5.3, qΦPSIIpot.i.5.2, qΦPSII.i.5.3, qqL.i.5.1, qqP.i.5.2 and qqP.i.5.3, associated with Φ_{NO}, $\Phi_{PSIIpot}$, Φ_{PSII}, qL and qP, respectively. Finally, the gene LOC_Os07g01480 is found in QTL qΦPo.i.7.1 and qΦPSII.i.7.1, associated with Φ_{Po} and Φ_{PSII}.

Discussion

Experimental characterization of the spectral quality of the environmental lighting and the actinic light used in this study allowed the quantitative description of its spectral. Thus, it was possible to work with a defined incident light spectrum. As reported by Terashima et al. (2009), Oguchi et al. (2011a), and Zavafer et al. (2015b), the lack of quantification of the spectral quality of white actinic light is a limitation for the interpretation and comparison of chlorophyll fluorescence results. This limitation is due to the fact that white light spectrum can build with of different intensities in each wavelength band. It is widely reported that the energy dissipation processes in PSII are closely linked to the spectral quality of the incident light (Jung and Kim 1990; Hakala et al. 2005; Ohnishi et al. 2005; Oguchi et al. 2011a, b; Schreiber and Klughammer 2013; Zavafer et al. 2015a, b; Hamdani et al. 2019; Zheng et al. 2019; Schreiber et al. 2019). Taking these considerations into account, in this work we proposed an index (QI) to quantify the spectral quality of actinic light, which defines the energy of the PPFD of each wavelength band. QI is proposed as an indicator for the quantitative description of the incident actinic light spectrum. Higher values of QI were obtained for blue and green bandwidth. This could explain why the dissipation process detected ($\Phi_{NPQ}+\Phi_{NO}$) are the final destination of the 80% of the energy reaches to PSII (Fig. 2a, b). Results agree with reported in Rice by Hamdani et al. (2019) who indicate that blue light increases the NPQ. Thus, the spectrum quality of incident light of this study is possible to infer that the high levels of $\Phi_{NPQ}+\Phi_{NO}$ observed could be associated with damage at manganese cluster of OEC (Hakala et al. 2005; Ohnishi et al. 2005; Terashima et al. 2009). The importance of thermal dissipation processes in PSII as a mechanism of photoinhibition or photoprotection in rice has been reported in numerous studies (Jiao et al. 2002; Kasajima et al. 2011; Murchie et al. 2015).

On the other hand, based on the values of QI, it was established that the spectral quality of the actinic light used for the determination of the fluorescence parameters is very similar to the spectral quality of the light environment in which the plants grew (Figs. 1b, 2b and ESM_2). In this sense, it can be inferred that the information generated on the energy partition processes of the PSII, based on the spectral quality of the actinic light, could be related to the effects of the light environment on the photosynthetic apparatus during plant growth. This is very important because it gives physiological support to the phenotyping strategy for the identification of genes related to photochemistry through GWAS.

The analysis of the PSII energy partitioning should be complemented with the use of multivariate analysis tools to reduce the dimensions of the fluorescence measurements (Goltsev et al. 2012; Rapacz et al. 2019). Analysis of PC indicates that Φ_{PSII} is related to both qP and qL, parameters associated frequently with models of excitation of the reaction center of PSII, "puddle" and "lake" models, respectively (Miyake et al. 2009; Zivcak et al. 2014). Agreeing with Miyake et al. (2009), a negative correlation between Φ_{Po} and qL was observed. This clustering strategy showed that all fluorescence variables can be grouped into three clusters. This contributes to the identification of rice advanced inbred lines with similar photochemical responses taking account of all variables in the same analysis and no analyzing the variables one by one.

Correspondence detected among the cluster generated by HCPC was performed using the first PCA component for all fluorescence parameters ($HCPC_{pheno}$) and obtained from genotypic information ($HCPC_{geno}$). This strengthens the idea that GWAS strategy is useful for identifying genes associated with regulation of photochemistry process in a Rice population. Also, correspondence among groups support the strategy of phenotypic clustering to select rice lines that are completely different when using all fluorescence variables analyzed together.

Although most of the genes that participate in the photosynthetic process are found in the chloroplast genome (Blankenship 2014; Herritt et al. 2018), genes encoding many of the structural proteins of PSII are located in the nuclear genome (Koussevitzky et al. 2007). For this reason, in this work it was possible to find 143 QTL associated with different photosynthetic processes, suggesting that selection and genetic improvement of these traits are possible (Frachebound et al. 2004; Kościelniak et al. 2005; Flood et al. 2011; Adachi et al. 2014, 2019; Ortiz et al. 2017).

QTL studies for chlorophyll fluorescence under optimal and stress conditions have been reported in rice (*Oryza sativa*) (Hu et al. 2009; Kasajima et al. 2011; Gu et al. 2012; Wang et al. 2017). In this work, we found that on chromosome 5 there is the largest amount of QTL shared between the different fluorescence parameters evaluated, 19 regions shared for k_1, one region for k_2, and six for the k_3. In addition, on chromosome 5, 22 QTL shared between k_1 and k_3, and 4 QTL shared between k_2 and k_3 were identified. Our results indicate that chromosome 5 has a significant importance on the genetic regulation of photochemistry of photosynthesis. This is consistent with several studies that report genomic regions of chromosome 5 related to the photosynthetic process (Zuo et al. 2007; Hu et al. 2009; Adachi et al. 2014, 2019; Ye et al. 2017).

To analyze the genetic architecture of photosynthesis, candidate genes linked to energy partitioning traits and other associated indirect parameters were selected. Most of the selected genes encode proteins of the subunits of the electronic transfer chain found in the thylakoid membrane (PSII, cytochrome b6f and PSI). In particular, genes encoding elements of the light-harvesting antenna complexes (LHCI and LHCII), reaction center and the manganese cluster belonging to the oxygen-evolving complex were found. Light-harvesting chlorophyll a/b-binding proteins are the most abundant proteins in the chloroplast and play a role in the light energy transference to the reaction center (Xia et al. 2012), and the expression level is regulated by light (Humbeck and Krupinska 2003). From 17 genomic loci in rice coding for the component of the light-harvesting complexes chlorophyll a/b-binding protein (Umate 2010), we were able to identify seven. In our study from the nine genes associated with $\Phi_{PSIIpot}$, five were associated with the light-harvesting chlorophyll a/b-binding (chromosomes 1, 7, 9 and 11). It is worth noting that $\Phi_{PSIIpot}$ is measured when all reaction centers of PSII are open, representing the potential quantum yield of PSII photochemistry for a light-adapted state (Lazár 2015). However, no regions coding for this protein associated with PSII were identified. According to the results obtained under our study conditions, light-harvesting complexes would be associated with the maximum PSII capacity in the light rather than with its operational capacity. On the other hand, the PsbP thylakoid lumen protein is codified at the nucleus level and plays an important role in the structural stability of PSII (Liu et al. 2012). In our work, the gene LOC_Os01g43070 that codes for this protein was found associated with the $\Phi_{PSIIpot}$. This gene was reported by Raorane et al. (2015) as downregulated in rice flag leaves during stress. Like the chlorophyll a/b-binding, PsbP participates in the structure of the PSII and is associated with the maximum capacity of the PSII and not with its functional operating capacity.

Here, the Φ_{PSII} was associated with a gene coding protein related to PSII oxygen-evolving complex (OEC) (LOC_Os07g01480) and three genes for PSI structural proteins (LOC_Os02g39740, LOC_Os05g48630, LOC_Os05g48630). These results suggest that the operational capacity of the PSII is related to the structural integrity of OEC; this makes sense in our work because the highest values of QI were observed in the blue bands of the incident light (actinic and light environment of growth) and these are the wavelengths that have a direct effect on the integrity of the OEC (Ohnishi et al. 2005). In turn, Φ_{PSII} was associated with genes encoding PSI structural proteins, which reinforces the idea that operational function of PSII depends on the flow of electrons through PSI (Nishiyama et al. 2011; Murata and Nishiyama 2017), and the PSII–PSI relation (Tikkanen and Aro 2012; Tikkanen et al. 2014; Brestic et al. 2016).

In the case of genes associated with Φ_{NPQ}, two of them code for 2Fe–2S iron–sulfur cluster binding domain containing protein, which are associated with ferredoxin related to PSI. This implies certain amount of energy must be dissipated in a regulated manner as heat and this linked to the final stages of the electron transfer chain in the chloroplast thylakoid. This is particularly important in rice, since Φ_{NPQ} is the main energy destination reaching PSII (Fig. 3a). In addition to the aforementioned genes, the LOC_Os03g44380 gene that codes for 9-cis-epoxycarotenoid dioxygenase (NCED3, chloroplastic) was also identified in a region associated with Φ_{NPQ}. This is particularly relevant, since this enzyme catalyzes the first limiting step of abscisic acid biosynthesis from carotenoids (Qin and Zeevaart 1999; Chernys and Zeevaart 2000). It is reported that carotenoids are a family of pigments related to photoprotection mechanisms and, therefore, to Φ_{NPQ} (Ruiz-Sola and Rodríguez-Concepción 2012; Pan et al. 2013; Adams et al. 2018; Malnoë 2018, Schreiber et al. 2019; Van Amerongen and Chmeliov 2019; Landi et al. 2020). This could determine under stress conditions a competition between the ABA synthesis and the levels of carotenoids required for maintaining the heat dissipation levels via NPQ in chloroplasts. Thus, the fine regulation of both processes would be necessary.

As for Φ_{NO}, it is worth mentioning that 2 of the 3 genes associated only with this trait (LOC_Os08g39430, LOC_Os08g40160) code for PSII structural proteins. This would indicate that the dissipative constitutive processes during the photochemical phase of photosynthesis are associated with the structural composition of PSII.

In conclusion, in this work we were able to identify, through a GWAS strategy, genes associated with the main parameters that define the quantum yield of PSII in rice. Our work shows the association between light-harvesting complexes and the potential quantum yield of PSII, as well as the relationship between regions that code for PSI-linked

proteins in energy distribution during the photochemical process of photosynthesis. Further studies are necessary to establish the action mechanisms of the spectral quality of light on PSI and how this defines the energy partition of PSII.

Compliance with ethical standards

Conflict of interest The authors declare that they have no conflict of interest.

References

Adachi S, Baptista LZ, Sueyoshi T et al (2014) Introgression of two chromosome regions for leaf photosynthesis from an indica rice into the genetic background of a japonica rice. J Exp Bot 65:2049–2056. https://doi.org/10.1093/jxb/eru047

Adachi S, Yamamoto T, Nakae T et al (2019) Genetic architecture of leaf photosynthesis in rice revealed by different types of reciprocal mapping populations. J Exp Bot 70:5131–5144. https://doi.org/10.1093/jxb/erz303

Adams PG, Vasilev C, Hunter CN, Johnson MP (2018) BBA—bioenergetics correlated fluorescence quenching and topographic mapping of light-harvesting complex II within surface-assembled aggregates and lipid bilayers. BBA Bioenergy 1859:1075–1085. https://doi.org/10.1016/j.bbabio.2018.06.011

Ahn TK, Avenson TJ, Peers G et al (2009) Investigating energy partitioning during photosynthesis using an expanded quantum yield convention. Chem Phys 357:151–158. https://doi.org/10.1016/j.chemphys.2008.12.003

Albanese P, Manfredi M, Meneghesso A et al (2016) Biochimica et biophysica acta dynamic reorganization of photosystem II supercomplexes in response to variations in light intensities. BBA Bioenergy 1857:1651–1660. https://doi.org/10.1016/j.bbabio.2016.06.011

Allakhverdiev SI, Murata N (2004) Environmental stress inhibits the synthesis de novo of proteins involved in the photodamage-repair cycle of Photosystem II in *Synechocystis* sp. PCC 6803. Biochim Biophys Acta 1657:23–32. https://doi.org/10.1016/j.bbabio.2004.03.003

Allakhverdiev SI, Mohanty P, Murata N (2003) Dissection of photodamage at low temperature and repair in darkness suggests the existence of an intermediate form of photodamaged photosystem II. Biochemistry 42:14277–14283. https://doi.org/10.1021/bi035205+

Allakhverdiev SI, Tsvetkova N, Mohanty P et al (2005) Irreversible photoinhibition of photosystem II is caused by exposure of Synechocystis cells to strong light for a prolonged period. Biochim Biophys Acta 1708:342–351. https://doi.org/10.1016/j.bbabio.2005.05.006

Allakhverdiev SI, Los DA, Mohanty P et al (2007) Glycinebetaine alleviates the inhibitory effect of moderate heat stress on the repair of photosystem II during photoinhibition. Biochim Biophys Acta 1767:1363–1371. https://doi.org/10.1016/j.bbabio.2007.10.005

Baker NR (2008) Chlorophyll fluorescence: a probe of photosynthesis in vivo. Annu Rev Plant Biol 59:89–113. https://doi.org/10.1146/annurev.arplant.59.032607.092759

Bates D, Maechler M, Bolker B, Walker S (2015) Fitting linear mixed effects models using lme4. J. Stat. Softw. 67:1–48. https://doi.org/10.18637/jss.v067.i01

Bergelson J, Roux F (2010) Towards identifying genes underlying ecologically relevant traits in *Arabidopsis thaliana*. Nat Rev Genet 11:867–879. https://doi.org/10.1038/nrg2896

Blanco P, Molina F, Pérez de Vida F, Avila S et al (2004) INIA Olimar: characterization and performance in season 2003–2004. Arroz 38:40–48 **(in Spanish)**

Blankenship RE (2014) Molecular mechanisms of photosynthesis. Wiley, Hoboken

Brestic M, Zivcak M, Kunderlikova K, Allakhverdiev SI (2016) High temperature specifically affects the photoprotective responses of chlorophyll b-deficient wheat mutant lines. Photosynth Res 130:251–266. https://doi.org/10.1007/s11120-016-0249-7

Brodersen CR, Vogelmann TC (2010) Do changes in light direction affect absorption profiles in leaves? Funct Plant Biol 37:403–412. https://doi.org/10.1071/FP09262

Campbell G, Norman J (1998) lntroduction to environmental biophysics. Springer, New York

Campbell DA, Tyystjärvi E (2012) Parameterization of photosystem II photoinactivation and repair. Biochim Biophys Acta 1817:258–265. https://doi.org/10.1016/j.bbabio.2011.04.010

Chen C, Zhang D, Li P, Ma F (2012) Partitioning of absorbed light energy differed between the sun-exposed side and the shaded side of apple fruits under high light conditions. Plant Physiol Biochem 60:12–17. https://doi.org/10.1016/j.plaphy.2012.07.016

Chen W, Gao Y, Xie W et al (2014) Genome-wide association analyses provide genetic and biochemical insights into natural variation in rice metabolism. Nat Genet 46:714–721. https://doi.org/10.1038/ng.3007

Chernys JT, Zeevaart JAD (2000) Characterization of the 9-cis-epoxycarotenoid dioxygenase gene family and the regulation of abscisic acid biosynthesis in Avocado. Plant Physiol 124:343–353. https://doi.org/10.1104/pp.124.1.343

Counce PA, Keisling TC, Mitchell AJ (2000) A uniform, objectives, and adaptive system for expressing rice development. Crop Sci 40:436–443. https://doi.org/10.2135/cropsci2000.402436x

Cullis BR, Smith AB, Coombes NE (2006) On the design of early generation variety trials with correlated data. J Agric Biol Environ Stat 11:381–393. https://doi.org/10.1198/108571106X154443

Dall'Osto L, Bressan M, Bassi R (2015) Biogenesis of light harvesting proteins. Biochim Biophys Acta 1847:861–871. https://doi.org/10.1016/j.bbabio.2015.02.009

DeLucia EH, Nelson K, Vogelmann TC, Smith WK (1996) Contribution of intercellular reflectance to photosynthesis in shade leaves. Plant Cell Environ 19:159–170. https://doi.org/10.1111/j.1365-3040.1996.tb00237.x

Demmig-Adams B, Adams WW, Barker DH et al (1996) Using chlorophyll fluorescence to assess the fraction of absorbed light allocated to thermal dissipation of excess excitation. Physiol Plant 98:253–264. https://doi.org/10.1034/j.1399-3054.1996.980206.x

Derks A, Schaven K, Bruce D (2015) Diverse mechanisms for photoprotection in photosynthesis. Dynamic regulation of photosystem II excitation in response to rapid environmental change. Biochim Biophys Acta 1847:468–485. https://doi.org/10.1016/j.bbabio.2015.02.008

Elshire RJ, Glaubitz JC, Sun Q et al (2011) A Robust, simple genotyping-by-sequencing (GBS) approach for high diversity species. PLoS ONE 6:1–10. https://doi.org/10.1371/journal.pone.0019379

Famoso AN, Zhao K, Clark RT et al (2011) Genetic architecture of aluminum tolerance in rice (*Oryza sativa*) determined through genome-wide association analysis and qtl mapping. PLoS Genet. https://doi.org/10.1371/journal.pgen.1002221

Flood PJ, Harbinson J, Aarts MGM (2011) Natural genetic variation in plant photosynthesis. Trends Plant Sci 16:327–335. https://doi.org/10.1016/j.tplants.2011.02.005

Fracheboud Y, Jompuk C, Ribaut JM et al (2004) Genetic analysis of cold-tolerance of photosynthesis in maize. Plant Mol Biol 56:241–253

Genty B, Briantais J, Baker NR (1989) The relationship between the quantum yield of photosynthetic electron transport and quenching of chlorophyll fluorescence. Biochim Biophys Acta 990:87–92. https://doi.org/10.1016/S0304-4165(89)80016-9

Glaubitz JC, Casstevens TM, Lu F et al (2014) TASSEL-GBS: a high capacity genotyping by sequencing analysis pipeline. PLoS ONE. https://doi.org/10.1371/journal.pone.0090346

Goltsev V, Zaharieva I, Chernev P et al (2012) Drought-induced modifications of photosynthetic electron transport in intact leaves: analysis and use of neural networks as a tool for a rapid non-invasive estimation. Biochim Biophys Acta 1817:1490–1498. https://doi.org/10.1016/j.bbabio.2012.04.018

Goltsev VN, Kalaji HM, Paunov M et al (2016) Variable chlorophyll fluorescence and its use for assessing physiological condition of plant photosynthetic apparatus. Russ J Plant Physiol 63:869–893. https://doi.org/10.1134/S1021443716050058

Gore MA, Chia JM, Elshire RJ et al (2009) A first-generation haplotype map of maize. Science 326:1115–1117. https://doi.org/10.1126/science.1177837

Gu J, Yin X, Struik PC et al (2012) Using chromosome introgression lines to map quantitative trait loci for photosynthesis parameters in rice (*Oryza sativa* L.) leaves under drought and well-watered field conditions. J Exp Bot 63:455–469. https://doi.org/10.1093/jxb/err292

Gutierrez L, Quero G, Fernandez S, Brandariz S (2016) lmem.gwaser: linear mixed effects models for genome-wide association studies. R package version 0.1.0. https://cran.r-project.org/src/contrib/Archive/lmem.gwaser/. Accessed 6 July 2019

Hakala M, Tuominen I, Keränen M et al (2005) Evidence for the role of the oxygen-evolving manganese complex in photoinhibition of photosystem II. Biochim Biophys Acta 1706:68–80. https://doi.org/10.1016/j.bbabio.2004.09.001

Hamdani S, Khan N, Perveen S et al (2019) Changes in the photosynthesis properties and photoprotection capacity in rice (*Oryza sativa*) grown under red, blue, or white light. Photosynth Res 139:107–121. https://doi.org/10.1007/s11120-018-0589-6

Hao D, Chao M, Yin Z (2012) Genome-wide association analysis detecting significant single nucleotide polymorphisms for chlorophyll and chlorophyll fluorescence parameters in soybean (*Glycine max*) landraces. Euphytica 186:919–931. https://doi.org/10.1007/s10681-012-0697-x

Havurinne V, Tyystjärvi E (2017) Action spectrum of photoinhibition in the diatom *Phaeodactylum tricornutum*. Plant Cell Physiol 58:2217–2225. https://doi.org/10.1093/pcp/pcx156

He J, Yang W, Qin L et al (2015) Photoinactivation of Photosystem II in wild-type and chlorophyll b-less barley leaves: Which mechanism dominates depends on experimental circumstances. Photosynth Res 126:399–407. https://doi.org/10.1007/s11120-015-0167-0

Hendrickson L, Furbank RT, Chow WS (2004) A simple alternative approach to assessing the fate of absorbed light energy using chlorophyll fluorescence. Photosynth Res 82:73–81. https://doi.org/10.1023/B:PRES.0000040446.87305.f4

Hendrickson L, Förster B, Pogson BJ, Wah SC (2005) A simple chlorophyll fluorescence parameter that correlates with the rate coefficient of photoinactivation of photosystem II. Photosynth Res 84:43–49. https://doi.org/10.1007/s11120-004-6430-4

Herritt M, Dhanapal AP, Fritschi FB (2018) Identification of genomic loci associated with the photochemical reflectance index by genome-wide association study in soybean. BMC Plant Biol 18:1–19. https://doi.org/10.1186/s12870-018-1517-9

Hu SP, Zhou Y, Zhang L et al (2009) Correlation and quantitative trait loci analyses of total chlorophyll content and photosynthetic rate of rice (*Oryza sativa*) under water stress and well-watered conditions. J Integr Plant Biol 51:879–888. https://doi.org/10.1111/j.1744-7909.2009.00846.x

Huang X, Wei X, Sang T et al (2010) Genome-wide association studies of 14 agronomic traits in rice landraces. Nat Genet 42:961–967. https://doi.org/10.1038/ng.695

Huang X, Zhao Y, Wei X et al (2012) Genome-wide association study of flowering time and grain yield traits in a worldwide collection of rice germplasm. Nat Genet 44:32–39. https://doi.org/10.1038/ng.1018

Humbeck K, Krupinska K (2003) The abundance of minor chlorophyll a/b-binding proteins CP29 and LCHI of barley (*Hordeum vulgare* L.) during leaf senescence is controlled by light. J Exp Bot 54:375–383. https://doi.org/10.1093/jxb/erg012

Jiao D, Huang X, Li X et al (2002) Photosynthetic characteristics and tolerance to photo-oxidation of transgenic rice expressing C4 photosynthesis enzymes. Photosynth Res 72:85–93. https://doi.org/10.1023/A:1016062117373

Jones LW, Kok B (1966) Photoinhibition of chloroplast reactions. I. Kinetics and action spectra. Plant Physiol 41:1037–1043. https://doi.org/10.1104/pp.41.6.1037

Jung J, Kim H (1990) The chromophores as endogenous sensitizers involved in the photogeneration of singlet oxygen in spinach thylakoids. Photochem Photobiol 52:1003–1009. https://doi.org/10.1111/j.1751-1097.1990.tb01817.x

Kalaji HM, Schansker G, Ladle RJ, Goltsev V (2014) Frequently asked questions about in vivo chlorophyll fluorescence : practical issues. Photosynth Res 122:121–158. https://doi.org/10.1007/s11120-014-0024-6

Kalaji HM, Schansker G, Brestic M, Bussotti F, Calatayud A, Ferroni L, Bąba W et al (2017) Frequently asked questions about chlorophyll fluorescence, the sequel. Photosynth Res 132:13–66. https://doi.org/10.1007/s11120-016-0318-y

Kasajima I, Takahara K, Kawai-Yamada M, Uchimiya H (2009) Estimation of the relative sizes of rate constants for chlorophyll de-excitation processes through comparison of inverse fluorescence intensities. Plant Cell Physiol 50:1600–1616. https://doi.org/10.1093/pcp/pcp102

Kasajima I, Ebana K, Yamamoto T et al (2011) Molecular distinction in genetic regulation of nonphotochemical quenching in rice. Proc Natl Acad Sci 108:13835–13840. https://doi.org/10.1073/pnas.1104809108

Kassambara A (2017) Practical guide to cluster analysis in R, 1st edn. https://www.sthda.com/english/download/3-ebooks/. Accessed 6 Aug 2019

Kitajima M, Butler WL (1975) Quenching of chlorophyll fluorescence and primary photochemistry in chloroplasts by dibromothymoquinone. BBA Bioenergy 376:105–115. https://doi.org/10.1016/0005-2728(75)90209-1

Klimov VV, Shafiev MA, Allakhverdiev SI (1990) Photoinactivation of the reactivation capacity of photosystem II in pea subchloroplast particles after a complete removal of manganese. Photosynth Res 23:59–65. https://doi.org/10.1007/BF00030063

Klughammer C, Schreiber U (2008) Complementary PS II quantum yields calculated from simple fluorescence parameters measured by PAM fluorometry and the saturation pulse method. PAM Appl Notes 1:27–35

Kościelniak J, Janowiak F, Kurczych Z (2005) Increase in photosynthesis of maize hybrids (*Zea mays* L.) at suboptimal temperature (15 °C) by selection of parental lines on the basis

of chlorophyll a fluorescence measurements. Photosynthetica 43:125–134. https://doi.org/10.1007/s11099-005-5134-0
Koussevitzky S, Nott A, Mockler TC, Hong F, Sachetto-Martins G, Surpin M, Lim J, Mittler R, Chory J (2007) Signals from chloroplasts converge to regulate nuclear gene expression. Science 316(5825):715–719
Kraakman ATW, Niks RE, Van Den Berg PMMM et al (2004) Linkage disequilibrium mapping of yield and yield stability in modern spring barley cultivars. Genetics 168:435–446. https://doi.org/10.1534/genetics.104.026831
Kramer DM, Johnson G, Kiirats O, Edwards GE (2004) New fluorescence parameters for the determination of QA redox state and excitation energy fluxes. Photosynth Res 79:209–218. https://doi.org/10.1023/B:PRES.0000015391.99477.0d
Krause H, Jahns P (2003) Pulse amplitude modulated chlorophyll fluorometry and its application in plant science. In: Beverley RG, Parson W (eds) Light-harvesting antennas in photosynthesis. Kluwer Academic, New York, pp 373–399
Laisk A, Oja V, Eichelmann H, Dall'Osto L (2014) Action spectra of photosystems II and I and quantum yield of photosynthesis in leaves in state 1. Biochim Biophys Acta 1837:315–325. https://doi.org/10.1016/j.bbabio.2013.12.001
Landi M, Zivcak M, Sytar O et al (2020) Plasticity of photosynthetic processes and the accumulation of secondary metabolites in plants in response to monochromatic light environments: a review. Biochim Biophys Acta 1861:148131
Langmead B, Salzberg SL (2012) Fast gapped-read alignment with Bowtie 2. Nat Methods 9:357–359. https://doi.org/10.1038/nmeth.1923
Lazár D (2015) Parameters of photosynthetic energy partitioning. J Plant Physiol 175:131–147. https://doi.org/10.1016/j.jplph.2014.10.021
Lê S, Josse J, Husson F (2008) FactoMineR: an R package for multivariate analysis. J. Stat. Softw. 25:1–18. https://doi.org/10.18637/jss.v025.i01
Li J, Ji L (2005) Adjusting multiple testing in multilocus analyses using the eigenvalues of a correlation matrix. Heredity 95:221–227. https://doi.org/10.1038/sj.hdy.6800717
Liu J, Yang H, Lu Q et al (2012) PSBP-DOMAIN PROTEIN1, a nuclear-encoded thylakoid lumenal protein, is essential for photosystem I assembly in *Arabidopsis*. Plant Cell 24:4992–5006. https://doi.org/10.1105/tpc.112.106542
Logan BA, Demmig-adams B, Adams W III, Bilger W (2014) Non-photochemical quenching and energy dissipation in plants, algae and cyanobacteria. In: Demmig-Adams B, et al. (eds) Non-photochemical quenching and energy dissipation in plants, algae and cyanobacteria. Springer, Dordrecht, pp 187–201
Lysenko V, Lazár D, Varduny T (2018) A method of a bicolor fast-Fourier pulse-amplitude modulation chlorophyll fluorometry. Photosynthetica 56:1447–1452. https://doi.org/10.1007/s11099-018-0848-y
Malnoë A (2018) Photoinhibition or photoprotection of photosynthesis ? Update on the (newly termed) sustained quenching component qH. Environ Exp Bot. https://doi.org/10.1016/j.envexpbot.2018.05.005
Malosetti M, Ribaut JM, Vargas M et al (2007) A multi-trait multi-environment QTL mixed model with an application to drought and nitrogen stress trials in maize (*Zea mays* L.). Euphytica 161:241–257. https://doi.org/10.1007/s10681-007-9594-0
McCouch SR, Wright MH, Tung CW et al (2016) Open access resources for genome-wide association mapping in rice. Nat Commun. https://doi.org/10.1038/ncomms10532
McCree KJ (1971) The action spectrum, absorptance and quantum yield of photosynthesis in crop plants. Agric Meteorol 9:191–216. https://doi.org/10.1016/0002-1571(71)90022-7
Mehta P, Allakhverdiev SI, Jajoo A (2010) Characterization of photosystem II heterogeneity in response to high salt stress in wheat leaves (*Triticum aestivum*). Photosynth Res 105:249–255. https://doi.org/10.1007/s11120-010-9588-y
Miyake C, Amako K, Shiraishi N, Sugimoto T (2009) Acclimation of tobacco leaves to high light intensity drives the plastoquinone oxidation system-relationship among the fraction of open PSII centers, non-photochemical quenching of Chl fluorescence and the maximum quantum yield of PSII in the dark. Plant Cell Physiol 50:730–743. https://doi.org/10.1093/pcp/pcp032
Müh F, Glöckner C, Hellmich J, Zouni A (2012) Light-induced quinone reduction in photosystem II. Biochim Biophys Acta 1817:44–65. https://doi.org/10.1016/j.bbabio.2011.05.021
Murata N, Nishiyama Y (2017) ATP is a driving force in the repair of photosystem II during photoinhibition. Plant Cell Environ 41:285–299. https://doi.org/10.1111/pce.13108
Murata N, Takahashi S, Nishiyama Y, Allakhverdiev SI (2007) Photoinhibition of photosystem II under environmental stress. Biochim Biophys Acta 1767:414–421. https://doi.org/10.1016/j.bbabio.2006.11.019
Murata N, Allakhverdiev SI, Nishiyama Y (2012) The mechanism of photoinhibition in vivo: re-evaluation of the roles of catalase, α-tocopherol, non-photochemical quenching, and electron transport. Biochim Biophys Acta 1817:1127–1133. https://doi.org/10.1016/j.bbabio.2012.02.020
Murchie EH, Ali A, Herman T (2015) Photoprotection as a trait for rice yield improvement: status and prospects. Rice 8:31. https://doi.org/10.1186/s12284-015-0065-2
Nishiyama Y, Allakhverdiev SI, Murata N (2011) Protein synthesis is the primary target of reactive oxygen species in the photoinhibition of photosystem II. Physiol Plant 142:35–46. https://doi.org/10.1111/j.1399-3054.2011.01457.x
Nobel PS (2009) Light. In: Nobel PS (ed) Physicochemical and environmental plant physiology, 4th edn. Academic Press, Cambridge, pp 176–226. https://doi.org/10.1016/B978-0-12-374143-1.00004-1
Oguchi R, Douwstra P, Fujita T et al (2011a) Intra-leaf gradients of photoinhibition induced by different color lights: implications for the dual mechanisms of photoinhibition and for the application of conventional chlorophyll fluorometers. New Phytol 191:146–159. https://doi.org/10.1111/j.1469-8137.2011.03669.x
Oguchi R, Terashima I, Kou J, Chow WS (2011b) Operation of dual mechanisms that both lead to photoinactivation of photosystem II in leaves by visible light. Physiol Plant 142:47–55. https://doi.org/10.1111/j.1399-3054.2011.01452.x
Ohnishi N, Allakhverdiev SI, Takahashi S, Murata N (2005) Two-step mechanism of photodamage to photosystem II: step 1 occurs at the oxygen-evolving complex and step 2 occurs at the photochemical reaction two-step mechanism of photodamage to photosystem II: step 1 occurs at the oxygen-evolving complex and step. Biochemistry 44:8494–8499. https://doi.org/10.1021/bi047518q
Ortiz D, Hu J, Salas Fernandez MG (2017) Genetic architecture of photosynthesis in Sorghum bicolor under non-stress and cold stress conditions. J Exp Bot 68:4545–4557. https://doi.org/10.1093/jxb/erx276
Oxborough K, Baker NR (1997) Resolving chlorophyll a fluorescence images of photosynthetic efficiency into photochemical and non-photochemical components—calculation of qP and Fv'/Fm' without measuring Fo'. Photosynth Res 54:135–142. https://doi.org/10.1023/A:1005936823310
Pan X, Liu Z, Li M, Chang W (2013) Architecture and function of plant light-harvesting complexes II. Curr Opin Struct Biol 23:515–525. https://doi.org/10.1016/j.sbi.2013.04.004
Parisseaux B, Bernardo R (2004) In silico mapping of quantitative trait loci in maize. Theor Appl Genet 109:508–514. https://doi.org/10.1007/s00122-004-1666-0

Pfündel E, Klughammer C, Schreiber U (2008) Monitoring the effects of reduced PS II antenna size on quantum yields of photosystems I and II using the dual—PAM—100 measuring system. PAM Appl Notes 1:21–24

Pfündel EE, Latouche G, Meister A, Cerovic ZG (2018) Linking chloroplast relocation to different responses of photosynthesis to blue and red radiation in low and high light-acclimated leaves of *Arabidopsis thaliana* (L.). Photosynth Res 137:105–128. https://doi.org/10.1007/s11120-018-0482-3

Price AL, Patterson NJ, Plenge RM et al (2006) Principal components analysis corrects for stratification in genome-wide association studies. Nat Genet 38:904–909. https://doi.org/10.1038/ng1847

Qin X, Zeevaart JAD (1999) The 9-cis-epoxycarotenoid cleavage reaction is the key regulatory step of abscisic acid biosynthesis in water-stressed bean. Proc Natl Acad Sci USA 96:15354–15361. https://doi.org/10.1073/pnas.96.26.15354

Quero G, Gutiérrez L, Monteverde E et al (2018) Genome-wide association study using historical breeding populations discovers genomic regions involved in high-quality rice. Plant Genome. https://doi.org/10.3835/plantgenome2017.08.0076

Quero G, Bonnecarrère V, Fernández S et al (2019) Light-use efficiency and energy partitioning in rice is cultivar dependent. Photosynth Res 140:51–63. https://doi.org/10.1007/s11120-018-0605-x

R Core Team (2018) R: a language and environment for statistical computing. R Foundation for Statistical Computing, Vienna, Austria. https://www.R-project.org/. Accessed 5 June 2019

Raorane ML, Pabuayon IM, Varadarajan AR, Kohli A (2015) Proteomic insights into the role of the large-effect QTL qDTY 12 1 for rice yield under drought. Mol Breed 35:139. https://doi.org/10.1007/s11032-015-0321-6

Rapacz M, Wójcik-Jagła M, Fiust A et al (2019) Genome-wide associations of chlorophyll fluorescence OJIP transient parameters connected with soil drought response in barley. Front Plant Sci. https://doi.org/10.3389/fpls.2019.00078

Ruiz-Sola MÁ, Rodríguez-Concepción M (2012) Carotenoid biosynthesis in *Arabidopsis*: a colorful pathway. Arabidopsis book 10:e0158. https://doi.org/10.1199/tab.0158

Russell L (2019) emmeans: estimated marginal means, aka least-squares means. R package version 1.4.2. https://CRAN.R-project.org/package=emmeans. Accessed 5 June 2019

Sager JC, McFarlane J (1997) Radiation. In: Langhans RW, Tibbitts TW (eds) Plant growth chamber handbook. Iowa State University, Ames, pp 1–29

Schreiber U, Klughammer C (2013) Wavelength-dependent photodamage to Chlorella investigated with a new type of multi-color PAM chlorophyll fluorometer. Photosynth Res 114:165–177. https://doi.org/10.1007/s11120-013-9801-x

Schreiber U, Klughammer C, Kolbowski J (2012) Assessment of wavelength-dependent parameters of photosynthetic electron transport with a new type of multi-color PAM chlorophyll fluorometer. Photosynth Res 113:127–144. https://doi.org/10.1007/s11120-012-9758-1

Schreiber U, Klughammer C, Schansker G (2019) Rapidly reversible chlorophyll fluorescence quenching induced by pulses of supersaturating light in vivo. Photosynth Res. https://doi.org/10.1007/s11120-019-00644-7

Schweder T, Spjøtvoll E (1982) Plots of p-values to evaluate many tests simultaneously. Biometrika 69:493–502. https://doi.org/10.1093/biomet/69.3.493

Smith HL, Mcausland L, Murchie EH (2017) Don't ignore the green light: exploring diverse roles in plant processes. J Exp Bot 68:2099–2110. https://doi.org/10.1093/jxb/erx098

Su Y (2019) The effect of different light regimes on pigments in *Coscinodiscus granii*. Photosynth Res 140:301–310. https://doi.org/10.1007/s11120-018-0608-7

Takahashi S, Milward SE, Yamori W et al (2010) The solar action spectrum of photosystem II damage. Plant Physiol 153:988–993. https://doi.org/10.1104/pp.110.155747

Terashima I, Fujita T, Inoue T et al (2009) Green light drives leaf photosynthesis more efficiently than red light in strong white light: revisiting the enigmatic question of why leaves are green. Plant Cell Physiol 50:684–697. https://doi.org/10.1093/pcp/pcp034

Tikkanen M, Aro EM (2012) Thylakoid protein phosphorylation in dynamic regulation of photosystem II in higher plants. Biochim Biophys Acta 1817:232–238. https://doi.org/10.1016/j.bbabio.2011.05.005

Tikkanen M, Mekala NR, Aro EM (2014) Photosystem II photoinhibition-repair cycle protects photosystem I from irreversible damage. Biochim Biophys Acta 1837:210–215. https://doi.org/10.1016/j.bbabio.2013.10.001

Umate P (2010) Genome-wide analysis of the family of light-harvesting chlorophyll a/b-binding proteins in Arabidopsis and rice. Plant Signal Behav 5:1537–1542. https://doi.org/10.4161/psb.5.12.13410

Van Amerongen H, Chmeliov J (2019) BBA bioenergetics instantaneous switching between different modes of non-photochemical quenching in plants. Consequences for increasing biomass production. BBA. https://doi.org/10.1016/j.bbabio.2019.148119

Vass I (2012) Molecular mechanisms of photodamage in the photosystem II complex. Biochim Biophys Acta 1817:209–217. https://doi.org/10.1016/j.bbabio.2011.04.014

Wang Q, Zhao H, Jiang J et al (2017) Genetic architecture of natural variation in rice nonphotochemical quenching capacity revealed by genome-wide association study. Front Plant Sci. https://doi.org/10.3389/fpls.2017.01773

Xia Y, Ning Z, Bai G et al (2012) Allelic variations of a light harvesting chlorophyll a/b-binding protein gene (Lhcb1) associated with agronomic traits in barley. PLoS ONE 7:1–9. https://doi.org/10.1371/journal.pone.0037573

Yan WJN, Rutger RJ, Bryant HE, Bockelman RG et al (2007) Development and evaluation of a core subset of the USDA rice germplasm collection. Crop Sci 47:869–876. https://doi.org/10.2135/cropsci2006.07.0444

Ye W, Hu S, Wu L et al (2017) Fine mapping a major QTL qFCC7L for chlorophyll content in rice (*Oryza sativa* L.) cv. PA64s. Plant Growth Regul 81:81–90. https://doi.org/10.1007/s10725-016-0188-5

Yoshida S, Forno D, Cock JH, Gomez KA (1976) Laboratory manual for physiological studies of rice, 3rd edn. International Rice Research Institute, Los Baños

Zavafer A, Cheah MH, Hillier W et al (2015a) Photodamage to the oxygen evolving complex of photosystem II by visible light. Sci Rep 5:1–8. https://doi.org/10.1038/srep16363

Zavafer A, Chow WS, Cheah MH (2015b) The action spectrum of photosystem II photoinactivation in visible light. J Photochem Photobiol B Biol 152:247–260. https://doi.org/10.1016/j.jphotobiol.2015.08.007

Zavafer A, Koinuma W, Chow WS et al (2017) Mechanism of photodamage of the oxygen evolving Mn cluster of photosystem II by excessive light energy. Sci Rep 7:11–14. https://doi.org/10.1038/s41598-017-07671-1

Zhao K, Tung C, Eizenga GC et al (2011) Genome-wide association mapping reveals a rich genetic architecture of complex traits in *Oryza sativa*. Nat Commun 2:1–10. https://doi.org/10.1038/ncomms1467

Zheng L, Ceusters J, Van Labeke MC (2019) Light quality affects light harvesting and carbon sequestration during the diel cycle of crassulacean acid metabolism in Phalaenopsis. Photosynth Res 41:195–207. https://doi.org/10.1007/s11120-019-00620-1

Zhu Z, Zhang F, Hu H et al (2016) Integration of summary data from GWAS and eQTL studies predicts complex trait gene targets. Nat Genet 48:481–487. https://doi.org/10.1038/ng.3538

Zivcak M, Brestic M, Kalaji HM (2014) Photosynthetic responses of sun- and shade-grown barley leaves to high light: is the lower PSII connectivity in shade leaves associated with protection against excess of light? Photosynth Res 119:339–354. https://doi.org/10.1007/s11120-014-9969-8

Zivcak M, Brestic M, Kunderlikova K et al (2015) Repetitive light pulse-induced photoinhibition of photosystem I severely affects CO_2 assimilation and photoprotection in wheat leaves. Photosynth Res 126:449–463. https://doi.org/10.1007/s11120-015-0121-1

Zivcak M, Brestic M, Botyanszka L et al (2018) Phenotyping of isogenic chlorophyll-less bread and durum wheat mutant lines in relation to photoprotection and photosynthetic capacity. Photosynth Res. https://doi.org/10.1007/s11120-018-0559-z

Zuo HL, Xiao K, Dong YJ, Xu JL, Li ZK et al (2007) Molecular detection of quantitative trait loci for leaf chlorophyll content at different growth-stages of rice (*Oryza sativa* L.). Asian J Plant Sci 6:518–522. https://doi.org/10.3923/ajps.2007.518.522

Affiliations

Gastón Quero[1] · Victoria Bonnecarrère[2] · Sebastián Simondi[3] · Jorge Santos[4] · Sebastián Fernández[5] · Lucía Gutierrez[6,7] · Silvia Garaycochea[2] · Omar Borsani[1]

Victoria Bonnecarrère
vbonnecarrere@inia.org.uy

Sebastián Simondi
ssimondi@uncu.edu.ar

Jorge Santos
jrsantos@uncu.edu.ar

Sebastián Fernández
sebfer@fing.edu.uy

Lucía Gutierrez
gutierrezcha@wisc.edu

Silvia Garaycochea
sgaraycochea@inia.org.uy

Omar Borsani
oborsani@fagro.edu.uy

[1] Departamento de Biología Vegetal, Facultad de Agronomía, Universidad de la República, Garzón 809, Montevideo, Uruguay

[2] Unidad de Biotecnología, Estación Experimental Wilson Ferreira Aldunate, Instituto Nacional de Investigación Agropecuaria (INIA), Ruta 48, Km 10, Rincón del Colorado, 90200 Canelones, Uruguay

[3] Área de Matemática, Facultad de Ciencias Exactas y Naturales, Universidad Nacional de Cuyo (FCEN-UNCuyo), Padre Contreras 1300, Mendoza, Argentina

[4] Área de Física, Facultad de Ciencias Exactas y Naturales, Universidad Nacional de Cuyo (FCEN-UNCuyo), Padre Contreras 1300, Mendoza, Argentina

[5] Facultad de Ingeniería, Instituto de Ingeniería Eléctrica, Universidad de La República, Julio Herrera y Reissig 565, Montevideo, Uruguay

[6] Department of Agronomy, University of Wisconsin-Madison, 1575 Linden Dr., Madison, WI 53706, USA

[7] Departamento de Biometría, Estadística y Cómputos, Facultad de Agronomía, Universidad de la República, Garzón 780, Montevideo, Uruguay

4.1.1 Material suplementario

El material suplementario del artículo precedente se encuentra en el siguiente enlace:

http://link.springer.com/article/10.1007/s11120-020-00721-2

5. CONCLUSIONES

En esta tesis se desarrollaron dos sistemas lumínicos en base LED. Ambos sistemas son capaces de generan niveles de radiación similares a los encontrados en situación de cultivo a cielo abierto (2000 µmol de fotones m^{-2} s^{-1}). Los sistemas LED desarrollados permiten generar ambientes lumínicos con diferentes calidades espectrales (Quero et al., 2019). Por otro lado, cuando se estudian procesos de conversión de energía durante la fotosíntesis conocer las características de la luz con la cual se realizan las mediciones es de suma importancia, debido al efecto que tiene esta sobre los proceso evaluados. Se estableció una estrategia analítica para la definición cuantitativa de la calidad espectral de la luz actínica incidente con la cual realizamos las mediciones de fluorescencia de clorofilas.

Los sistemas lumínicos desarrollados permiten obtener en condiciones controladas valores de eficiencia de uso de radiación (EUR) para arroz muy similares a los reportados en la literatura (Sinclair y Muchow, 1999, Mitchell et al., 1998). Esta validación de la información generada en condiciones controlada es de relevancia, porque permite comprender los procesos que regulan la EUR en arroz a nivel productivo.

En los cuatro cultivares de arroz analizados la disminución de la EUR en relación al incremento de la intensidad lumínica estuvo asociada a la calidad espectral del ambiente lumínico. Por otra parte, se observó una interacción genotipos ambiente en los valores de EUR evaluadas. Estas interacciones genotipo por ambiente presenta oportunidades para seleccionar aquellos cultivares que son más eficientes en el uso de la radiación en ambientes lumínicos específicos.

A nivel del aparato fotosintético, se observó que tanto el ambiente lumínico de crecimiento como el cultivar condicionan la partición de energía en el PSII. En ambientes de luz blanca, los bajos niveles de energía aumentan el daño de PSII y conducen a una disminución en los procesos fotoquímicos debido al cierre de los centros de reacción. La partición de energía en el PSII depende de los niveles de energía y de la calidad espectral de la luz incidente. Duplicar la energía de irradiación

en ambientes azules y rojos no genera la misma respuesta que duplicar la energía en ambientes blancos.

Los cultivares de arroz evaluados en este estudio mostraron ser sensibles a bajos niveles de radiación. En ambientes de baja intensidad lumínica se observó un incremento de los procesos disipativos vinculados con la fotoinhibición del PSII. La importancia de los mecanismos de fotoprotección en arroz fue comprobada al evaluar la población de mapeo donde se pudo observar el más del 60% de la energía que llega al PSII se disipa en forma de calor. Este trabajo concuerda con los reportado por Murchie et al. (2015) y Kasajima et al. (2011) quienes resaltan la relevancia de los mecanismos de fotoprotección en los procesos de conversión de energía durante la fotosíntesis en arroz.

En este trabajo, pudimos encontrar QTL putativos asociados con la calidad del grano y con los procesos primarios de conversión de energía durante la fotosíntesis en arroz. La estrategia de mapeo asociativo utilizada en este trabajo permitió identificar regiones genómicas claves de la arquitectura genética que codifica los procesos fotosintéticos en arroz. Esto es importante no solo por la implicancias que puede tener en los programas de mejoramiento, sino que es una estrategias para le generación de hipótesis sobre el funcionamiento y la regulación de los diferentes mecanismo fotosintéticos.

Por otra parte el uso de germoplasma adaptado localmente con una variación genética pequeña proporcionó la oportunidad de mapear diferencias fenotípicas sutiles que probablemente se pasarán por alto con un panel de germoplasma más diverso. Además, una población localmente adaptada de materiales de mejoramiento de élite permite la aplicación inmediata en programas de mejoramiento, incluida la introgresión asistida por marcadores de regiones genómicas favorables que confieren rasgos de interés en arroz o edición dirigida del genoma como base para futuros experimentos genéticos y aplicaciones en el mejoramiento.

6. BIBLIOGRAFÍA

Battello C. 2008. El arroz en Uruguay. Revista Arroz. Publicación de la Asociación Cultivadores de Arroz del Uruguay. Montevideo. 53: 34 – 40.

Berger B, Parent B, Tester M. 2010. High-throughput shoot imaging to study drought responses. Journal of Experimental Botany, 61 (13): 3519–3528. doi:10.1093/jxb/erq201.

Blum A. 1988. Plant Breeding for Stress Environments. USA. CRC Press. Boca Raton. FL.

Forrester JW.1961. Industrial Dynamics. Cambridge. MS. USA. MIT Press.

Gutiérrez L, Quero G, Fernández S, Brandariz S. 2016. lmem.gwaser: Linear mixed effects models for genome-wide association studies. R package version 0.1.0. The R Foundation (accessed 17 Jan. 2017). https://CRAN.R-project.org/package=lmem.gwaser.

Jones JW, Tsuji GY, Hoogenboom G, Hunt LA, Thornton PK, Wilkens PW, Imamura DT, Bowen WT, Singh U.1998. Decision support system for agrotechnology transfer DSSAT v3. En: Tsuji GY, Hoogenboom G, Thornton PK. (Eds.). Understanding Options for Agricultural Production. Kluwer Academic Publishers. Dordrecht. The Netherlands. pp. 157 – 177.

Kasajima I, Ebana K, Yamamoto T, Takahara K, Yano M, Kawai-Yamada M, Uchimiya H. 2011. Molecular distinction in genetic regulation of nonphotochemical quenching in rice. Proceedings of the National Academy of Sciences of the United States of America, 108 (33):13835–13840.doi: 10.1073/pnas.1104809108.

Khush GS. 2005. What it will take to Feed 5.0 Billion Rice consumers in 2030. Plant Molecular Biology, 59 (1):1–6.doi: 10.1007/s11103-005-2159-5.

Long SP, Zhu X, Naidu SL, Ort DR .2006. Can improvement in photosynthesis increase crop yields? Plant Cell and Environment 29 (3):315–330. doi:10.1111/j.1365-3040.2005.01493.x

Mitchell PL, Sheehy JE, Woodward FI. 1998. Potential yields and the efficiency of radiation use in rice. Manila (Philippines): IRRI Discussion Paper Series No. 32. 62 p

Monneveux P, Ribaut JM. 2006. Secondary traits for drought tolerance improvement in cereals. En: Ribaut JM. (Eds.). Drought Adaptation in Cereals. New York. Food Products Press.pp. 97 – 122.

Monteith JL. 1994. Principles of resource capture by crop stands. En: Monteith JL. Scott RK. Unsworth MH. (Eds.). Proceedings of the 52nd Easter School in Agricultural Sciences. Nottingham University Press; Loughborough, Leicestershire, University of Nottingham. pp.469.

Monteith J .1977. Climate and the efficiency of crop production in Britain. Philosophical Transactions of the Royal Society B. 281(980):277–294. doi:10.1098/rstb.1977.0140

Murchie EH, Ali A, Herman T. 2015. Photoprotection as a Trait for Rice Yield Improvement: Status and Prospects. Rice 8(1):1-9.doi: 10.1186/s12284-015-0065-2.

Pérez de Vida FB, Macedo I. 2013. Estimación de brecha y reserva tecnológica en arroz. Arroz Resultados Experimentales 2010-11. Actividades de Difusión 713. INIA Treinta y Tres.

Pérez de Vida FB. 2011. Aspectos de la ecofisiología del cultivo de arroz en Uruguay: III. Potencial biológico en la región Este. Arroz Resultados Experimentales 2010-11. Actividades de Difusión 651. INIA Treinta y Tres.

Quero G, Bonnecarrère V, Fernández S, Simondi S, Borsani O. 2019. Light-use efficiency and energy partitioning in rice is cultivar dependent. Photosynthesis Research. 140 (1):51–63.doi: 10.1007/s11120-018-0605-x.

Quero G, Gutiérrez L, Monteverde E, Blanco P, Pérez de Vida F, Rosas J, Fernández S, Garaycochea S, McCouch S, Berberian N, Simondi S, Bonnecarrère V. 2018. Genome-Wide Association Study Using Historical Breeding Populations Discovers Genomic Regions Involved in High-Quality Rice. Plant Genome 11(3):1-12.doi: 10.3835/plantgenome2017.08.0076.

Quero G, Simondi S, Bonnecarrère V, Gutiérrez L. 2017. Clusterhap: Clustering genotypes in haplotypes. R package version 0.1.0. The R Foundation. (accessed 5 June 2018). https://CRAN.R-project.org/package=clusterhap.

Russell G, Jarvis PG, Monteith JL. 1989. Absorption of radiation by canopies and stand growth. En: Russell G, Marshall B, Jarvis PG. (Eds). Plant canopies: their growth form and function. Society for Experimental Biology Seminar Series 31. Cambridge: Cambridge University Press. pp. 21-39.

Sadras VO, O'Leary GJ, Roget DK. 2005. Crop responses to compacted soil: Capture and efficiency in the use of water and radiation. Field Crops Research, 91 (2): 131 – 148. doi:10.1016/j.fcr.2004.06.011.

Sinclair TR, Muchow RC .1999. Radiation Use Efficiency. Advances in Agronomy, 65:215–265. doi:10.1016/S0065-2113(08)60914-1.

Stöckle CO, Kemanian AR. 2009. Crop Radiation Capture and Use Efficiency : A Framework for Crop Growth Analysis to canopy. En: Sadras V, Calderini D. (Eds.). Crop Physiology. San Diego. Academic Press, Elsevier Inc. pp.145–170.

Swaminathan MS. 2007. Can science and technology feed the world in 2025 ? Field Crops Research, 104 (2): 3 – 9. doi:10.1016/j.fcr.2007.02.004.

van Ittersum MK, Rabbinge R. 1997. Concepts in production ecology for analysis and quantification of agricultural input-output combinations. Field Crops Research, 52 (93): 197 – 208.doi: 10.1016/S0378-4290(97)00037-3.

Williams JR, Jones CA, Dyke PT. 1984. A modeling approach to determining the relationship between erosion and soil productivity. Transactions of the ASAE, 27(1). 129 – 144. doi: 10.13031/2013.32748.